AD-A054 699 ARINC RESEARCH CORP ANNAPOLIS MD F/G 20/5
HYDROSTATIC-BEARING MODIFICATION FOR MODEL 120RD02 CONSTANT-SPE--ETC(U)
AUG 69 R F WAMELING, G K GANTSCHNIGG F34601-69-C-1400
UNCLASSIFIED 595-01-1-990 NL

1 OF 2
ADA 054699

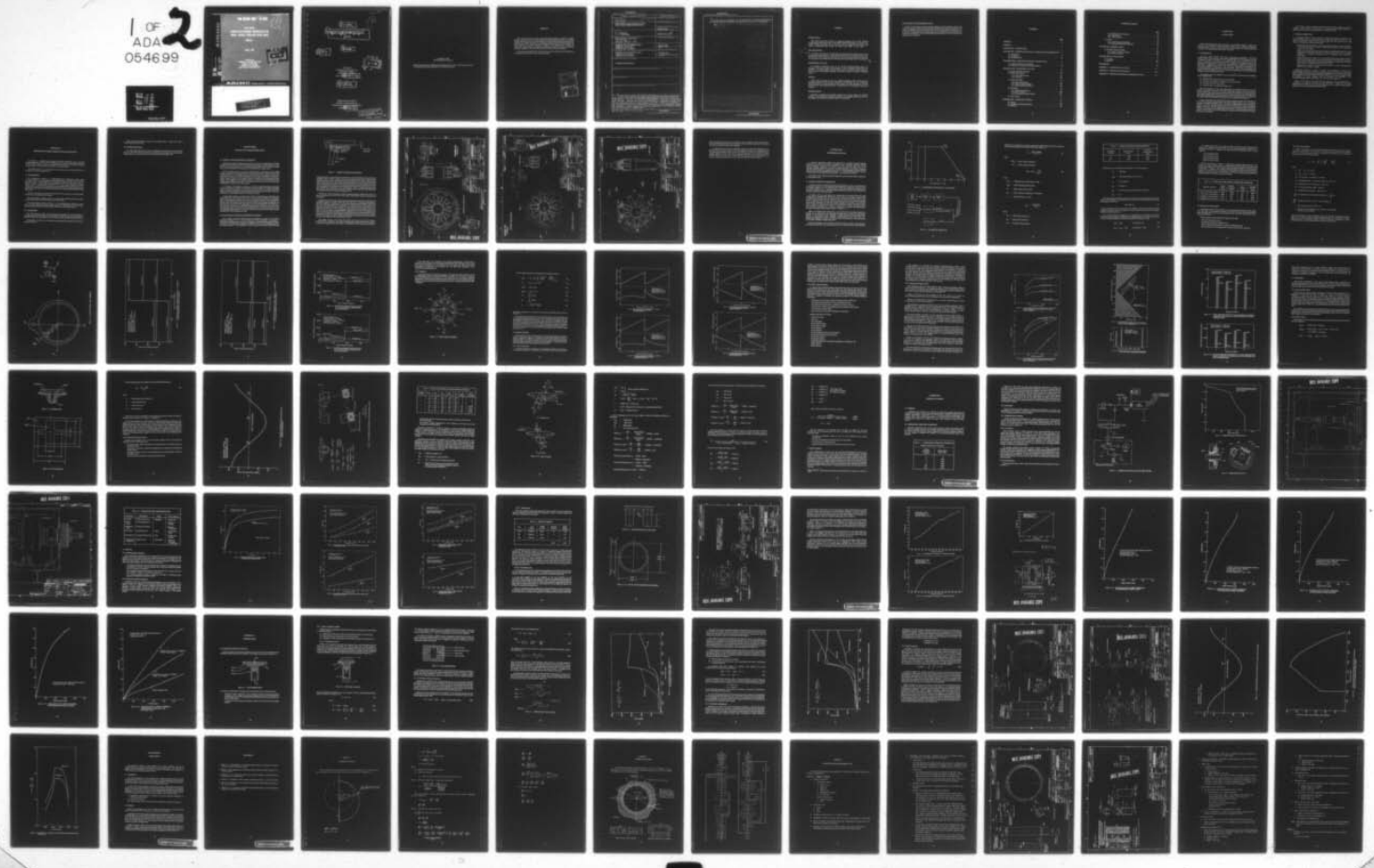

Publication 595-01-1-990

FOR ANOTHER TOWN

FINAL REPORT
HYDROSTATIC-BEARING MODIFICATION FOR MODEL 120RD02 CONSTANT-SPEED DRIVE
PHASE I

August 1968

Prepared for
OKLAHOMA CITY AIR MATERIEL AREA
TINKER AIR FORCE BASE
OKLAHOMA CITY, OKLAHOMA
under Contract F34601-68-C-1400

ARINC RESEARCH CORPORATION

R7W

1

9 Final Report,

6 HYDROSTATIC-BEARING MODIFICATION FOR MODEL 12ORD02 CONSTANT-SPEED DRIVE, PHASE I.

11 August 1969

12 97 p.

Prepared for
Oklahoma City Air Materiel Area
Tinker Air Force Base
Oklahoma City, Oklahoma

15 under Contract F34601-69-C-1400

by

10 R. F. Wameling
G. K. Gantschnigg

ARINC Research Corporation
a Subsidiary of Aeronautical Radio, Inc.
2551 Riva Road, Annapolis, Maryland 21401

14 Publication 595-01-1-990

400 247 SB

Prepared under Contract F34601-69-C-1400 which grants to the U.S. Government a license to use any material in this publication for Government purposes.

ABSTRACT

This report presents the results of an engineering program conducted by ARINC Research Corporation on the Model 120RD02 Constant Speed Drive used on the B-52H aircraft. The main objective of this program was to provide the engineering data required to determine the technical feasibility of a hydrostatic-bearing system as a replacement for the roller bearing in the CSD. Analytical calculations were performed to establish the hydrostatic bearing design, and laboratory testing was conducted to obtain a quantified empirical comparison of the hydrostatic-bearing and roller-bearing configurations.

In this report the details of the calculations and tests are presented, the problem areas are examined, and corrective actions are recommended.

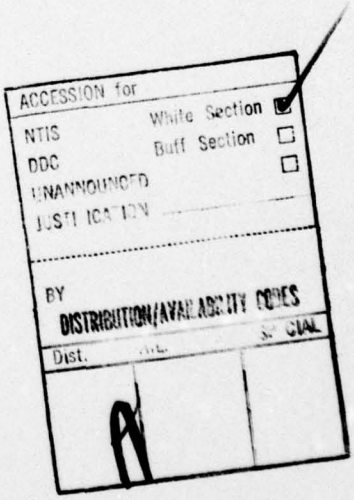

UNCLASSIFIED

SECURITY CLASSIFICATION OF THIS PAGE (When Data Entered)

REPORT DOCUMENTATION PAGE		READ INSTRUCTIONS BEFORE COMPLETING FORM
1. REPORT NUMBER 595-01-1-990	2. GOVT ACCESSION NO.	3. RECIPIENT'S CATALOG NUMBER
4. TITLE (and Subtitle) HYDROSTATIC-BEARING MODIFICATION FOR MODEL 120RD02 CONSTANT-SPEED DRIVE		5. TYPE OF REPORT & PERIOD COVERED
		6. PERFORMING ORG. REPORT NUMBER 595-01-1-990
7. AUTHOR(s) R. F. Wameling G. K. Gantschnigg		8. CONTRACT OR GRANT NUMBER(s) F34601-69-C-1400
9. PERFORMING ORGANIZATION NAME AND ADDRESS ARINC Research Corporation 2551 Riva Road Annapolis, Maryland 21401		10. PROGRAM ELEMENT, PROJECT, TASK AREA & WORK UNIT NUMBERS
11. CONTROLLING OFFICE NAME AND ADDRESS OKLAHOMA CITY AIR MATERIEL AREA TINKER AIR FORCE BASE OKLAHOMA CITY, OKLAHOMA		12. REPORT DATE August 1969 13. NUMBER OF PAGES 52
14. MONITORING AGENCY NAME & ADDRESS (if different from Controlling Office) OKLAHOMA CITY AIR MATERIEL AREA TINKER AIR FORCE BASE OKLAHOMA CITY, OKLAHOMA		15. SECURITY CLASS. (of this report) UNCLASSIFIED 15a. DECLASSIFICATION/DOWNGRADING SCHEDULE

16. DISTRIBUTION STATEMENT (of this Report)

UNCLASSIFIED/UNLIMITED

17. DISTRIBUTION STATEMENT (of the abstract entered in Block 20, if different from Report)

18. SUPPLEMENTARY NOTES

19. KEY WORDS (Continue on reverse side if necessary and identify by block number)

20. ABSTRACT (Continue on reverse side if necessary and identify by block number)

This report presents the results of an engineering program conducted by ARINC Research Corporation on the Model 120RD02 Constant Speed Drive used on the B-52H aircraft. The main objective of this program was to provide the engineering data required to determine the technical feasibility of a hydrostatic-bearing system as a replacement for the roller bearing in the CSD. Analytical calculations were performed to establish the hydrostatic bearing design, and laboratory testing was conducted to obtain a quantified empirical comparison of the hydrostatic-bearing and roller-bearing configurations. → over

DD FORM 1 JAN 73 1473 EDITION OF 1 NOV 65 IS OBSOLETE

UNCLASSIFIED

SECURITY CLASSIFICATION OF THIS PAGE (When Data Entered)

In this report the details of the calculations and tests are presented, the problem areas are examined, and corrective actions are recommended.

SUMMARY

INTRODUCTION

This report presents the results of an engineering program for the Model 120RD02 Constant-Speed Drive (CSD) used on the B-52H aircraft. The program was conducted by ARINC Research Corporation for the Oklahoma City Air Materiel Area (OCAMA) under Contract F34601-69-C-1400 during the period April 1969 to July 1969.

CSD DESCRIPTION

The CSD is a hydraulically operated differential transmission that transfers and converts variable-engine-speed rotation to constant-speed rotation for the aircraft alternator. Since the alternator output frequency varies directly with the speed of rotation, the alternator must be driven at a constant speed so that a constant output frequency will be maintained.

ENGINEERING ANALYSIS

An analytical engineering study of the selected hydrostatic-bearing design was performed. This study included the definition of critical operating conditions and the calculation of bearing loading, expected leakage flows, and frictional power dissipation. Each component was analyzed separately to determine its ability to perform its specified mission.

TESTING

Testing was conducted for both the original-configuration roller bearing and the prototype hydrostatic bearing. These comparative tests indicated that the hydrostatic bearing operated at a lower temperature, more quietly, and with less vibration and drag torque than the roller bearing. However, oil leakage flow in the hydrostatic bearing was excessive.

PROBLEM AREAS

Excessive oil leakage at the pad/race interface was a major obstacle to successful operation of the hydrostatic bearing. This problem was thoroughly analyzed, the cause of the leakage was identified, and a specific solution was developed.

CONCLUSIONS AND RECOMMENDATIONS

Because of the excessive pad/race interface leakage, it was not possible to obtain a true empirical comparison between the roller-bearing and hydrostatic-bearing configurations. The cause of this problem has been identified and a corrective design modification developed. It is therefore recommended that prototype parts for the modification be manufactured and tested. The determination of technical feasibility should be delayed until such modification testing has been completed.

CONTENTS

CONTENTS (continued)

CHAPTER ONE

INTRODUCTION

This report presents the results of Phase I of a two-phase program to improve the operation of the 12ORDO2 Constant Speed Drive (CSD). Phase I consisted of designing a hydrostatic-bearing system to replace the present roller-bearing system and determining the feasibility of incorporating this modification in the CSD.

1.1 BACKGROUND

In May 1968 ARINC Research Corporation completed a six-month reliability-improvement program under Contract F34601-68-C-0284 to determine the causes of premature wearout and failure of the 120RD02 CSD, and to recommend corrective actions to eliminate or minimize these failures. Program tasks included analysis of data acquired from unsatisfactory reports (UR), the preparation of engineering reports, and observation of disassembly and overhaul of failed units and damaged parts to identify the most critical problems contributing to CSD unreliability. Engineering investigations of the identified problems were conducted to determine specific causes of failure and appropriate solutions. These investigations included load analysis, determination of friction levels and temperature effects, and laboratory tests.

Four problem areas were identified as the most significant contributors to unreliability of the 120RDO2 CSD:

(1) Scuffing of the pump and motor race and pistons

(2) Excessive wear of gears and bearings in the accessory drive

(3) Excessive wear of the valve plates

(4) Excessive wear of the input and output shafts

The most significant of these was determined to be scuffing between the race and pistons of the pump and motor. Under certain operating conditions, the friction between moving elements (e.g., pistons and cylinders, rollers and retainer-ring pockets, rollers and race) causes a sliding motion between the piston heads and the inner race. With high loads and high differential speeds, this sliding motion results in overload and wearout (scuffing) of the contact surfaces and subsequent contamination of the hydraulic/lubricating oil.

It was concluded from the reliability-improvement program that the intrinsic features of the current pump/motor design would not permit a simple solution (one not involving redesign) to the basic scuffing problem. Preliminary engineering examination of existing oil supply in the drive indicated that the unit would be amenable to a hydrostatic-bearing system. However, an intensive engineering study of the entire CSD would be necessary to determine what effects such a design approach would have on supporting devices such as oil pumps, oil lines, filters, and valves. Characteristic changes such as temperature and leakage also had to be considered.

On the basis of these conclusions derived from the six-month reliability-improvement program, ARINC Research proposed that a hydrostatic-bearing design program be undertaken to improve the operation and the service life of the CSD.

1.2 PROGRAM OBJECTIVES

A two-phase program is being conducted to eliminate the premature wear-out of the Model 120RD02 CSD as a result of piston/race scuffing. This report covers Phase I — the design of a hydrostatic bearing system to eliminate parts that cause wear-out in the pump element. The design encompasses the following:

- Replace the roller bearing with a hydrostatic bearing, using the internal oil pressure of the CSD system as the source of hydrostatic lubrication, and investigate the capacity of the oil supply.
- Design the new hydrostatic bearing for complete interchangeability with the current rolling-element bearings without affecting other parts and devices (such as oil-pump capacities), or changing performance, weight, installation, and maintenance characteristics.
- Design the hydrostatic bearing to prevent metal-to-metal contact between the race and wobbler bearing surfaces under all environmental and operational conditions, such as start-up, high speed, and low speed (including zero speed), and at any type of relative motion and applied loads specified for the CSD.
- Design parts to modify the pump element, allowing for as much interchangeability with the motor element as possible.

Additional objectives of Phase I include the manufacture of one set of hydrostatic-bearing prototype parts, and laboratory testing of these parts to demonstrate design feasibility. Analytical and empirical engineering data were to be acquired to quantify design characteristics of the hydrostatic-bearing modification. The results of Phase I are to be evaluated by OCNE engineers, who will determine the feasibility of the hydrostatic-bearing approach and whether or not to proceed with Phase II.

Phase II will consist of a detailed engineering analysis of the entire CSD system — including the oil reservoir, oil cooler, oil lines, and filters — followed by the actual modification and testing of individual CSDs, preparation of a complete engineering data package, and revision of applicable Technical Orders.

CHAPTER TWO

DESCRIPTION OF MODEL 120RD02 CONSTANT-SPEED DRIVE

The CSD is a hydraulically operated differential transmission used to convert variable-engine-speed rotation (4475 to 7980 rpm) to constant-speed rotation (8000 rpm) for the aircraft alternator. Since the alternator output frequency varies directly with the speed of rotation, the alternator must be driven at a constant speed.

The CSD consists of (1) a transmission, (2) accessories, and (3) interface devices, as described in the following subsections.

2.1 TRANSMISSION

The transmission consists of a variable-displacement radial-piston pump whose oil-output volume can be controlled, a governing system that controls the rate of flow from the pump, and a constant-displacement radial-piston hydraulic motor whose speed of rotation depends on how much oil the pump forces into it. The pump/motor assembly consists of (1) a cylinder-block assembly, (2) a pump-wobbler assembly, and (3) a motor-wobbler assembly. The cylinder-block assembly contains the pump and motor pistons and the pump and motor valve plates, and is driven by the aircraft engine through the input drive shaft.

The rate of oil flow from the pump is determined by the position of the pump wobbler, which in turn is controlled by the governor.

The pump-wobbler assembly consists of a nonrotating variable-displacement wobbler, an inner race, and two roller bearings with roller retainer rings.

The motor-wobbler assembly consists of a constant-displacement wobbler, an inner race, two roller bearings with roller retainer rings, and a ball bearing with retainer ring. During operation, the motor-wobbler assembly rotates at the CSD output speed.

2.2 ACCESSORIES

The CSD accessories consist of a charge pump that supplies oil to the transmission, a scavenge pump that recirculates used and surplus oil from the sump to the reservoir, a governor charge pump that supplies oil to the control system, and basic and limit governors.

These devices are driven by a common accessory gear-drive assembly from the motor output of the CSD.

Other nonrotating accessories include a recirculating valve, a charge relief valve, a proportional valve, and a filter.

2.3 INTERFACE DEVICES

The CSD connecting devices consist of installation parts between the aircraft-engine gear box, the CSD, and the generator. These include the input shaft, double-spline shaft, thermal disconnect, output shaft, and two quick-attach/detatch (QAD) pads.

CHAPTER THREE

HYDROSTATIC-BEARING MODIFICATION

3.1 GENERAL CHARACTERISTICS OF BEARINGS

Bearings that exhibit primarily rolling friction are known as rolling-element bearings. Examples are the ball, roller, and needle bearings. Rolling-element bearings generally consist of two races (inner and outer), a set of rolling elements (balls, rollers, or needles) between the races, and a separator for keeping the set of rolling elements equally spaced.

When the bearing friction is essentially sliding friction, the bearing is called a sliding bearing. Lubrication of a sliding bearing may be such that the bearing surfaces are separated by the creation of a load-carrying continuous fluid film. When this condition is present, the lubrication is referred to as either hydrodynamic or hydrostatic. Hydrodynamic lubrication requires relative motion of the bearing surfaces to generate the load-reacting lubricant pressures. The magnitude of the lubricant pressures is a function of the relative speed of the bearing surfaces. When relative speeds of the bearing surfaces are low or the loads are high, hydrodynamic lubrication may not be possible.

In contrast to hydrodynamic bearings, in which the lubricant pressure is generated within the bearing by relative motion between bearing surfaces, the hydrostatic-bearing lubricant pressure is generated at an external source and fed into the bearing. The CSD, because it has the potential for providing a pressurized lubrication source that is external to the bearing, is an ideal application for the hydrostatic bearing.

A hydrostatic bearing in its simplest form consists of a pad and runner. The pad in turn incorporates three basic elements, the recess, sill, and restrictor (Figure 3-1). Pressurized fluid is fed through the restrictor into the recess. When the product of the recess pressure and the recess area becomes greater than the load holding the pad and runner together, the pad and runner will separate and fluid will flow from the source through the restrictor and recess and out over the sill, thus establishing the load-carrying fluid film. The thickness of the fluid film is determined by the bearing supply pressure, restrictor size and type, fluid type and temperature, recess and sill areas, and applied load. If the applied load ever exceeds the maximum supply pressure at zero flow, the pad and runner will seat, metal-on-metal rubbing will occur, and damage may result.

3.2 EVOLUTION OF COMPOUND HYDROSTATIC BEARING

The originally proposed hydrostatic-bearing modification consisted of nine simple hydrostatic bearings (one for each piston pair). This modification incorporated a shrink-fitted steel-ring insert as the runner, together with individual bearing pads, as shown in ARINC Research Drawings C-000392 and C-000394. This concept was abandoned after a brief design analysis. It was impossible to achieve pad/runner separation against the high

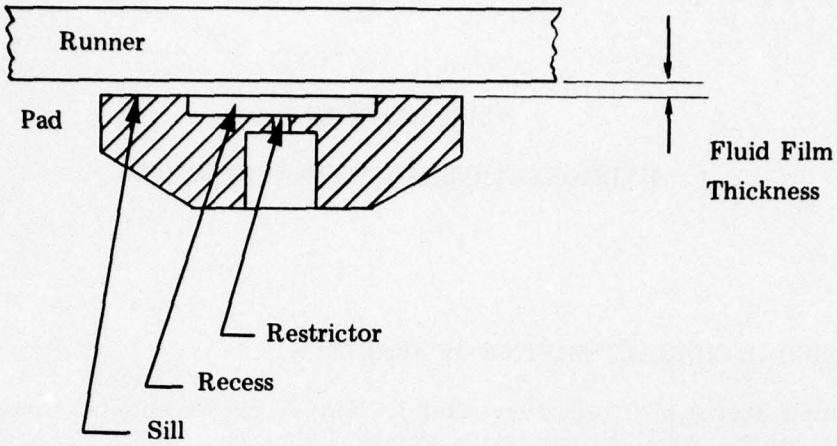

Figure 3—1. **SIMPLE HYDROSTATIC BEARING**

centrifugal loads by using pads that conformed to the space limitations imposed. Without separation, there would be metal-to-metal contact during relative motion. A load analysis revealed that under certain operating conditions the product of the relative sliding velocity between surfaces and the surface-contact bearing pressure (PV factor) would be excessively high. A hybrid bearing pad that would utilize both hydrodynamic and hydrostatic lift forces was then considered. This approach was abandoned because at maximum input speed, where the centrifugal load is greatest and the hydrodynamic effect is needed most, the relative speed between the cylinder block and motor wobbler is only 20 rpm. This speed differential is too small to generate the required hydrodynamic lift.

Finally, the concept illustrated in ARINC Research drawing C-000419 was chosen. As shown, the ring insert is free to rotate, and an array of hydrostatic recesses is located around its periphery.

Pressurized fluid is fed into recesses located at the pad surfaces; it acts on the recess area to partially support the applied radial load. Thus the pad is a hydrostatic bearing but is specifically designed to operate with zero fluid-film thickness (metal-to-metal contact with ring I.D.). The pressurized fluid is supplied to the ring recesses from the pad recesses through appropriate restrictors located in the ring. Each pad recess communicates at all times with at least one of these ring-recess feed restrictors. Fluid pressure acts on the ring-recess areas located at the ring periphery to support the vector sum of the applied loads from all of the piston/pad assemblies. Here, the applied load is completely supported, and a pressurized fluid film at the ring periphery prevents metal-to-metal contact between ring and wobbler. This bearing is called a compound hydrostatic bearing because there are actually two hydrostatic bearings in the same fluid series circuit.

The relative motion of the pads with respect to the ring is due to the wobbler eccentricity and is oscillatory. The relative sliding velocity between these parts, a function of eccentricity magnitude and input speed, is considerably lower than that for the case in

REVISIONS				
SYM	ZONE	DESCRIPTION	DATE	APPROVED

PRELIMINARY DATA

ARINC RESEARCH CORP

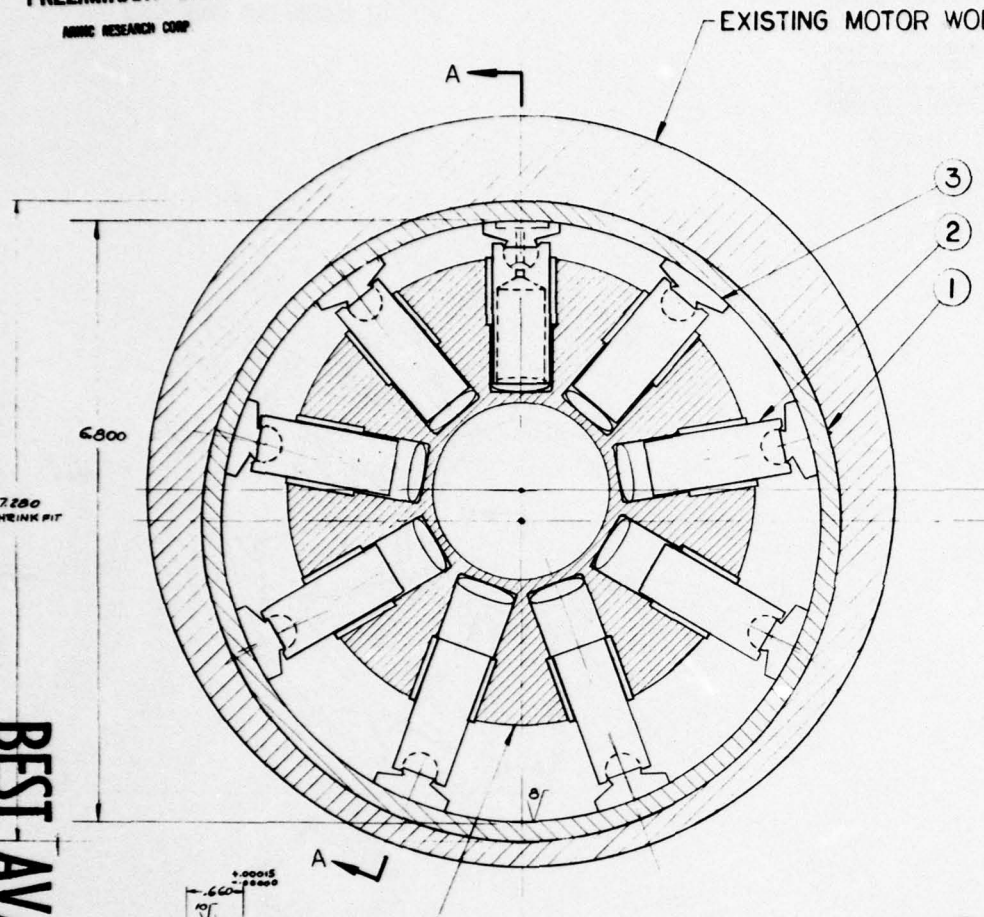

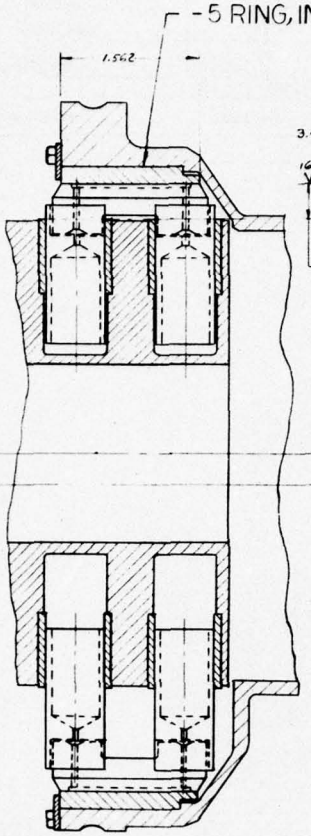

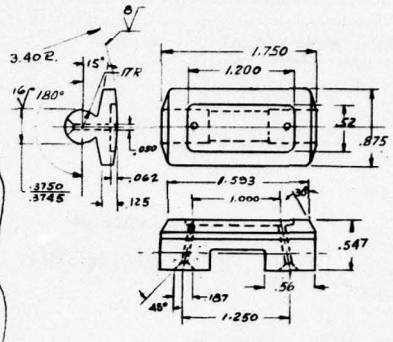

-9 PAD

PRELIMINARY DATA

ARINC RESEARCH CORP.

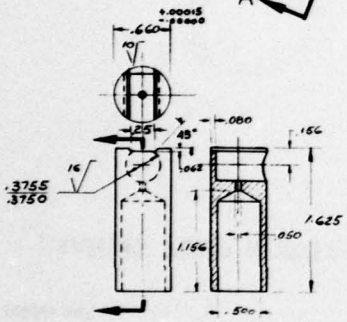

-7 PISTON

BEST AVAILABLE COPY

QTY.REQ.	DESCRIPTION	PART NO.	MATERIAL	SPECIFICATION	ZONE	ITEM
9	PAD, MOTOR	-9	BRONZE			3
18	PISTON, MOTOR	-7	STEEL			2
1	RING, INSERT	-5	STEEL			1

LIST OF MATERIALS

ITEM	QTY.	NEXT ASSY	USED ON
		APPLICATION	

UNLESS OTHERWISE SPECIFIED DIMENSIONS ARE IN INCHES

TOLERANCES ON:
FRACT. ± 1/64
DECIMALS .XX ± .010, .XXX ± .005
ANGLES ± .50°

MATERIAL

TREATMENT

FINISH

DFTM.		DATE
DES. ENG.		
CHKD.		
APPD.		

WORK ORDER NO. 568-01

CONTRACT NO. F34601-68-C-0254

ARINC RESEARCH CORPORATION

TITLE

MOTOR WOBBLER

B-52H, CSD-MODFL 120RD02

HYDROSTATIC PISTON PAD

SIZE C | DWG. NO. C000392

SCALE 1/1 | SHEET 1 OF 1

PRELIMINARY DATA

ARINC RESEARCH CORP.

REVISIONS				
SYM	ZONE	DESCRIPTION	DATE	APPROVED

EXISTING PUMP WOBBLER

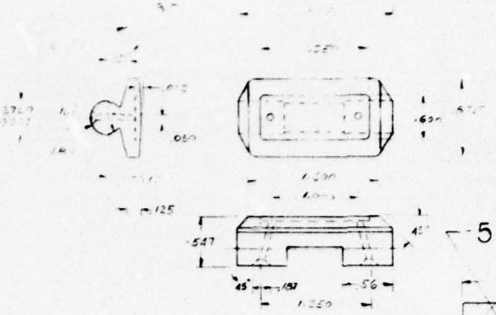

-9 PAD

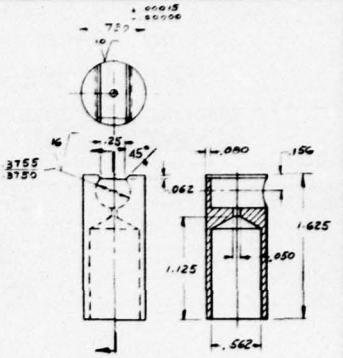

-7 PISTON

5 RING INSERT

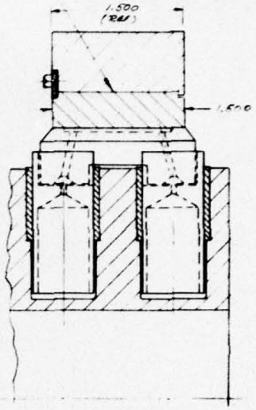

A-A

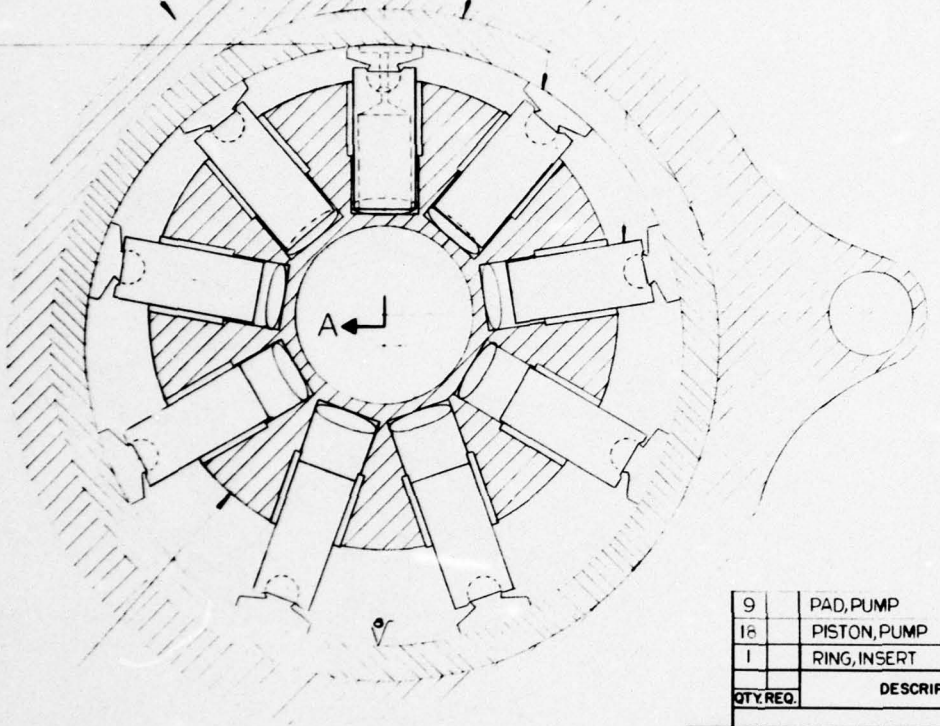

EXISTING CYLINDER BLOCK

PRELIMINARY DATA

ARINC RESEARCH CORP.

BEST AVAILABLE COPY

QTY. REQ.	DESCRIPTION	PART NO.	MATERIAL	SPECIFICATION	ZONE	ITEM
9	PAD, PUMP	-9	BRONZE			3
18	PISTON, PUMP	-7	STEEL			2
1	RING, INSERT	-5	STEEL			1

LIST OF MATERIALS

ITEM	QTY	NEXT ASSY	USED ON

APPL ON

UNLESS OTHERWISE SPECIFIED DIMENSIONS ARE IN INCHES

TOLERANCES ON:
FRACT. ± 1/64
DECIMALS .XX ± .010 .XXX ± .005
ANGLES ± .50°

MATERIAL

TREATMENT

FINISH

DFTM.		DATE 6-5-68
DES. ENG.		
CHKD.		
APPD.		

WORK ORDER NO. 568-1

CONTRACT NO. 3462 C 025

ARINC RESEARCH CORPORATION

TITLE

PUMP WOBBLER

B-52 H, CSD-MODEL 120 RD02

HYDROSTATIC PISTON PAD

SIZE C DWG. NO. C 000394

SCALE

SHEET OF 1

REVISIONS				
SYM	ZONE	DESCRIPTION	DATE	APPROVED

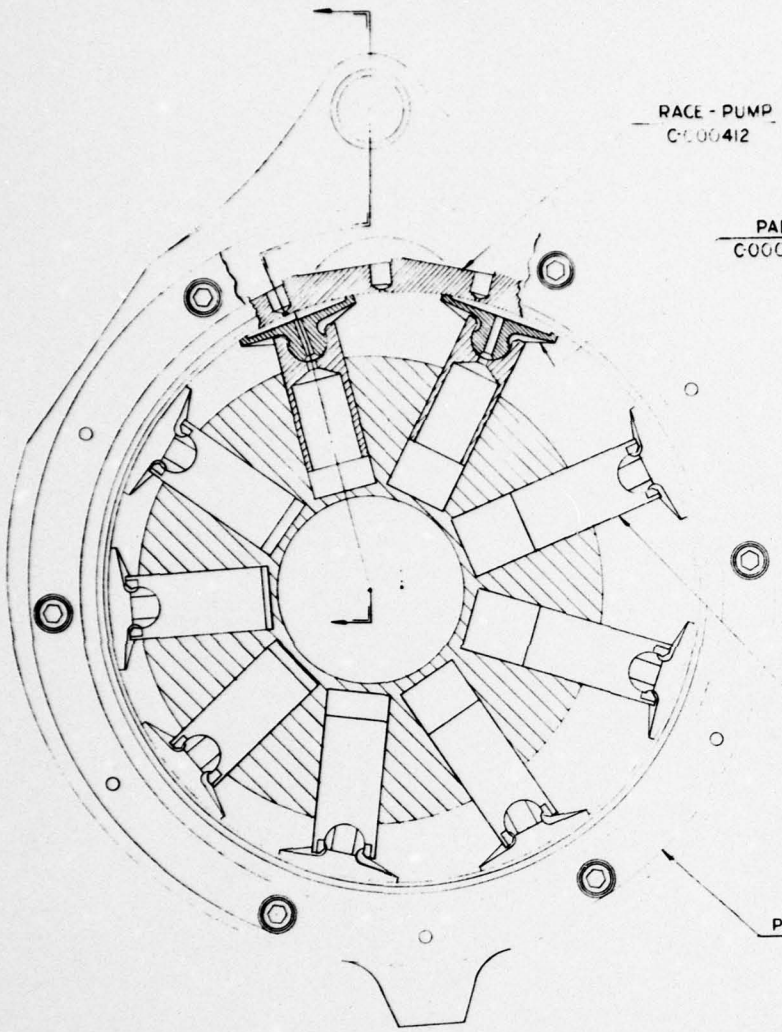

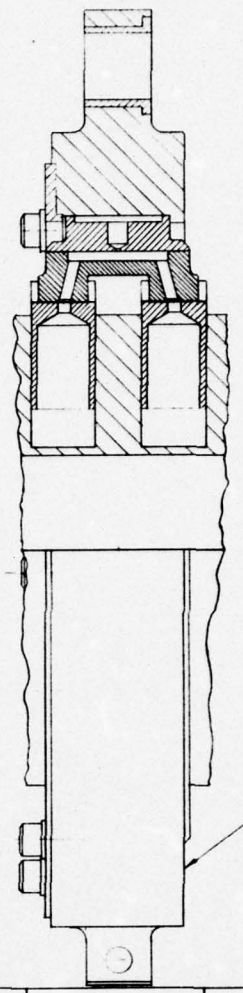

QTY. REQ.	DESCRIPTION	PART NO.	MATERIAL	SPECIFICATION	ZONE	ITEM

LIST OF MATERIALS

ITEM	QTY.	NEXT ASSY	USED ON
APPLICATION			

UNLESS OTHERWISE SPECIFIED DIMENSIONS ARE IN INCHES
TOLERANCES ON:
FRACT. ± DECIMALS .XX ± .XXX ± ANGLES ±
MATERIAL
TREATMENT
FINISH

		DATE
DFTM.	L. Litton	8/2/69
DES. ENG.		
CHKD.		
APPD.		

WORK ORDER NO. 595-01
CONTRACT NO.

ARINC RESEARCH CORPORATION

TITLE
PUMP ASSEMBLY
8.52 H CSD MODEL 120-RD02
COMPOUND HYDROSTATIC BEARING

SIZE C | DWG. NO. C 000419

SCALE 1/1 | SHEET 1 OF 1

4 3 2 1

D C A

which the ring was fixed. Because of this lower velocity, together with the partial reaction of the applied bearing load and the availability of good boundary lubrication, the interface PV factor is small and wear should be negligible.

At CSD start-up and very low initial input speeds some piston/pad assemblies will be retracted because of their weight. As the cylinder block accelerates, the centrifugal force of the piston/pad assemblies increases until it is sufficient to move the assemblies radially outward against the ring. After all 18 piston/pad assemblies of the pump and motor elements have been forced into contact with the ring I.D., system charge pressure will increase to supply pressurized fluid to the compound hydrostatic-bearing system.

CHAPTER FOUR

ENGINEERING ANALYSIS

A rigorous engineering analysis was performed to determine specific hardware dimensions and ensure the theoretical feasibility of the compound hydrostatic bearing. Critical operating conditions were defined and loads calculated. Each part of the hydrostatic-bearing modification was then analyzed separately to determine compliance with the specified mission. To supplement the ARINC Research analysis, Franklin Institute Research Laboratories, Philadelphia, Pennsylvania — an acknowledged authority in the field of hydrostatic- and hydrodynamic-bearing design — was retained as consultant.

The results of the engineering analysis suggested that the proposed design modification was technically sound.

4.1 CRITICAL OPERATING CONDITIONS

The pump, as shown in ARINC Research Drawing C000419, consists of a cylinder block containing a double row of nine radial cylinders and pistons, a single row of pads each with two pistons attached to it, a free-floating race with hydrostatic-bearing recesses spaced around the periphery, and a nonrotating variable-displacement wobbler. The cylinder block is directly driven by the CSD input shaft.

At start-up and low input speeds, the cylinder block is centered within the pump wobbler and no pumping action takes place. As the input speed increases to between 1000 and 2000 rpm, the basic governor causes actuation of the control piston, which in turn moves the pump wobbler into the maximum eccentric position. The minimum governing speed is 4475 rpm. Once the input has reached this speed, the output is at the desired constant value of 8000 rpm. As the input speed increases from 4475 to the maximum rated speed of 7980, the basic governor causes a control piston to position the pump wobbler from maximum eccentricity to a near-zero eccentricity in a manner that maintains the constant output speed. This operation is shown in Figure 4—1.

Figure 4—2 illustrates the primary power flow of the CSD. The power demands are imposed at any speed above the minimum governing speed of 4475 rpm. The power required for the accessories was calculated in ARINC Research Report 568-01-1-901, Analysis of Sundstrand Model 120RD02 Constant-Speed Drive, May 1968. The alternator-electrical-power demand was obtained from T.O. 9H6-3-21-2, Technical Manual for the Model 120RD02 Constant Speed Drive.

With the knowledge of the horsepower which the CSD must deliver to the alternator and accessories and of the fact that this power must be delivered at the constant speed of

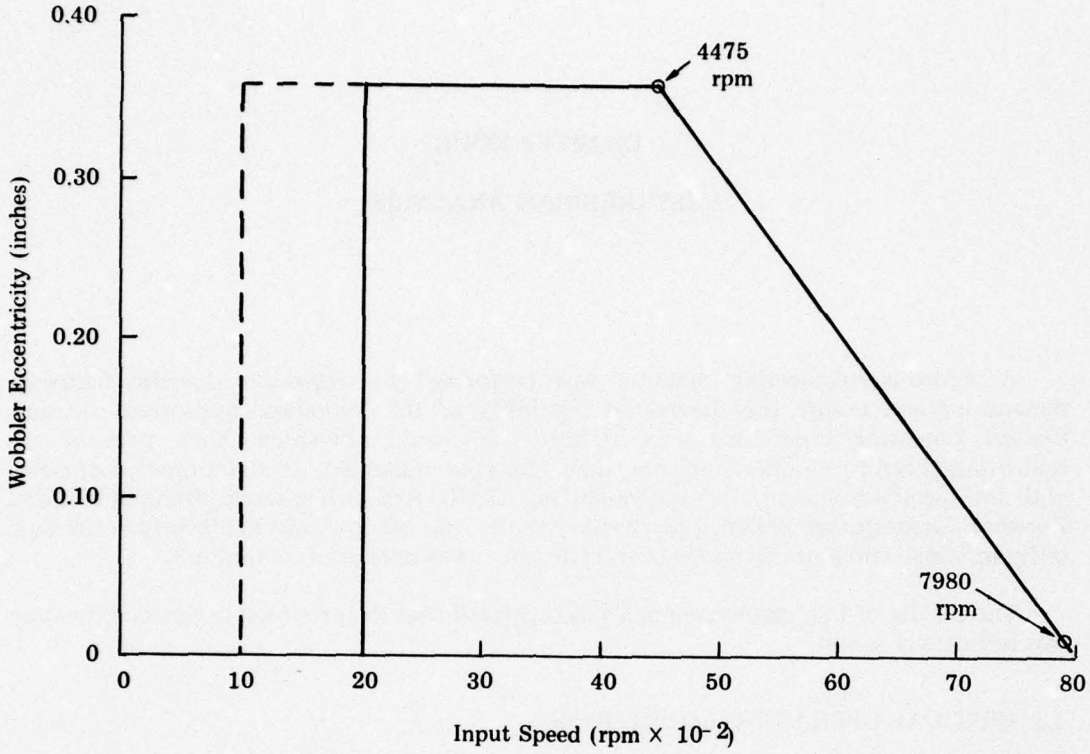

Figure 4—1. **PUMP-WOBBLER ECCENTRICITY VS INPUT SPEED**

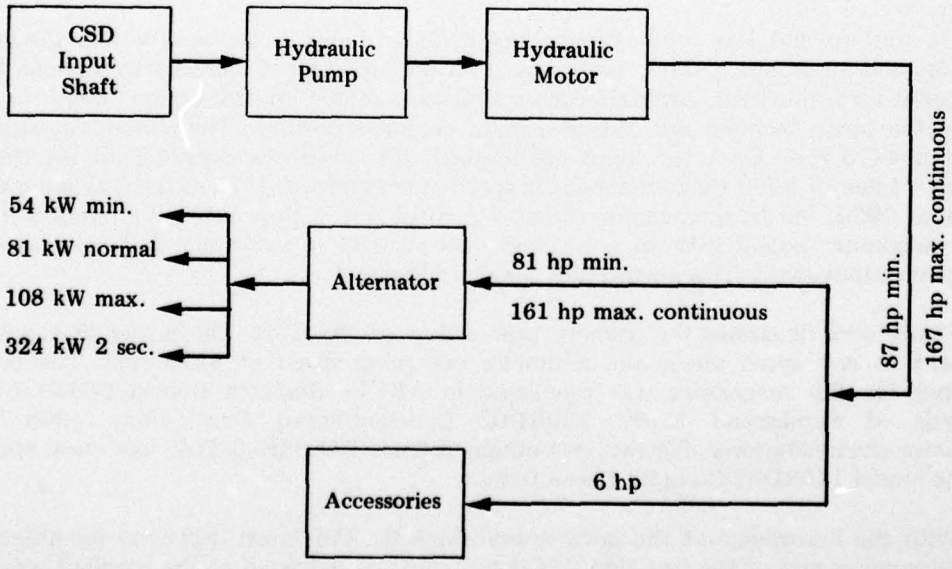

Figure 4—2. **CSD PRIMARY POWER FLOW**

8000 rpm, the hydraulic-motor output torque and required supply pressure were calculated from the following equations (results are tabulated in Table 4—1):

$$T_o = \frac{(HP)_o\ (63000)}{n_o} \qquad (1)$$

where

$(HP)_o$ = Motor output horsepower

N_o = Motor output speed (rpm)

$$P_{ms} = P_{md} + \frac{T_o}{D_m\ \eta_t} \qquad (2)$$

where

P_{ms} = Required motor supply pressure (psig)

P_{md} = Motor discharge pressure (psig)

T_o = Motor output torque (in-lb)

D_m = Motor volumetric displacement (In^3/radian)

η_t = Torque efficiency of motor

$$D_m = \frac{A_m\ S_m\ N_m}{2\pi} \qquad (3)$$

where

A_m = Motor piston area (sq. in.)

S_m = Motor piston stroke (in)

N_m = Number of motor pistons

Table 4—1. **HYDRAULIC-MOTOR CHARACTERISTICS**

Horsepower Demand	Output Torque (in-lb_f)	Required Supply Pressure (psig)
87	684	1675
167	1320	2980

Constants used in calculating the results (Table 4—1) were as follows:

N_o = 8000 rpm

P_{md} = 280 psig (maximum value per T.O.)

η_t = 0.7 (assumed)

A_m = 0.349 sq in

S_m = 0.70 (twice motor-wobbler fixed eccentricity)

N_m = 18

The hydraulic-pump discharge pressure must equal the motor supply pressure plus the pressure drop associated with transporting the fluid from the pump through the valve and porting and into the motor:

$$P_{pd} = P_{ms} + P_\ell \tag{4}$$

It was assumed that for the maximum flow condition, which occurs when the pump wobbler is eccentric 0.35 in., the pressure loss (P_ℓ) is about 10 percent of the maximum required motor supply pressure.

For turbulent flow, the pressure loss is proportional to the square of the flow. Therefore, at pump-wobbler eccentricities and resulting pump flow near zero, the pressure loss was considered negligible. Applying this assumption to Equation 4 yields

$$P_{pd} = P_{ms} \qquad \text{(eccentricity = 0)} \tag{5}$$

$$P_{pd} = P_{ms} + 300 \qquad \text{(eccentricity = 0.35)} \tag{6}$$

It is apparent that there are an infinite number of operating modes as determined by output power demand and speed differential. The proposed hydrostatic bearing can be adequately analyzed by considering the following four representative modes of pump operation:

- Low Flow/High Pressure
- Low Flow/Low Pressure
- High Flow/High Pressure
- High Flow/Low Pressure

The two circled points on Figure 4—1 indicate the conditions of high and low flow. The desired four modes of pump operation are determined by superimposing conditions of high and low power demand on these points and using the hydraulic pressure relationships given in Equations 1 through 6. The resulting critical operating conditions are summarized in Table 4—2. Oil inlet pressure was established at 240 psig for the analysis. This is the lowest possible inlet pressure, and it was selected to create the maximum pressure differential across the pump. It represents a worst-case condition.

Table 4—2. **HYDRAULIC-PUMP CRITICAL OPERATING CONDITIONS**

Operating Condition	Input Speed (rpm)	Wobbler Eccentricity (Inches)	Inlet Pressure (psig)	Discharge Pressure (psig)
A (Low flow, high pressure)	7980	0.009	240	2980
B (Low flow, low pressure)	7980	0.009	240	1675
C (High flow, high pressure)	4475	0.35	240	3280
D (High flow, low pressure)	4475	0.35	240	1975

4.2 RADIAL-LOAD ANALYSIS

A radial-load analysis was performed on both the piston-pad assembly and the pump race. The loads on the piston-pad assembly are inertial, frictional, and pressure-induced loads. Resultant loads on the race are essentially the vector sum of the loads imposed by the piston-pad assemblies.

For this analysis, several simplifying assumptions were made:

- Piston side-wall friction is zero.
- Cylinder-block angular acceleration is zero.
- There is instantaneous transition from inlet to discharge pressure.
- The reactive force of the ring against the pad acts along the piston center line.

4.2.1 Piston-Pad Assembly

Figure 4—3 illustrates a single piston-pad assembly traversing a complete revolution about the cylinder-block axis of rotation. The dashed arrows indicate the inertia-force vectors. The total radial reactive load was calculated (in accordance with the assumptions given above) from the following equation:

$$F_t = PA_p + \frac{W}{g}\left[r\left(\frac{d\theta}{dt}\right)^2 - \frac{d^2r}{dt^2}\right] \qquad (7)$$

where

$P = P_1 \quad (0^\circ < \theta \leqslant 180^\circ)$

$P = P_2 \quad (180^\circ < \theta \leqslant 360^\circ)$

P_1 = Inlet pressure - case pressure = 240 psid

P_2 = Discharge pressure - case pressure (psid) (See Table 4—2)

A_p = Total piston area of two pistons = 0.82 sq in

W = Piston-pad assembly weight = 0.263 lb

g = Gravitational acceleration = 386 in/sec/sec

$\frac{d\theta}{dt}$ = Cylinder-block rotational speed (radians/sec) = $\left(\frac{\pi}{30}\right)$ N

$\frac{d^2r}{dt^2}$ = Radial acceleration (in/sec/sec) (See Appendix A)

N = Input speed (rpm) (See Table 4—2)

r = Distance from cylinder-block axis of rotation to piston/pad assembly center of gravity

Values for cylinder-block speed, discharge pressure, and wobbler eccentricity were taken from the four critical operating conditions described above. The resulting plots of total radial piston force versus angle of rotation are shown in Figures 4—4 through 4—7. These curves indicate not only the total load but the component loads as well.

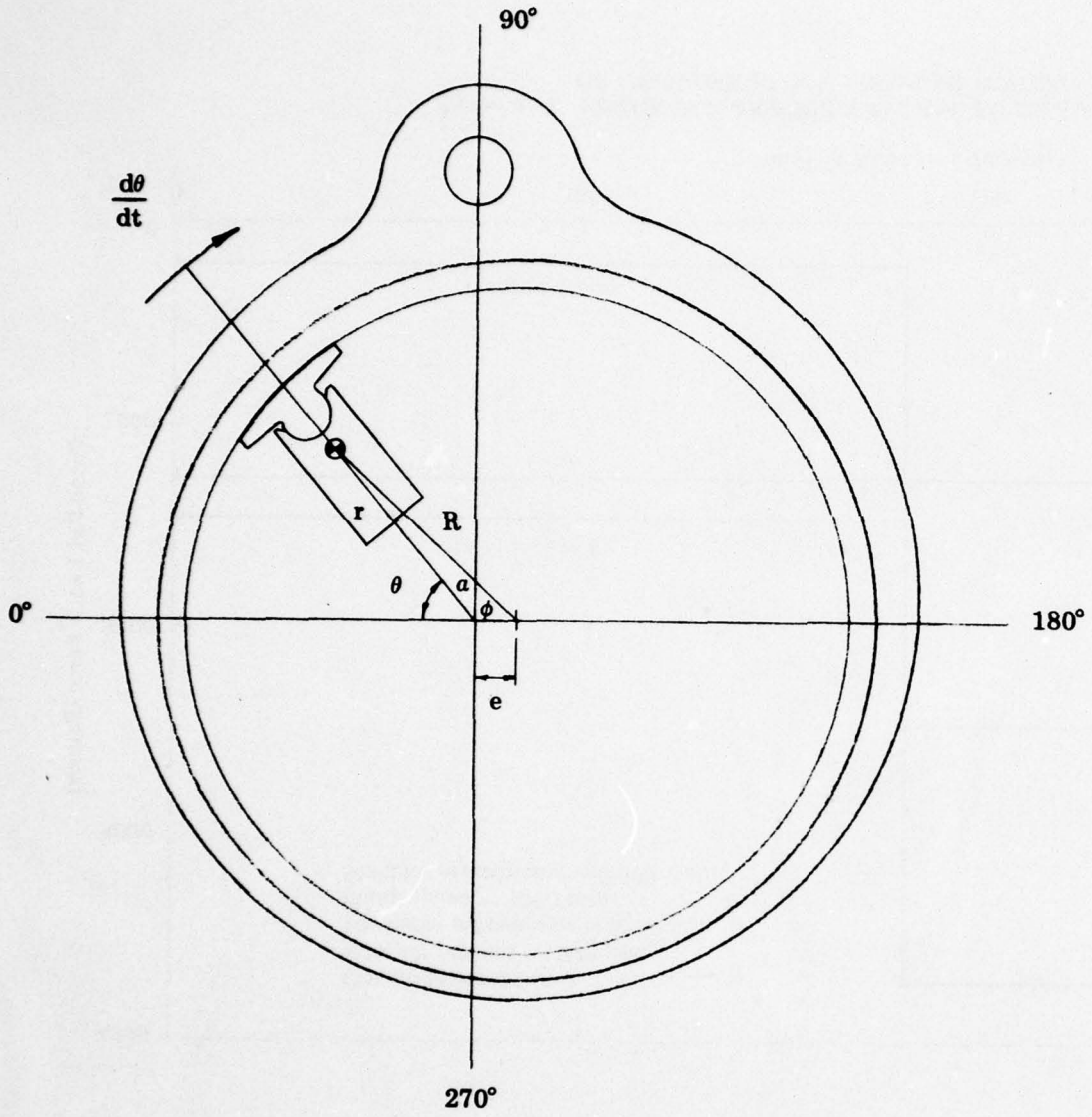

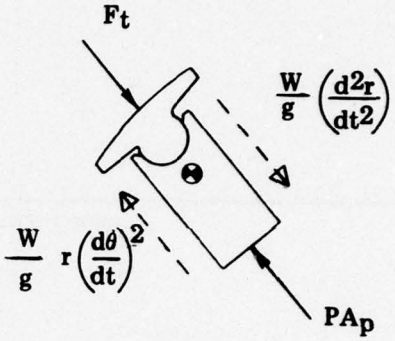

Figure 4—3. **SINGLE PISTON—PAD ASSEMBLY**

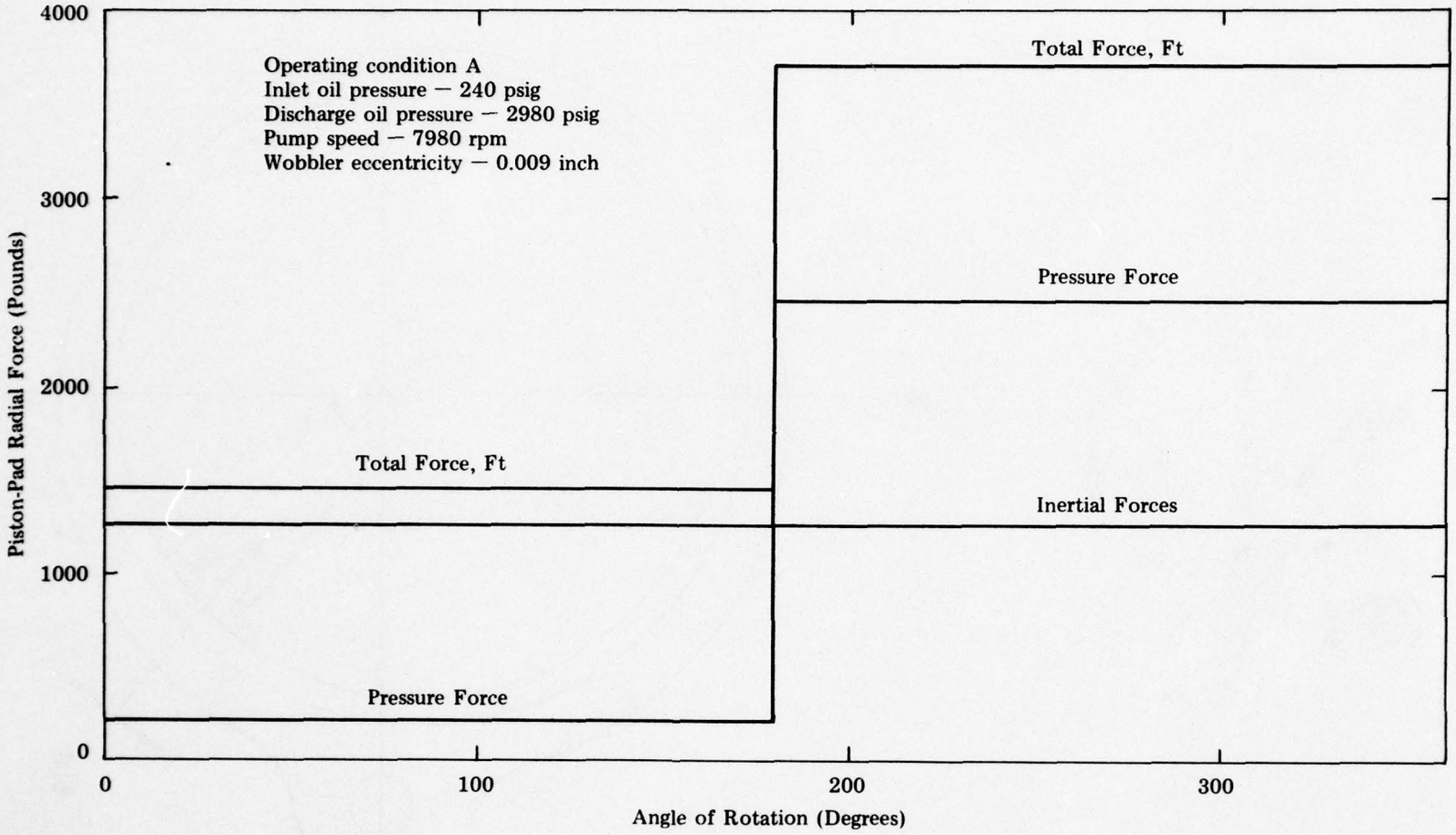

Figure 4—4. **PISTON-PAD ASSEMBLY RADIAL FORCES AS A FUNCTION OF CYLINDER-BLOCK ANGULAR POSITION**

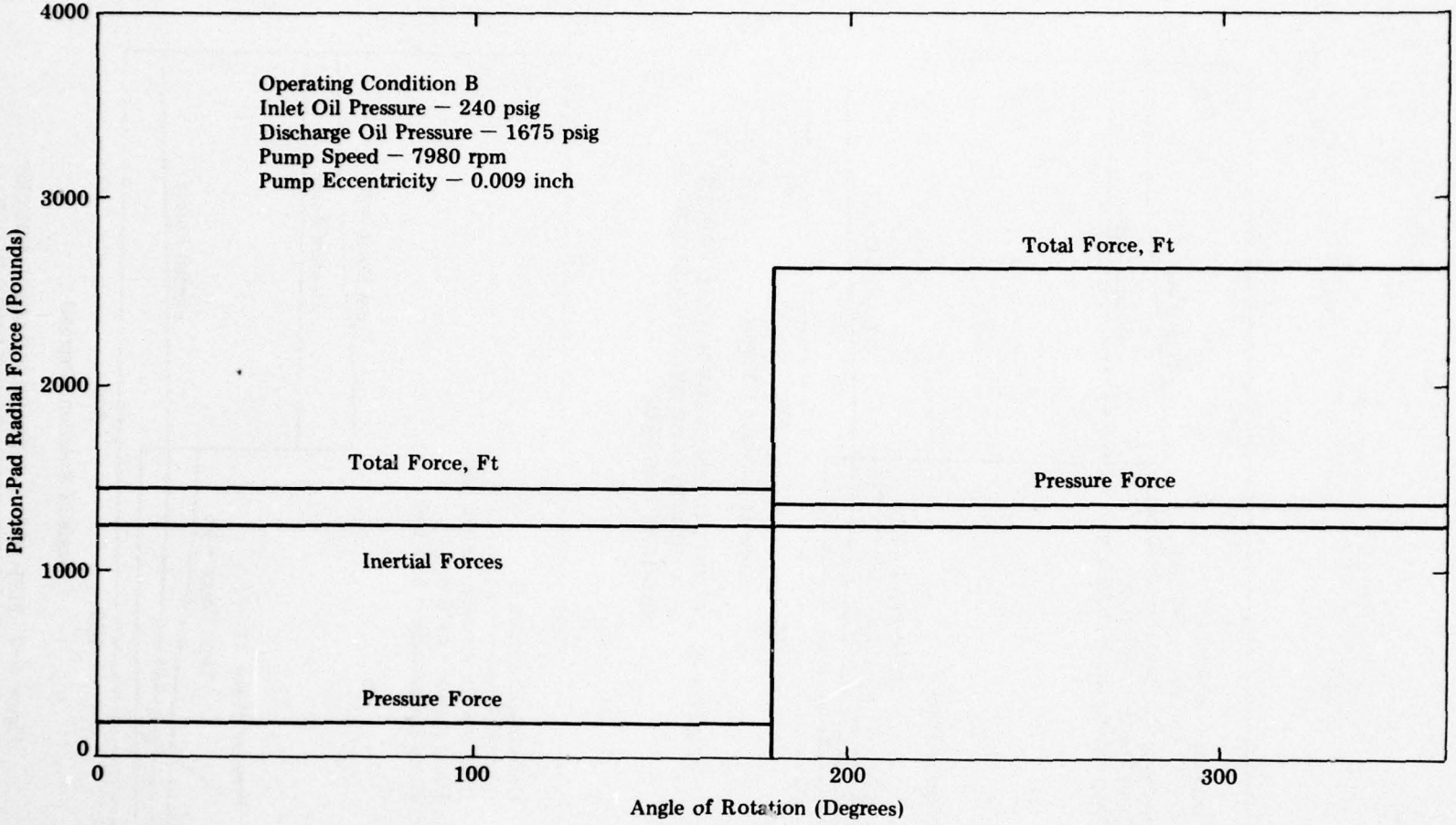

Figure 4—5. **PISTON-PAD ASSEMBLY RADIAL FORCES AS A FUNCTION OF CYLINDER-BLOCK ANGULAR POSITION**

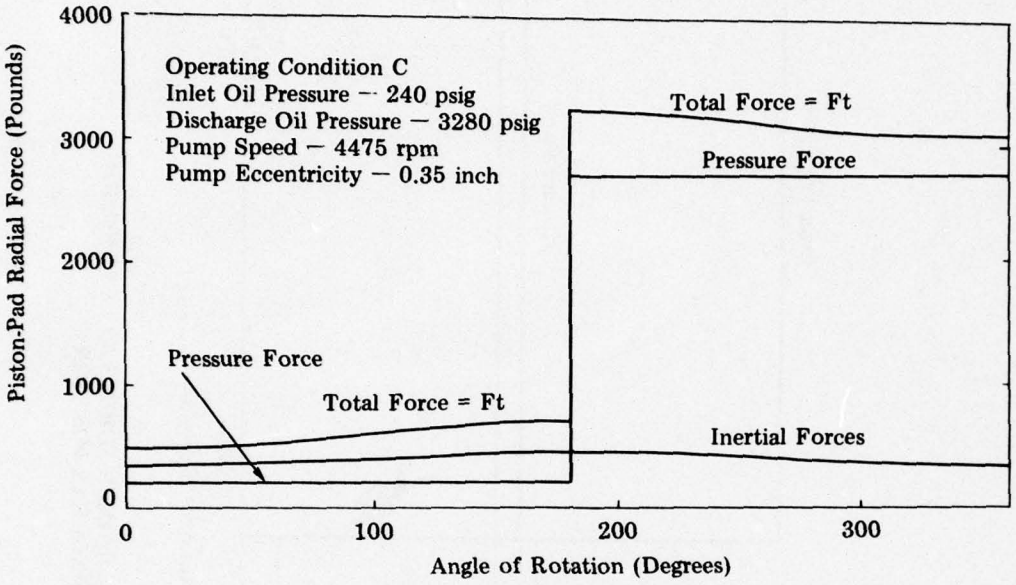

Figure 4—6. **PISTON-PAD ASSEMBLY RADIAL FORCES AS A FUNCTION OF CYLINDER-BLOCK ANGULAR POSITION**

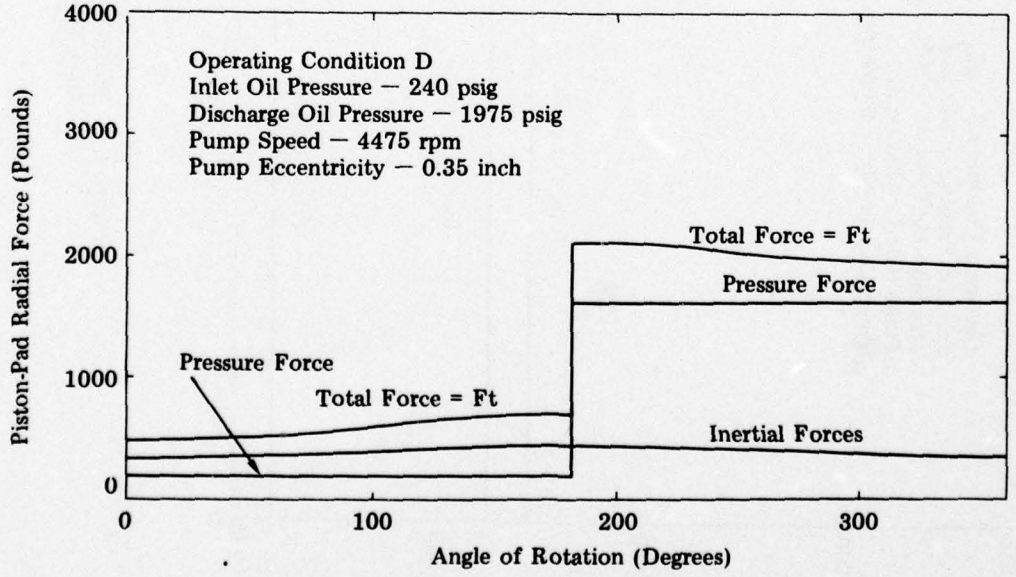

Figure 4—7. **PISTON-PAD ASSEMBLY RADIAL FORCES AS A FUNCTION OF CYLINDER-BLOCK ANGULAR POSITION**

Only radial loads were considered in this analysis. Quantification of radial loads is necessary for the design of the hydrostatic-bearing system that will support these loads. Piston side loads, however, are not expected to be any more severe than in the present roller-bearing configuration and therefore will not affect the feasibility of the hydrostatic-bearing modification.

4.2.2 Pump Race

As stated previously, the radial load acting on the pump race is the vector sum of the total radial loads of all nine piston-pad assemblies. In Figure 4—8, F_{rl}, F_{r2}, etc., represent the total radial piston force of pistons 1, 2, etc., respectively. $\theta 1$ is the angle of rotational displacement of the first piston-pad assembly from the zero position. It is apparent that the resultant ring load is periodic and will repeat itself each 40° of cylinder-block rotation (360° ÷ 9 pistons).

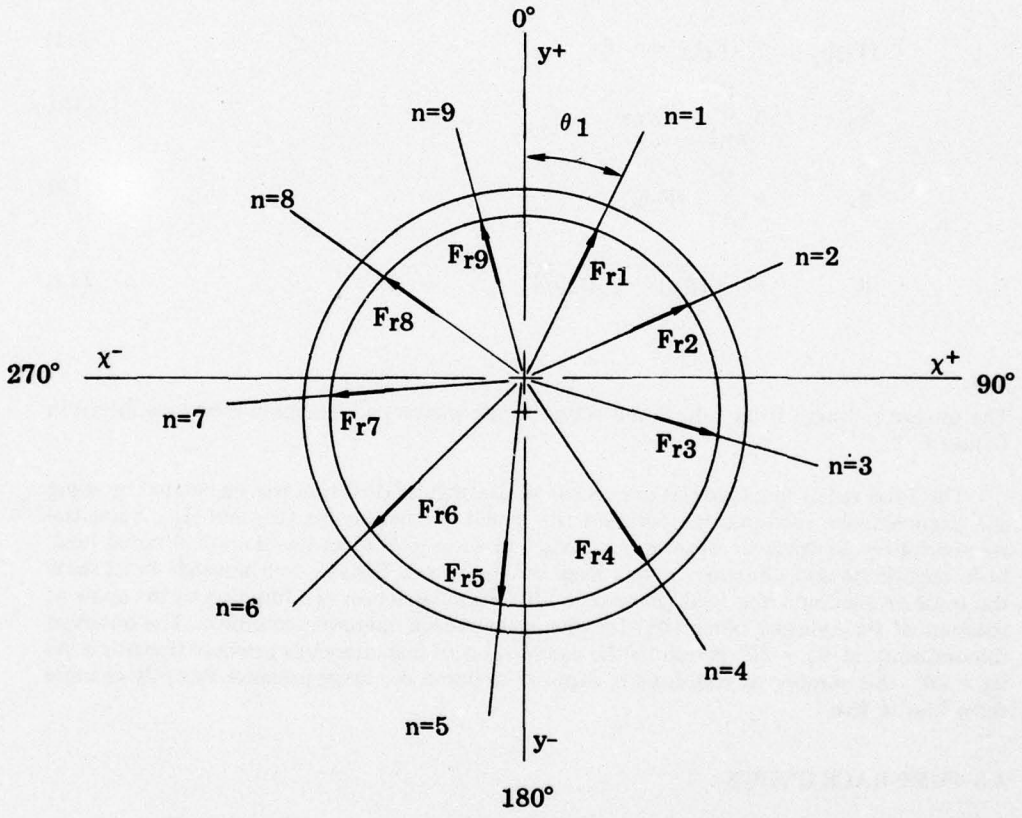

Figure 4—8. **RING RADIAL LOADING**

The total radial ring load was calculated from the following equations:

$$(F_r)_n = F_t = PA_p + \frac{W}{g}\left[r\left(\frac{d\theta}{dt}\right)^2 - \frac{d^2r}{dt^2}\right]\Bigg|_{\theta = \theta_n} \quad (8)$$

$$\theta_n = \theta_1 + (n - 1)\ 40^\circ \quad (9)$$

$$(F_r)_{nx} = (F_r)_n \sin\theta_n \quad (10)$$

$$(F_r)_{ny} = (F_r)_n \cos\theta_n \quad (11)$$

$$R_x = \sum_{n=1}^{9} (F_r)_{nx} \quad (12)$$

$$R_y = \sum_{n=1}^{9} (F_r)_{ny} \quad (13)$$

$$R = \sqrt{(R_x)^2 + (R_y)^2} \quad (14)$$

The integer n ranges from 1 to 9 and serves as the piston-pad assembly index, as shown in Figure 4—8.

The total radial ring load (R) is a vector whose angular direction was calculated by using the trigonemetric relationships between the x and y components (R_x and R_y). Since the race-periphery hydrostatic bearing must react to the resultant outward-applied radial load, both magnitude and direction of this load are important. Figures 4—9 through 4—12 show the total or resultant ring load (R) and the direction of action as a function of the angle of rotation of the cylinder block (0_1) for one cycle at each operating condition. The observed discontinuity at $0_1 = 20^\circ$ is due to the assumption of instantaneous pressure transition. At $0_1 = 20^\circ$, the number of piston pairs exposed to pump discharge pressure abruptly changes from four to five.

4.3 PUMP-RACE DESIGN

The pump race is the key to the uniqueness of the proposed modification. To produce a satisfactory prototype design, it was necessary to consider such fundamental aspects as material, strength, and installation. In addition, Franklin Institute Research Laboratory, under subcontract as consultants, originated a computer program to aid in selecting critical hydrostatic-bearing dimensions. The final ring design emerged as a compromise selection after all pertinent facts and design parameters were considered.

4.3.1 Basic Considerations

As indicated in Figures 4—9 through 4—12, the resultant ring load varies with time in both magnitude and direction. For this reason it was desirable to make the ring as massive as

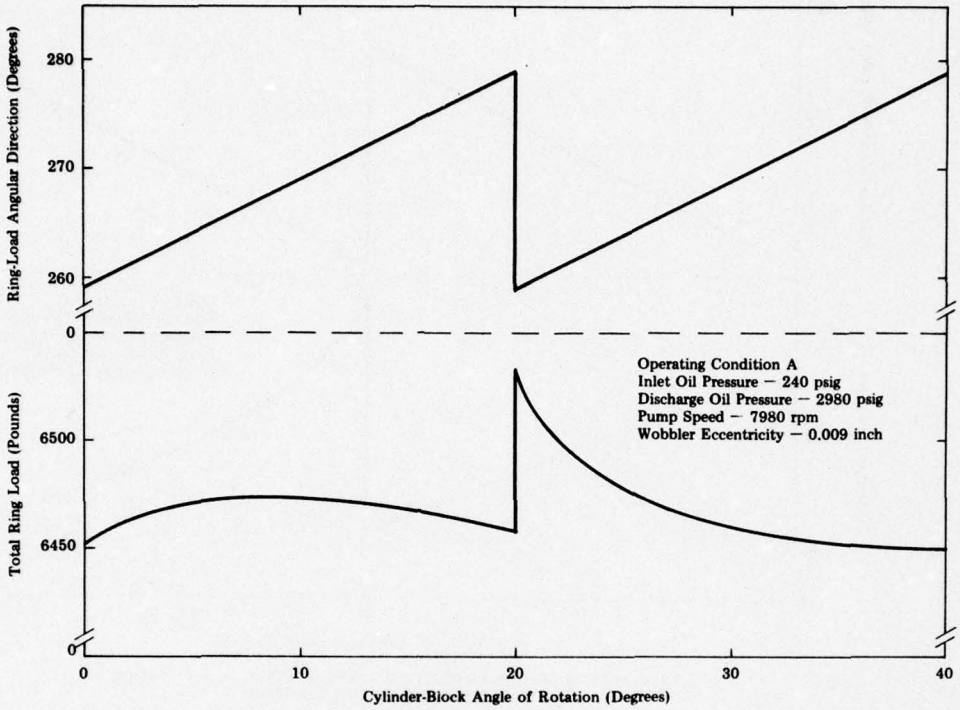

Figure 4—9. **RING-LOAD MAGNITUDE AND DIRECTION AS A FUNCTION OF CYLINDER-BLOCK ANGULAR POSITION (OPERATING CONDITION A)**

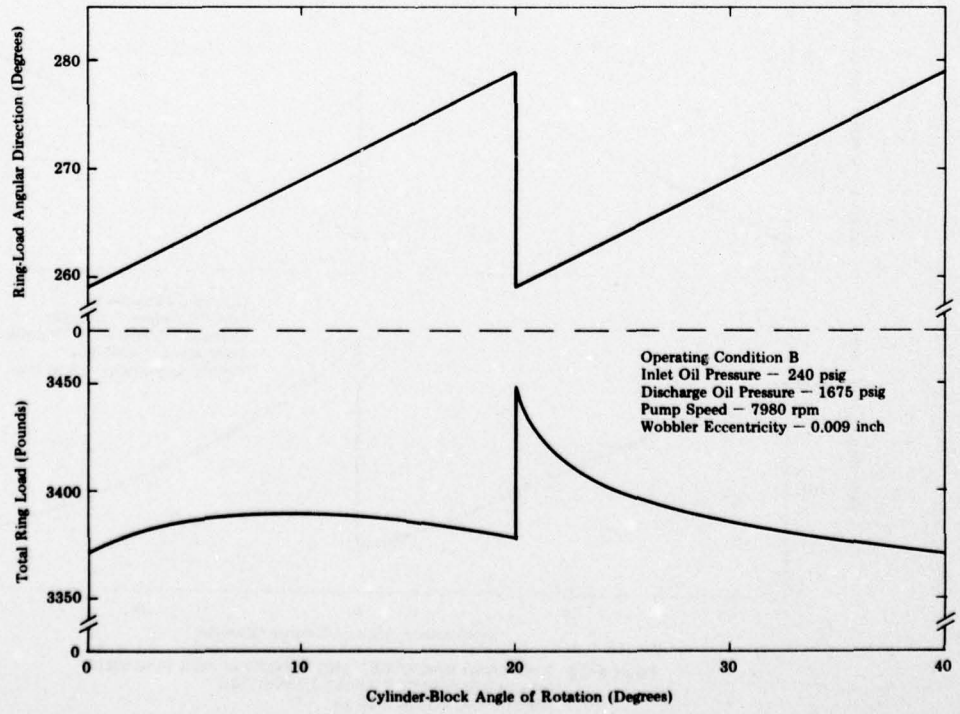

Figure 4—10. **RING-LOAD MAGNITUDE AND DIRECTION AS A FUNCTION OF CYLINDER-BLOCK ANGULAR POSITION (OPERATING CONDITION B)**

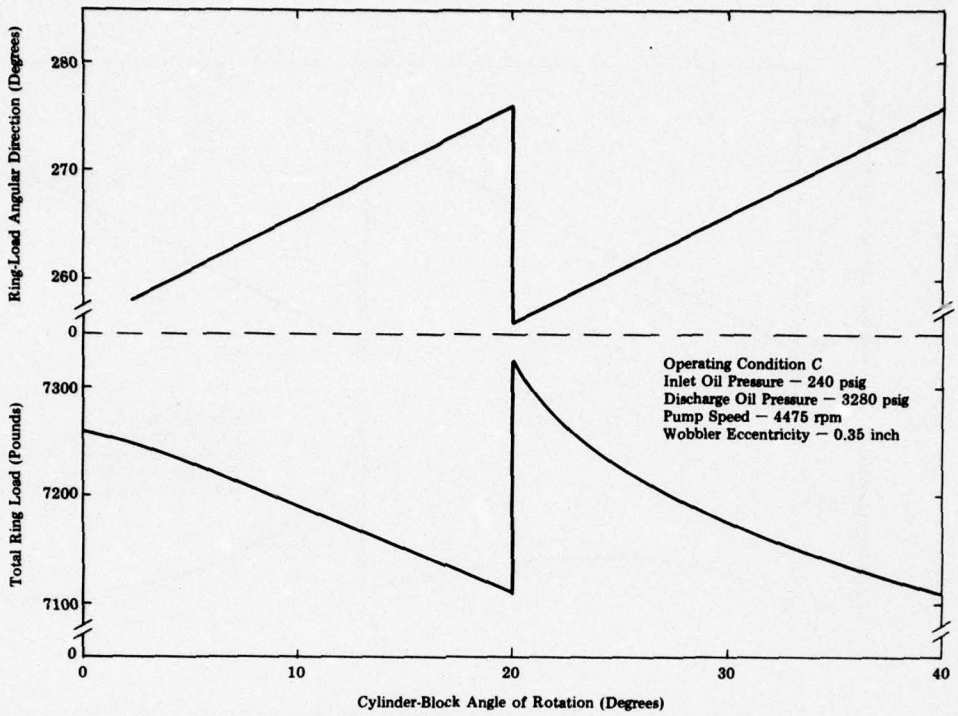

Figure 4—11. **RING-LOAD MAGNITUDE AND DIRECTION AS A FUNCTION OF CYLINDER-BLOCK ANGULAR POSITION (OPERATING CONDITION C)**

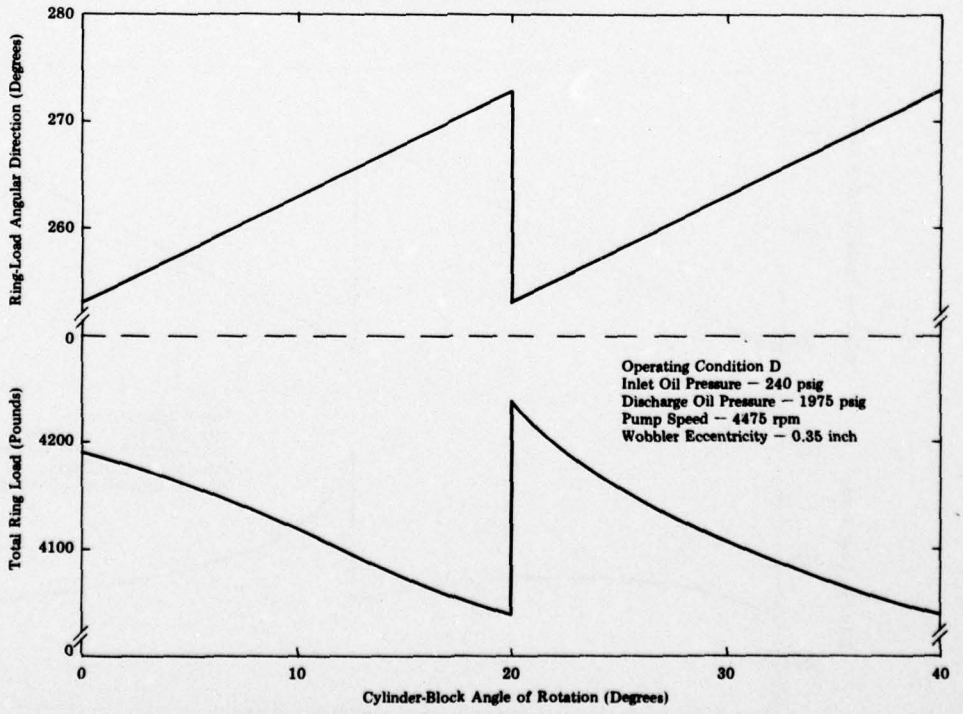

Figure 4—12. **RING-LOAD MAGNITUDE AND DIRECTION AS A FUNCTION OF CYLINDER-BLOCK ANGULAR POSITION (OPERATING CONDITION D)**

possible to provide inertial resistance against the forced vibration. AISI-E-52100 bearing steel hardened to 60 R_C was selected for the race. It was believed that a porous bearing material such as cast iron was not needed, since the pads that slide on the race I.D. would be bronze and the hydrostatic bearing at the race O.D. would preclude metal-to-metal rubbing contact with the wobbler I.D. On the other hand, steel, with its higher allowable stress levels and modulus of elasticity, would be more resistant to deflection, a quality important to satisfactory hydrostatic-bearing operation. A stress analysis was not considered necessary at this time since the hydrostatic race is made of the same material and is subjected to essentially the same loads but has a larger cross section than the roller-bearing race. In addition, the load balance between the outward radial loads of the pistons and the inward radial pressure of the hydrostatic oil film tends to eliminate the race hoop stress.

4.3.2 FIRL Computer Program

In selecting the hydrostatic-bearing critical dimensions such as recess size and shape, radial clearance between race O.D. and wobbler I.D., and restrictor type and size, it was necessary to consider various bearing-performance parameters quantitatively. These included running eccentricity, leakage, and viscous friction. It was for these particular quantifications that Franklin Institute was consulted. A flow chart of the Franklin Institute program is presented in Appendix B. Basically, this program was based on the following simplifying assumptions:

- Operation is at steady state, making all transient dynamic effects zero.
- The bearing is pure hydrostatic, with no hydrodynamic assist.
- The pressure drop from recess to periphery across the sill is linear.
- Under all flow conditions, full supply pressure is available at the restrictor.
- The restrictor is an ideal orifice.
- Pressure transition from inlet to discharge is instantaneous.

Program input data are as follows:

- Number of recesses
- Race O.D.
- Race axial length
- Recess effective width
- Recess effective length
- Load coefficient
- Flow coefficient
- Pump discharge pressure minus case pressure
- Pump inlet pressure minus case pressure
- Oil absolute viscosity
- Ring rotational speed
- Angle defining direction of applied load (Figures 4—9 through 4—12)
- Orifice diameter
- Radial clearance

The program now calculates the fluid-film radial-load-carrying ability, leakage, temperature rise due to viscous friction, and viscous frictional horsepower as a function of race eccentricity within the wobbler. These calculations are for eccentricities of +80 percent to -80 percent of the input programmed radial clearance in the direction of the applied load. The engineer using the program must compare the actual applied load (Figures 4—9 through 4—12) with the range of calculated load capacities to determine, for a load-balanced condition, the running eccentricity, leakage, and other critical parameters. The objective is for the race to run with perfect concentricity within the wobbler, with minimum leakage and friction under all operating conditions and for all fluid temperatures. Of course, this is an impossibility; thus a design compromise must be made.

4.3.3 Compromise-Design Selection

The quantitative effects of orifice diameter, radial clearance, ring position relative to cylinder block, fluid temperature, and operating condition on the critical parameters leakage and eccentricity at a balanced load condition were established by numerous computer runs. Some of the results are plotted in Figures 4—13 through 4—18.

Figure 4—13 shows the flow through all the race recesses as a function of race-to-wobbler radial clearance and orifice diameter for a fixed inlet oil temperature.

Figure 4—14 indicates the total bearing flow as a function of radial clearance and inlet oil temperature for a fixed orifice diameter.

The bearing flow is directly affected by the race-to-wobbler eccentricity, which is self-adjusting and is established when the load-carrying capacity of the fluid film at the race periphery exactly equals the resultant applied load as shown in Figure 4—9. These steady-state running eccentricities at load equilibrium are plotted in Figure 4—15 as a function of radial clearance and inlet oil temperature for a fixed orifice diameter.

The race-to-wobbler eccentricity can never physically exceed the radial clearance. If active and reactive load equilibrium cannot be established at an eccentricity less than the radial clearance, metal-to-metal contact will occur at the race periphery. Such a condition is indicated by the shaded portion of Figure 4—15. This figure shows, for example, that with an orifice diameter of 0.025″ and a radial clearance of 0.003″, metal-to-metal contact would not occur at any anticipated inlet oil temperature.

The race is a free-floating member and can assume any angular position with respect to the cylinder block. The position assumed determines the location of the orifices with respect to the pad recesses and, consequently, which ring recesses are pressurized and which are open. Figure 4—16 shows that the total bearing flow is not significantly affected by the angular position of the race. The angular location of the first pressurized recess serves merely as a convenient index of race position.

Figures 4—13 through 4—16 were all constructed for operating condition A. Figures 4—17 and 4—18 illustrate the comparative effect of the other three critical operating conditions (B, C, and D) on total bearing flow and race-to-wobbler eccentricity. Both figures illustrate, for two different inlet oil temperatures, that neither parameter is appreciably affected by a change in operating condition.

The power required to overcome viscous friction and the oil temperature rise due to this friction vary inversely with the ambient oil temperature. Thus the hotter the ambient oil temperature, the less the viscous friction and the smaller the additional temperature rise.

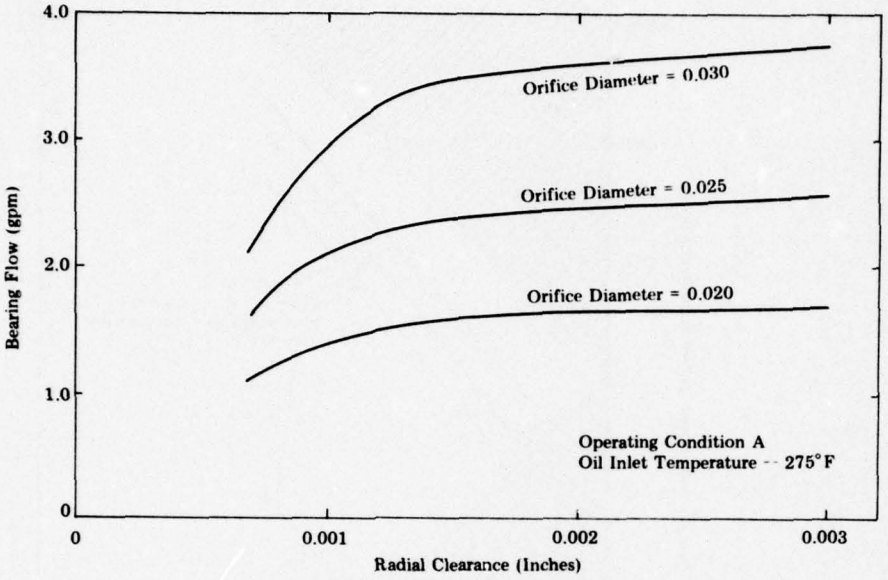

Figure 4–13. **TOTAL BEARING FLOW AT LOAD BALANCE AS A FUNCTION OF RACE-TO-WOBBLER RADIAL CLEARANCE FOR SEVERAL ORIFICE DIAMETERS**

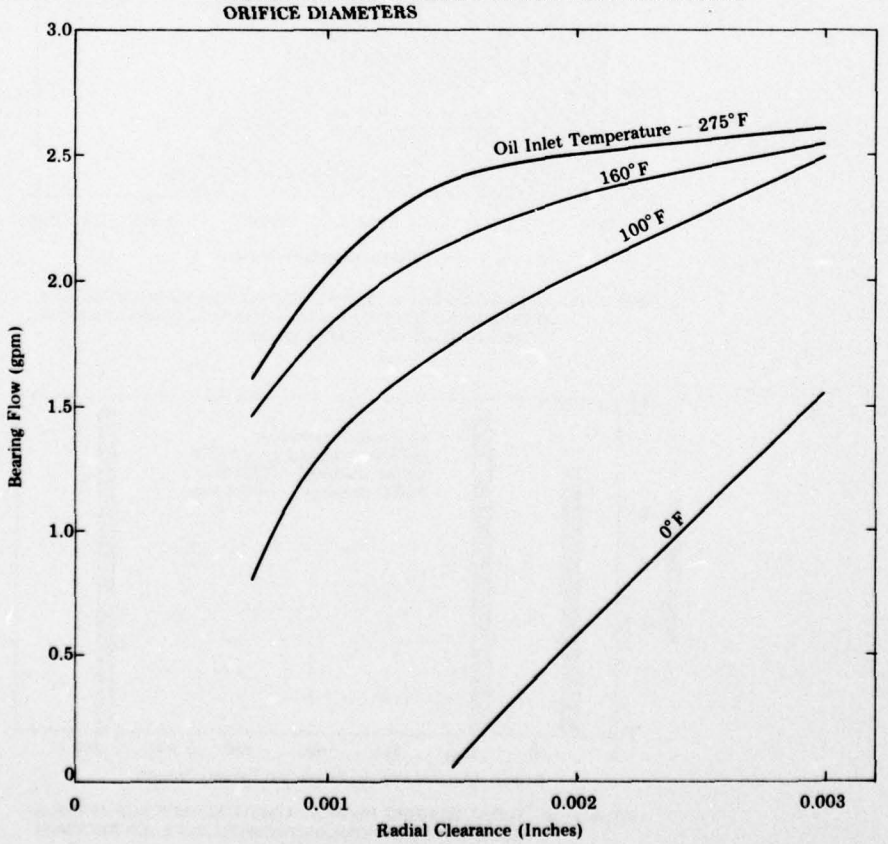

Figure 4–14. **TOTAL BEARING FLOW AT LOAD BALANCE AS A FUNCTION OF RACE-TO-WOBBLER RADIAL CLEARANCE FOR SEVERAL OIL INLET TEMPERATURES**

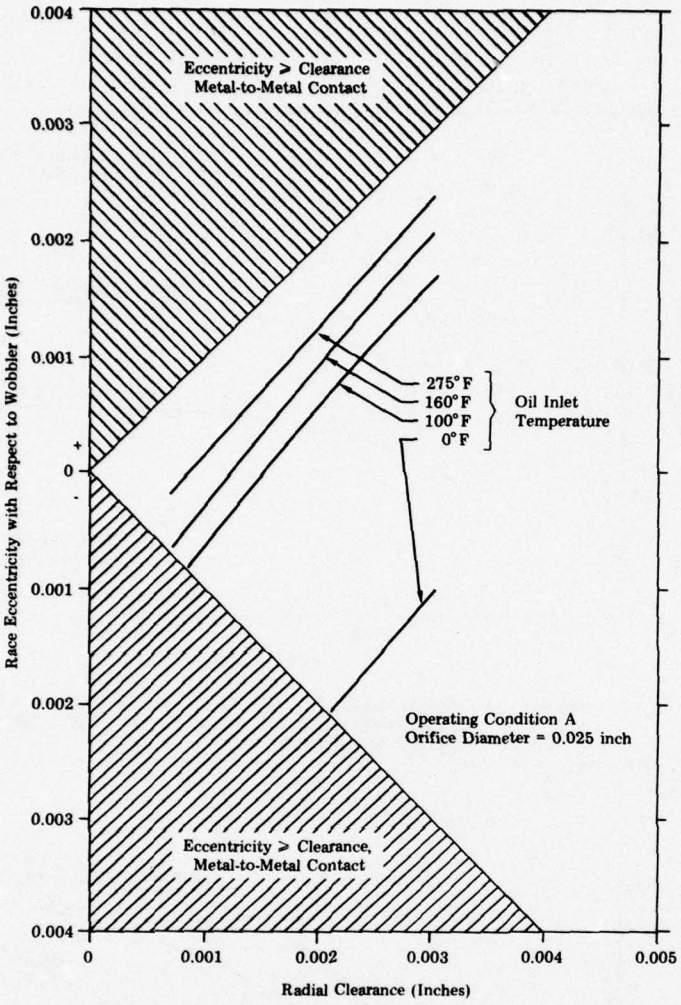

Figure 4—15. **RACE-TO-WOBBLER ECCENTRICITY AT LOAD BALANCE AS A FUNCTION OF RACE-TO-WOBBLER RADIAL CLEARANCE FOR SEVERAL OIL INLET TEMPERATURES**

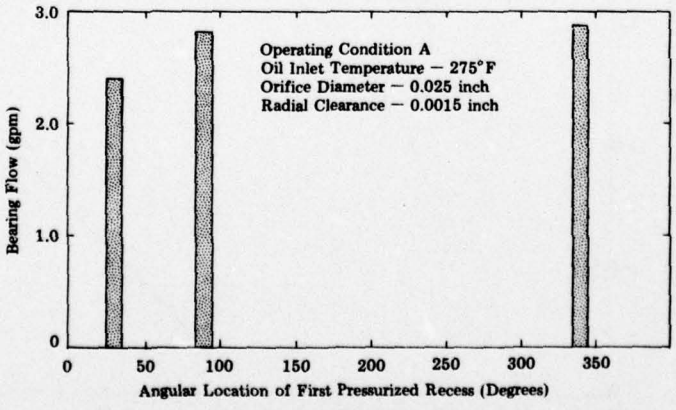

Figure 4—16. **TOTAL BEARING FLOW AT LOAD BALANCE FOR SEVERAL ANGULAR LOCATIONS OF PRESSURIZED RACE RECESSES**

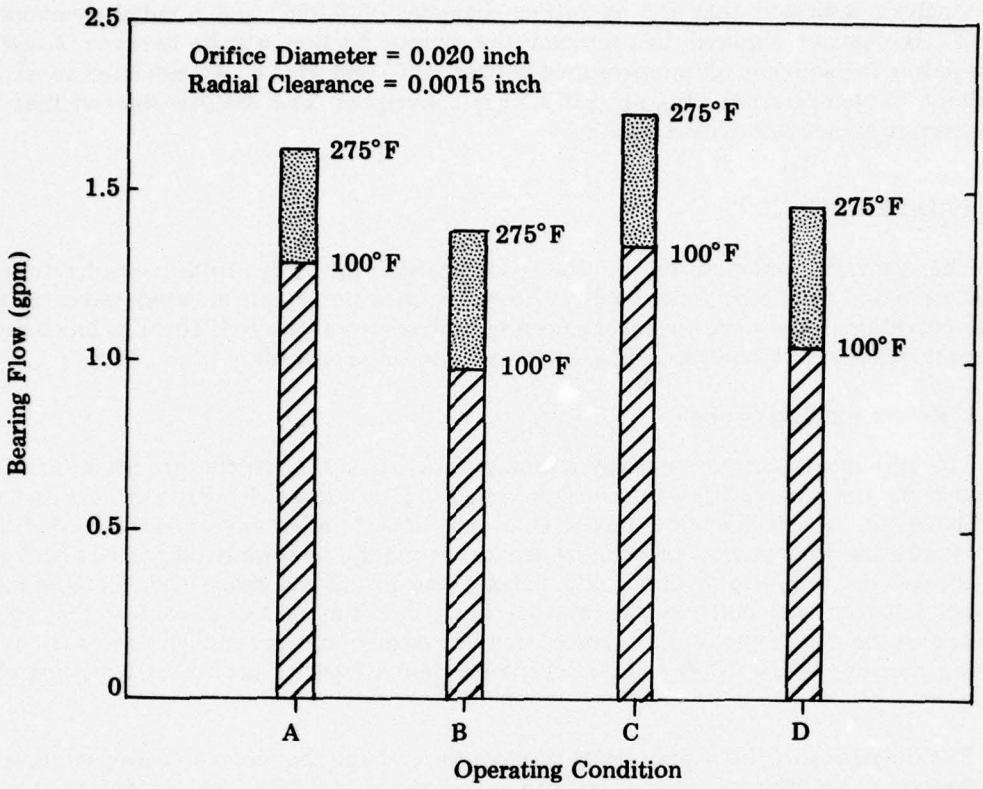

Figure 4—17. **TOTAL BEARING FLOW AT LOAD BALANCE FOR CRITICAL OPERATING CONDITIONS AT TWO DIFFERENT OIL INLET TEMPERATURES**

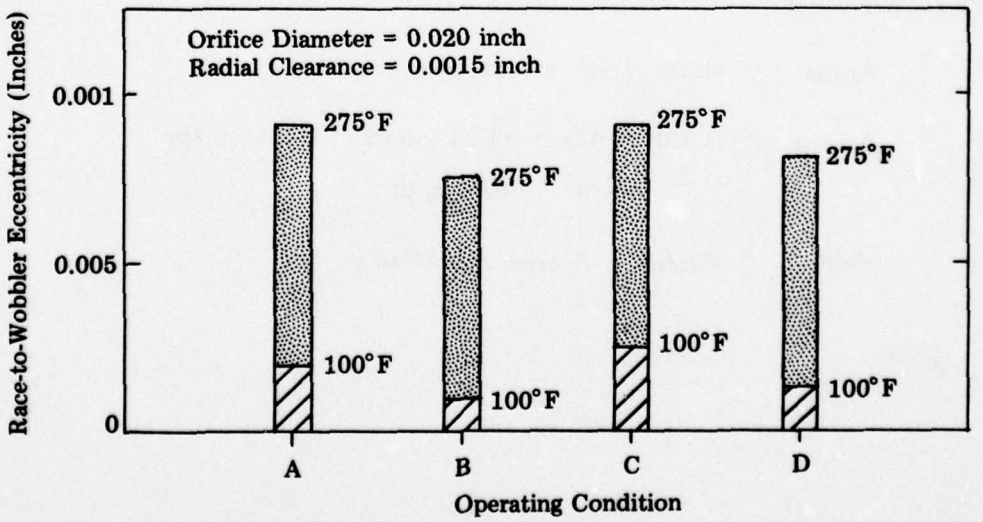

Figure 4—18. **RACE-TO-WOBBLER ECCENTRICITY AT LOAD BALANCE FOR CRITICAL OPERATING CONDITIONS AT TWO DIFFERENT OIL INLET TEMPERATURES**

The analysis indicated that for an orifice diameter of 0.025″ and a radial clearance of 0.003″, the power required to overcome the viscous friction will be between 3 and 13 horsepower for ambient oil temperatures between 275 and 100°F. As indicated above, the resultant oil temperature ($T_{ambient} + \Delta T$) is convergent. The analysis showed that this temperature should not exceed 325°F.

4.4 PAD DESIGN

The general configuration of the pad evolved primarily from consideration of installation and geometric functionality. However, once the layout drawings indicated that these conditions were met, several engineering analyses were required. These included recess and port sizing, sill PV analysis, and a critical-section stress analysis.

4.4.1 Recess and Port Sizing

The pad recess serves essentially a dual purpose. It is the vehicle through which oil is supplied to the ring restrictors. Thus its length (ℓ in Figure 4—19) is critical and was calculated to ensure that the recess is at all times, under any operating condition, communicating with at least one ring restrictor. Secondly, the supply oil pressure acting on the recess area tends to hydraulically balance the piston-pad radial load. Metal-to-metal contact between pad and race is essential since it is this frictional contact that causes rotation of the race. Therefore, the recess area was made only large enough to reduce the sill bearing pressure below 1300 psi, an acceptable design level for bronze on hardened alloy steel.

The diameters of the supply ports through the pad and the recess area perpendicular to the direction of oil flow were made large to minimize pressure losses and restrictor approach velocity. Flow cross-sectional area was made approximately equal to that of a round hole with a diameter ten times the orifice diameter.

4.4.2 Sill PV Analysis

From Figure 4—20, which illustrates approximate pad-surface dimensions, the following values are calculated:

$$A_{total} = (1.40)(1.60) = 2.24 \text{ sq in}$$

$$A_{recess} = (1.15)(0.43) + (1.18 - 0.43 - 0.19)(0.19) + \frac{\pi}{4}(0.19)^2 = 0.64 \text{ sq in}$$

$$A_{sill} = A_{total} - A_{recess} = 1.60 \text{ sq in}$$

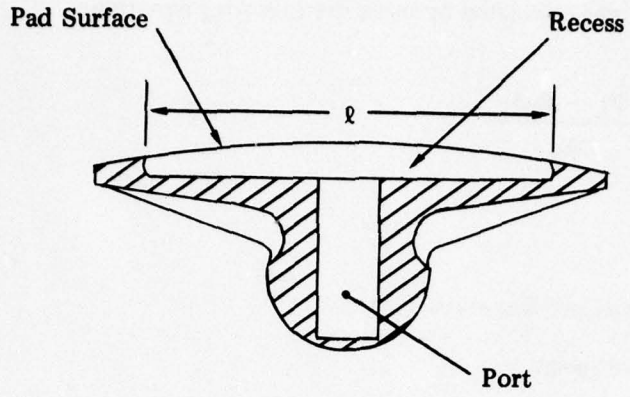

Figure 4—19. **BEARING PAD**

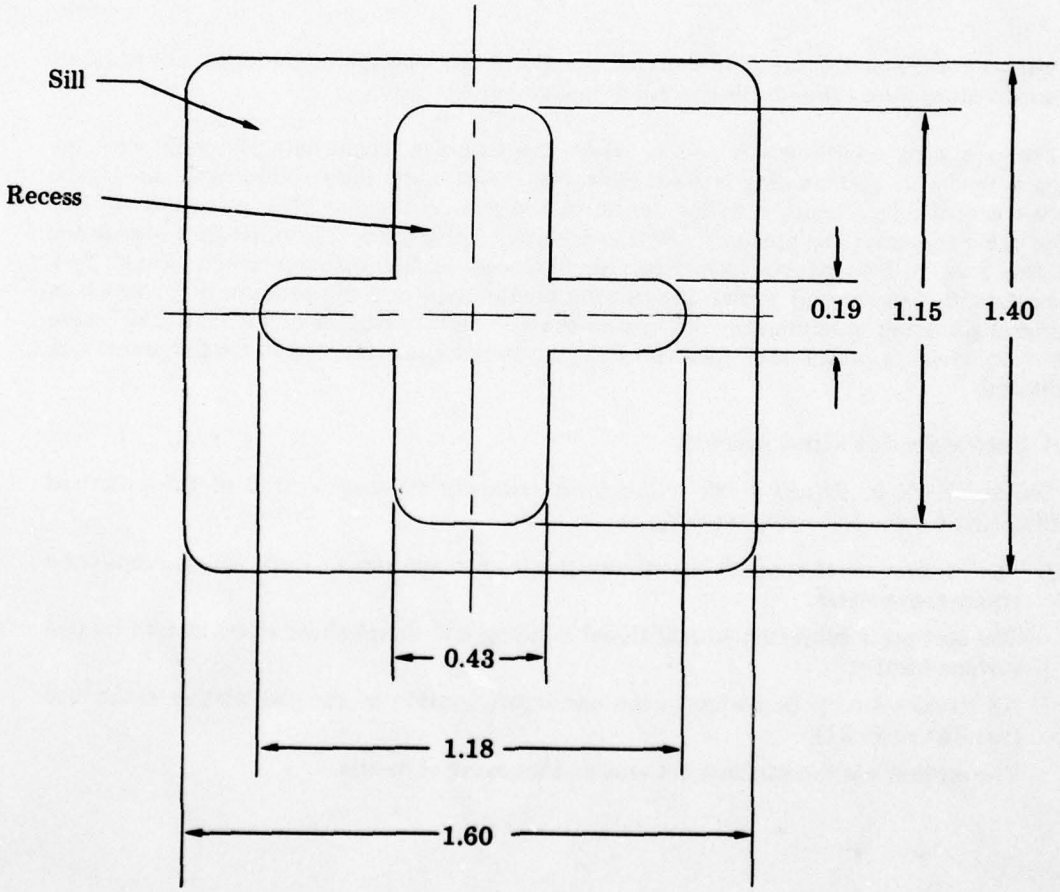

Figure 4—20. **PAD SURFACE**

The sill bearing pressure was calculated by using the following equation:

$$S_b = \frac{F_t - P_r A_r}{A_s} \tag{15}$$

where

F_t = Total radial load per Equation 7

P_r = Recess pressure (psig)

A_r = Recess area (sq in)

A_s = Sill area (sq in)

Values for F_t and P are functions of the particular operating condition and angle of rotation. Values were taken from Figures 4—4 through 4—7.

For operating conditions A and B, where the wobbler eccentricity is nearly zero, the sliding velocity of pad on ring is zero. However, under operating conditions C and D, the wobbler eccentricity creates a sliding action of the pad on the ring. The magnitude of this sliding velocity versus the angle of rotation is shown in Figure 4—21, in which it is assumed that the ring rotates at the same rotational speed as the cylinder block. Table 4—3 summarizes the above and shows the bearing pressure(s_b) and the product S_bV, which in bearing engineering is commonly known as the PV factor. Angles of 55° and 230° were chosen to yield approximately average PV factors for both inlet- and discharge-pressure conditions.

4.4.3 Critical-Section Stress Analysis

Section X—X in Figure 4—22 is the most critically stressed section of the proposed modification for the following reasons:

- The section must support essentially the total radial piston load, which produces a compressive stress.
- The section is subjected to additional bending and direct shear stress caused by pad surface friction.
- All stresses are cyclic owing to the oscillatory motion of the pad relative to the race (see Figure 4—21).
- The section has the smallest net area and moment of inertia.

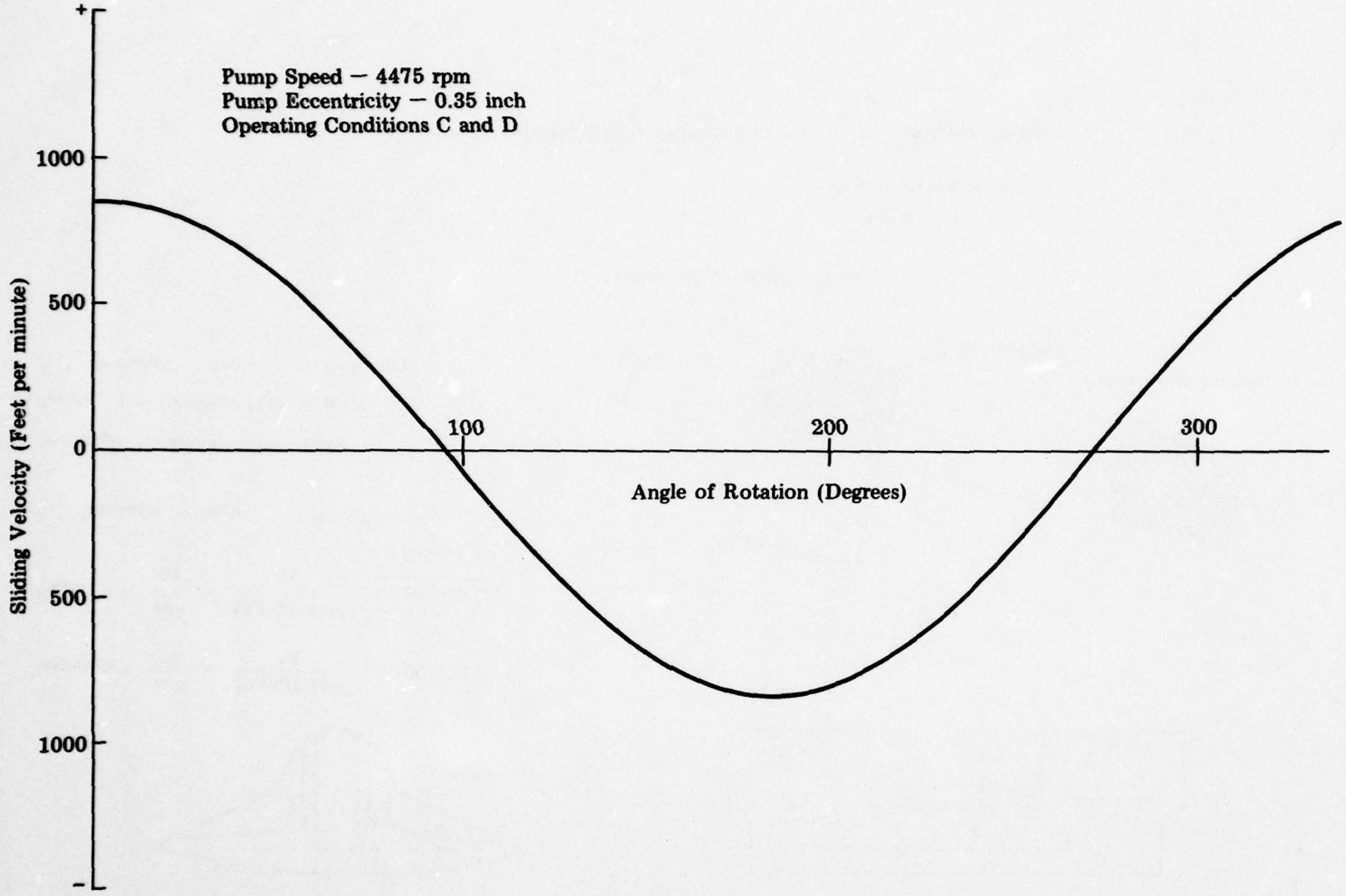

Figure 4—21. **SLIDING VELOCITY OF PAD ON RING VS. ANGLE OF ROTATION**

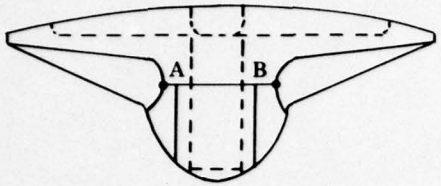

$$I_{rectangle} = \frac{bh^3}{12} = \frac{(0.48)(0.35)^3}{12} = 0.001715 \text{ in}^4$$

$$I_{circle} = \frac{\pi d^4}{64} = \frac{(3.14)(0.15)^4}{64} = \underline{0.000025 \text{ in}^4}$$

$$0.001690 \text{ in}^4$$

$$I = I_{rectangle} - I_{inch} \approx 0.0017 \text{ in}^4$$

$$A_{rectangle} = (0.48)(0.35) = 0.168$$

$$A_{circle} = (0.785)(0.15)^2 = 0.018$$

$$A = A_{rectangle} - A_{circle} = 0.150 \text{ sq in}$$

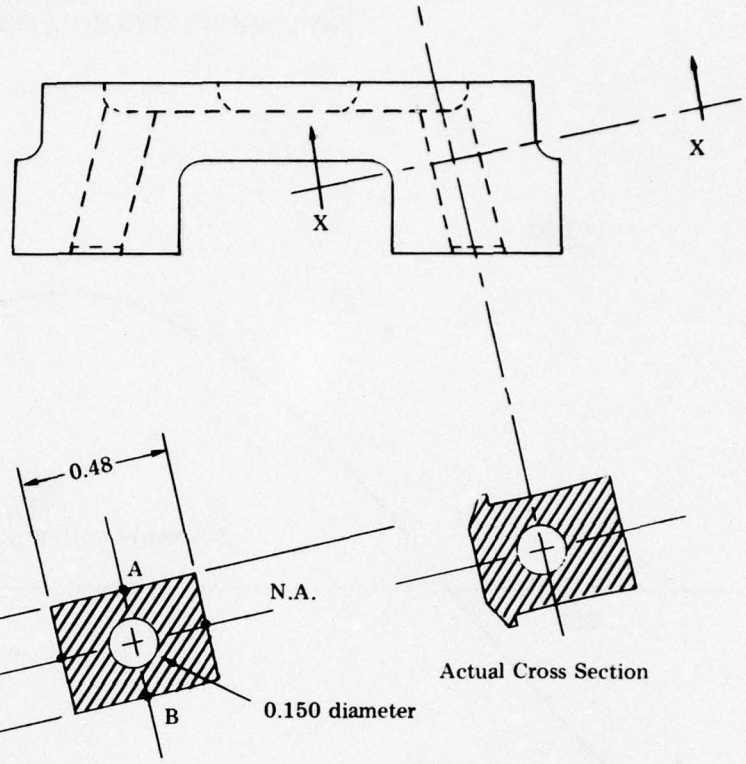

Section XX

Critical-Stress Section

Figure 4—22. **GEOMETRICAL PROPERTIES OF CRITICAL-STRESS SECTION**

Table 4—3. BEARING PARAMETERS FOR VARIOUS OPERATING CONDITIONS

Operating Condition	Degrees	P_r (psig)	F_t (pounds)	P_rA_r (pounds)	S_b (psi)	V (Feet per Minute)	S_bV (psi × Feet) per Minute)
A	55	240	1450	154	810	0	0
	230	2980	3700	1910	1120	0	0
B	55	240	1450	154	810	0	0
	230	1675	2640	1070	980	0	0
C	55	240	600	154	280	500	140,000
	230	3280	3100]	2100	620	500	310,000
D	55	240	600	154	280	500	140,000
	230	1975	2000	1260	460	500	230,000

- Actual stress levels are increased because of stress-concentration effects of the required side radii.
- The intrinsic strength characteristics of the material are the lowest of all part materials in the modified design.

The stress calculation is a worst-case analysis, in which all unfavorable aspects are maximized. Operating condition A was assumed since this yields the highest radial loads (Figure 4—4). The coefficient of friction decreases to a lower value as soon as the pad begins to slide. However, the higher value was used exclusively for this analysis. This coefficient was selected on the basis of dry operation when, actually, boundary lubrication is always available.

The analysis was simplified by assuming that the angle ψ (Figure 4—23a) due to the pad-surface curvature is zero. It should be noted that Figure 4-23a illustrates motion impending, with F_{py} created by discharge oil pressure. After the pad has traversed 180° rotation about the cylinder-block axis, F_{py} is then being caused by inlet oil pressure; the pad free-body diagram is shown in Figure 4—23b. Values for F_{py} were taken from Figure 4—4, and a friction coefficient $\mu = 0.52$ was obtained from Reference 3. The values used in the stress calculations are described as follows:

F_{py} = Radial load (Figure 4—4)

F_{px} = Load required to overcome friction

F_f = μF_r = Friction force between ring and pad

F_r = Reactive load of ring on pad perpendicular to pad surface and acting through the geometric center of the bearing-pressure distribution

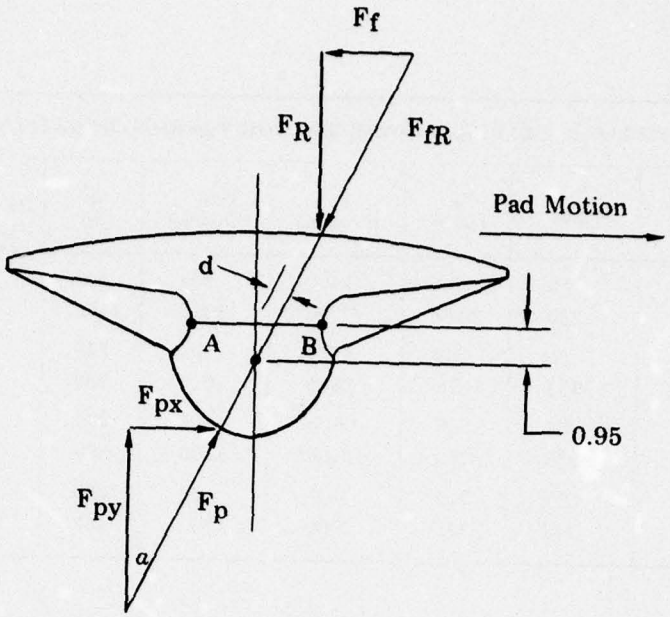

(a) Discharge Side

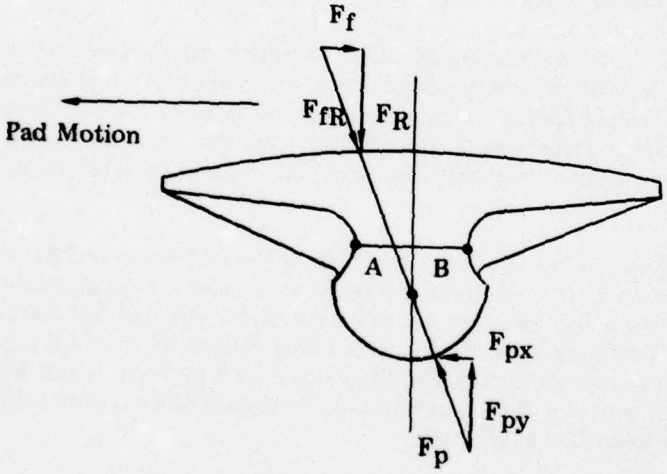

(b) Inlet Side

Figure 4—23. **PAD LOADING**

$F_{px} = F_f$
$F_r = F_{py}$ } surface curvature assumed zero

$F_p = \sqrt{(F_{py})^2 + (F_{px})^2}$

$a = \text{Tan}^{-1} \frac{F_{px}}{F_{py}} = \text{Tan}^{-1}\ \mu = \text{Tan}^{-1}\ 0.52 = 27^\circ\ 30'$

$d = 0.095\ \text{Sin}\ a = 0.044$ inch

$c = 0.175$ = distance from neutral axis to maximum-stressed fiber

$M = F_p d$ = bending moment

For the discharge side of the pump (Figure 4—23a) the following calculation is performed:

$F_{py} =$ 1850 pounds

$F_{px} =$ 960 pounds

$F_p =$ 2080 pounds

$M =$ 91.5 inch-pounds CCW

$(S_b)\text{Point A} = \frac{Mc_a}{I} = \frac{(91.5)\ (0.175)}{0.0017} =$ 9400-psi tensile

$(S_b)\text{Point B} = \frac{Mc_b}{I} = \frac{(91.5)\ (0.175)}{0.0017} =$ 9400-psi compression

$(S_c)\text{Points A and B} = \frac{F_{py}}{A} = \frac{1850}{0.15} =$ 12,300-psi compression

$(S_s)\text{Points A and B} = \frac{F_{px}}{A} = \frac{960}{0.15} =$ 6,400-psi shear

Total Normal Stress Point A = 12,300 - 9400

= 2900-psi compression

Total Normal Stress Point B = 12,300 + 9400

= 21,700-psi compression

Total Shear Stress Points A and B = 6,400 psi

For the inlet side of the pump (Figure 4—23b) the following calculation is performed:

F_{py} = 730 pounds

F_{px} = 380 pounds

F_p = 820 pounds

M = 36.1 in-lb CW

$$(S_b)\text{Point A} = \frac{Mc_a}{I} = \frac{(36.1)\,(.175)}{0.0017} = 3700\text{-psi compression}$$

$$(S_b)\text{Point B} = \frac{Mc_b}{I} = \frac{(36.1)(.175)}{0.0017} = 3700\text{-psi tensile}$$

$$(S_c)\text{Points A and B} = \frac{F_{py}}{A} = \frac{730}{0.15} = 4900\text{-psi compression}$$

$$(S_s)\text{Points A and B} = \frac{F_{px}}{A} = \frac{380}{0.15} = 2500\text{-psi shear}$$

From the preceding, it is evident that point B is the critical stress point. Using the maximum-shear-stress theory of failure for combined normal and shear stresses in conjunction with Soderberg fatigue criteria (Reference 2) results in the following equation for calculating the factor of safety (F.S.):

$$F.S. = \frac{S_{sy}}{\sqrt{¼\,[S_{av} + (S_y/S_e)\,K_f S_r]^2 + [S_{s,av} + (S_{sy}/S_{se})\,K_{fs} S_{s,r}]^2}} \qquad (16)$$

For point B, the following values are used:

$$S_{av} = \frac{21{,}700 + 1200}{2} = 11{,}450 \text{ psi}$$

$$S_r = \frac{21{,}700 - 1200}{2} = 10{,}250 \text{ psi}$$

$$S_{s,av} = \frac{6400 + (-2500)}{2} = 1950 \text{ psi}$$

$$S_{s,r} = \frac{6400 - (-2500)}{2} = 4450 \text{ psi}$$

S_{sy} = 23,500 psi
S_{se} = 16,000 psi
S_y = 44,000 psi
S_e = 30,000 psi

} Values taken from June 1958 *Alloy Digest* for AMPCO-15 material

K_f = 1.32
K_{fs} = 1.23

} *

Thus, the factor of safety for point B is as follows:

$$\text{F.S.} = \frac{23{,}500}{\sqrt{\tfrac{1}{4}[11{,}450 + 19{,}850]^2 + [1950 + 8040]^2}} = \frac{23{,}500}{18{,}600}$$

$$\text{F. S.} = 1.26$$

For this application, the calculated factor of safety is slightly low. However, consideration of the following aspects led to the conclusion that it was adequate for the prototype design:

- All factors contributing toward the low F.S. were maximized, some perhaps unrealistically.
- The types and magnitudes of applied loads were well defined.
- The material was considered reliable.
- Fatigue properties were taken for completely reversed stress cycles.

4.5 PISTON DESIGN

The modified piston is made of the same material (AISI-E-52100 steel 60 R_C) and is subjected to essentially the same loads as the roller-bearing-configuration piston. To obtain precise dimensions, therefore, it was necessary only to consider installation geometry. Length was calculated to yield engaged length and bottom clearance identical to that of the existing piston. Diametral clearance was also duplicated. The upper shape, which allows free pad angular motion, was evolved through construction of a series of 10X layouts. Oil-port diameter was selected in accordance with the concept that the total flow area of both piston ports should approximately equal the area of a single port having a diameter ten times the race-orifice diameter. This was done to minimize pressure losses as the fluid flows to the restrictors.

---

*Phelan, Richard M., *Fundamentals of Mechanical Design*, McGraw-Hill Book Company, Inc., New York, 1962.

CHAPTER FIVE

LABORATORY TESTING

5.1 PURPOSE

A laboratory test program was conducted to provide the necessary information for validating the feasibility of the hydrostatic-bearing system. Comparative data for both the existing roller-bearing configuration and the hydrostatic-bearing modification were obtained. These data included quantification of system-oil-flow demand, wobbler and oil-temperature increases over ambient, and input torque required to overcome system friction.

5.2 LABORATORY OPERATING CONDITIONS

Laboratory duplication of the pump's critical operating conditions as indicated in Table 4—2 was not possible. Therefore, the modified operating conditions shown in Table 5—1 were selected. By subjecting both bearing configurations to these same operating conditions, the data required to establish the feasibility of the hydrostatic-bearing system were obtained.

Table 5—1. LABORATORY OPERATING CONDITIONS
(Supply Pressure 250 to 1000 psig)

Wobbler Eccentricity (inches)	Cylinder-Block Speed (rpm)
0	0
0	2000
0	4750
0	7000
0.35	2000
0.35	4750

Figure 5—1 shows that the pump was hydraulically dead-ended. All testing was performed with a special Government-furnished cylinder block that was assembled without valve plates. Eighteen domed motor pistons were installed on the motor side of the cylinder block and retained with a balanced, concentric aluminum ring. Oil at supply pressure was thus allowed to act on all 36 pistons. When the pump wobbler was moved eccentric to the cylinder block, causing pump-element piston reciprocation, the oil was merely agitated within the cylinder-block cavity. The oil was neither raised to a higher pressure level nor discharged into a downstream circuit. The only flow through this system was external oil leakage. Measurement of this leakage permitted a numerical comparison between the roller and hydrostatic bearings.

5.3 FACILITIES

Primary laboratory facilities included a hydraulic power generator, a test fixture, and instrumentation. In addition, a 20-HP electric motor and V-belt drive were used to rotate the two bearing specimens at the required speeds.

5.3.1 Hydraulic Power Generator

A Racine Hydraulics and Machinery Inc. modified hydraulic power unit was used to generate the required fluid power. The unit included a 30-gallon reservoir; a 100-mesh (149 micron) suction screen filter; a pressure-compensated, variable-displacement, vane-type pump; and a 5-HP electric drive motor. The maximum-hydraulic-power curve for this generator is shown in Figure 5—2.

5.3.2 Text Fixture

The test fixture shown in ARINC Research layout Drawing D000263 was used for testing both bearing specimens. It consists of a center shaft, simply supported on two pillow-block bearings, through which pressurized oil is fed to the cylinder block's inner cavity. Cylinder-block rotation was effected through a specially modified V-belt pulley mounted on an extension of the center shaft. The pump wobbler was supported in a manner that provided wobbler-to-cylinder-block eccentricity adjustment. The entire fixture, with the exception of the pulley, was enclosed in an aluminum box containing plexiglass windows. Leakage oil was collected in this enclosure and fed back to the supply reservoir through a suitable drain manifold and hose.

The specially modified V-belt pulley is shown in Figure 5—3. Torque is transmitted through the pulley to the shaft by a set of tangential extension springs. Spring deflection is a function of the torque transmitted and is indicated as angular relative displacement on the scale provided. Prior to operation, the scale was calibrated for the particular set of springs used. Quantitative measurements of torque were obtained by using a stroboscope to stop motion during testing. At this same time the stroboscope was indicating the cylinder-block rotational speed.

5.3.3 Instrumentation

Various instrumentation used to obtain data and monitor system performance is listed in Table 5—2.

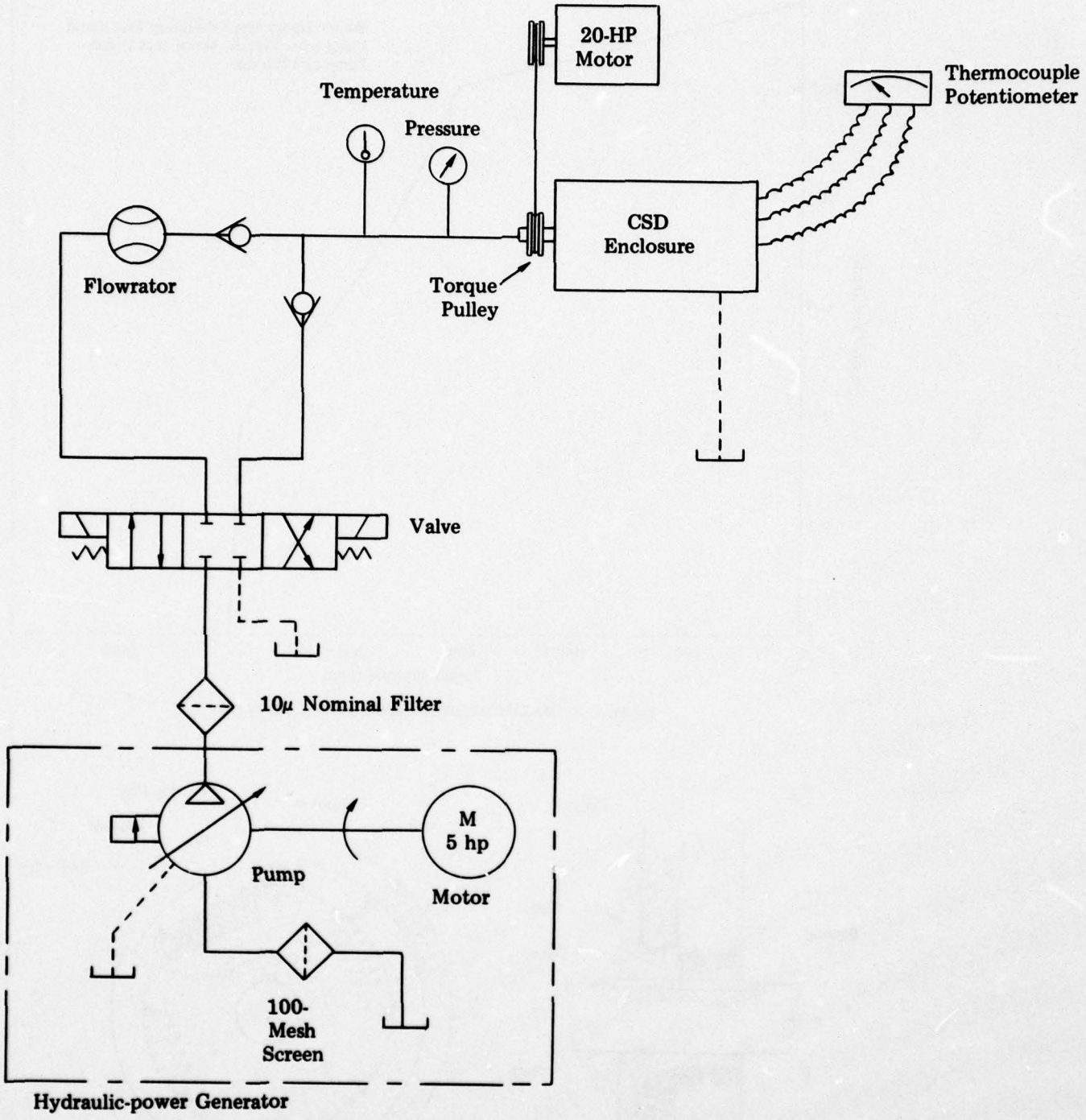

Figure 5—1. **SCHEMATIC DIAGRAM OF CSD TEST SYSTEM**

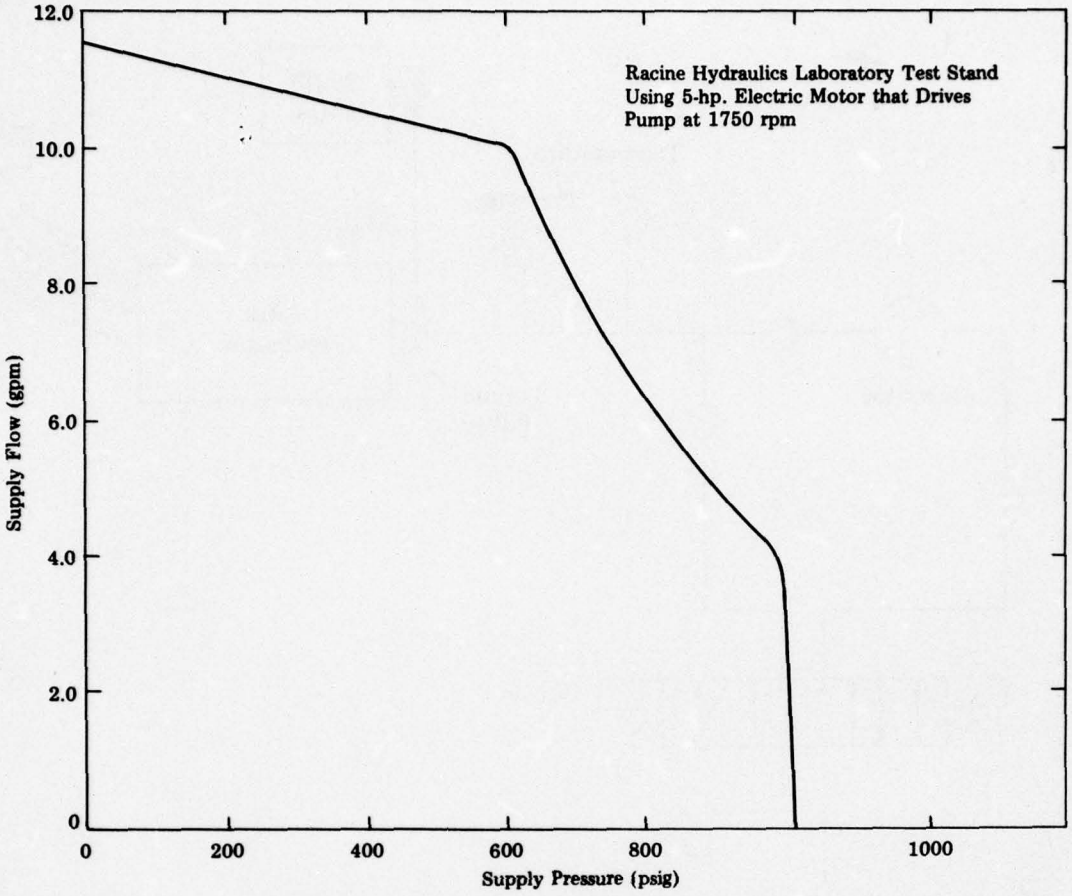

Figure 5—2. **MAXIMUM OBTAINABLE PRESSURE FLOW**

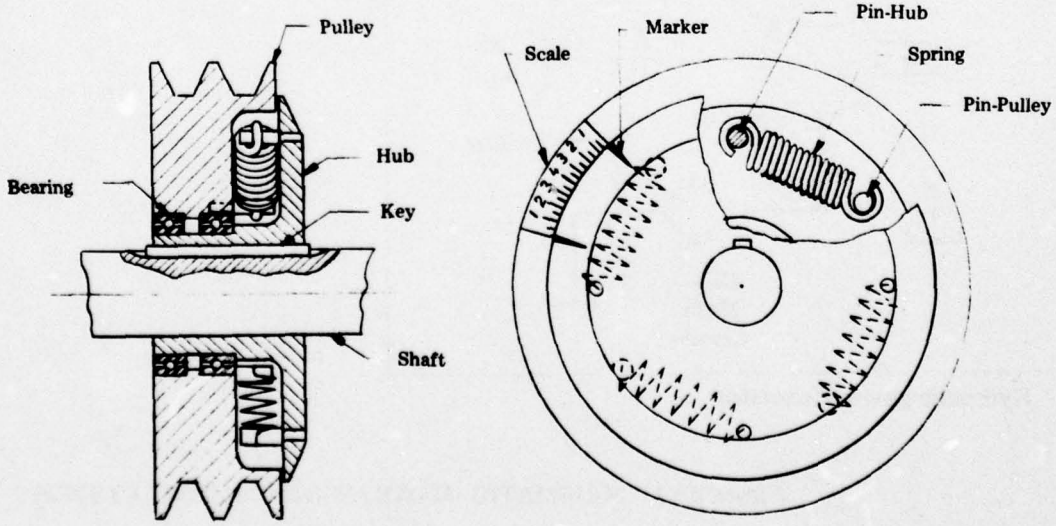

Figure 5—3. **TORQUE-MEASURING PULLEY**

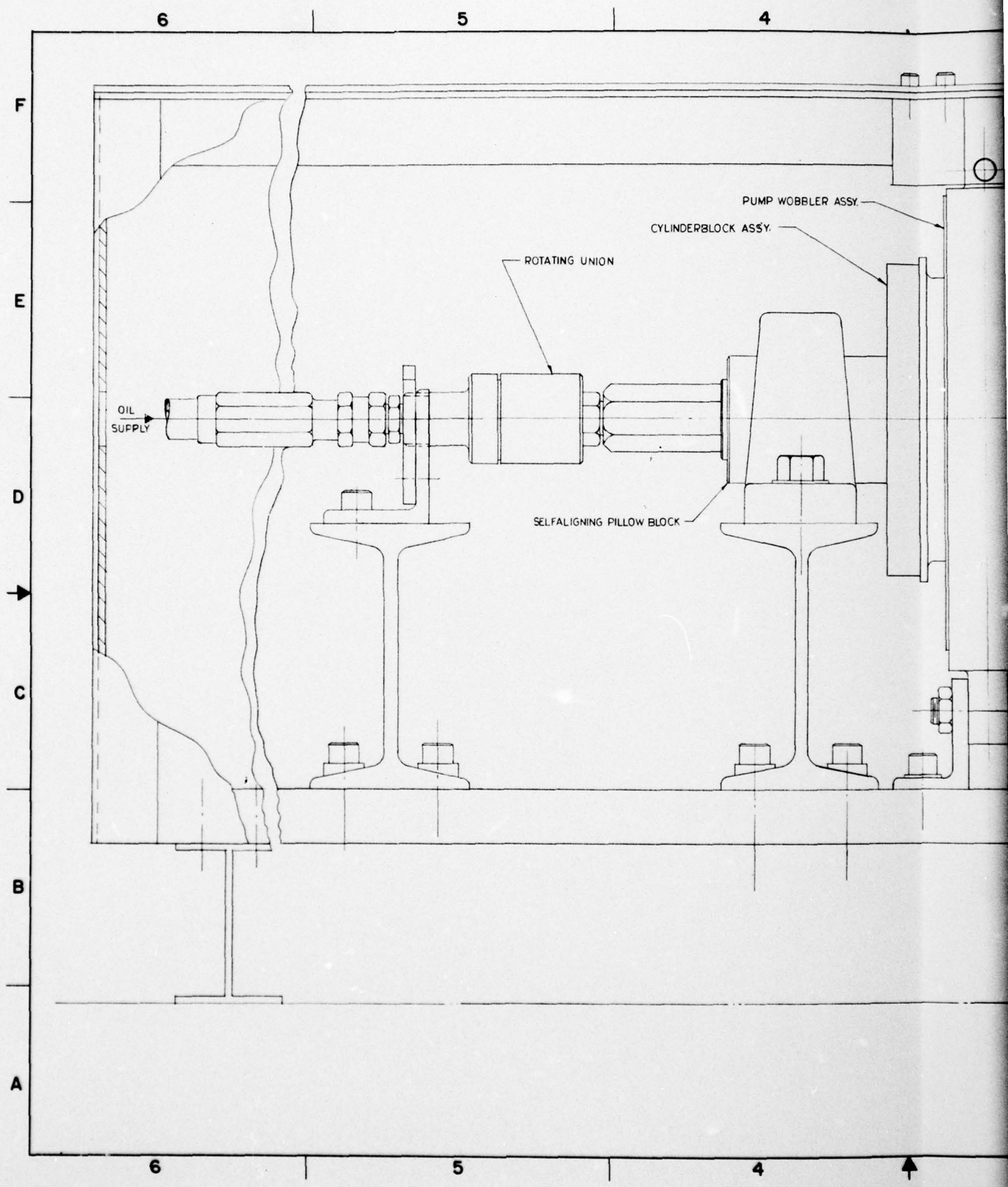

REVISIONS				
SYM	ZONE	DESCRIPTION	DATE	APPROVED

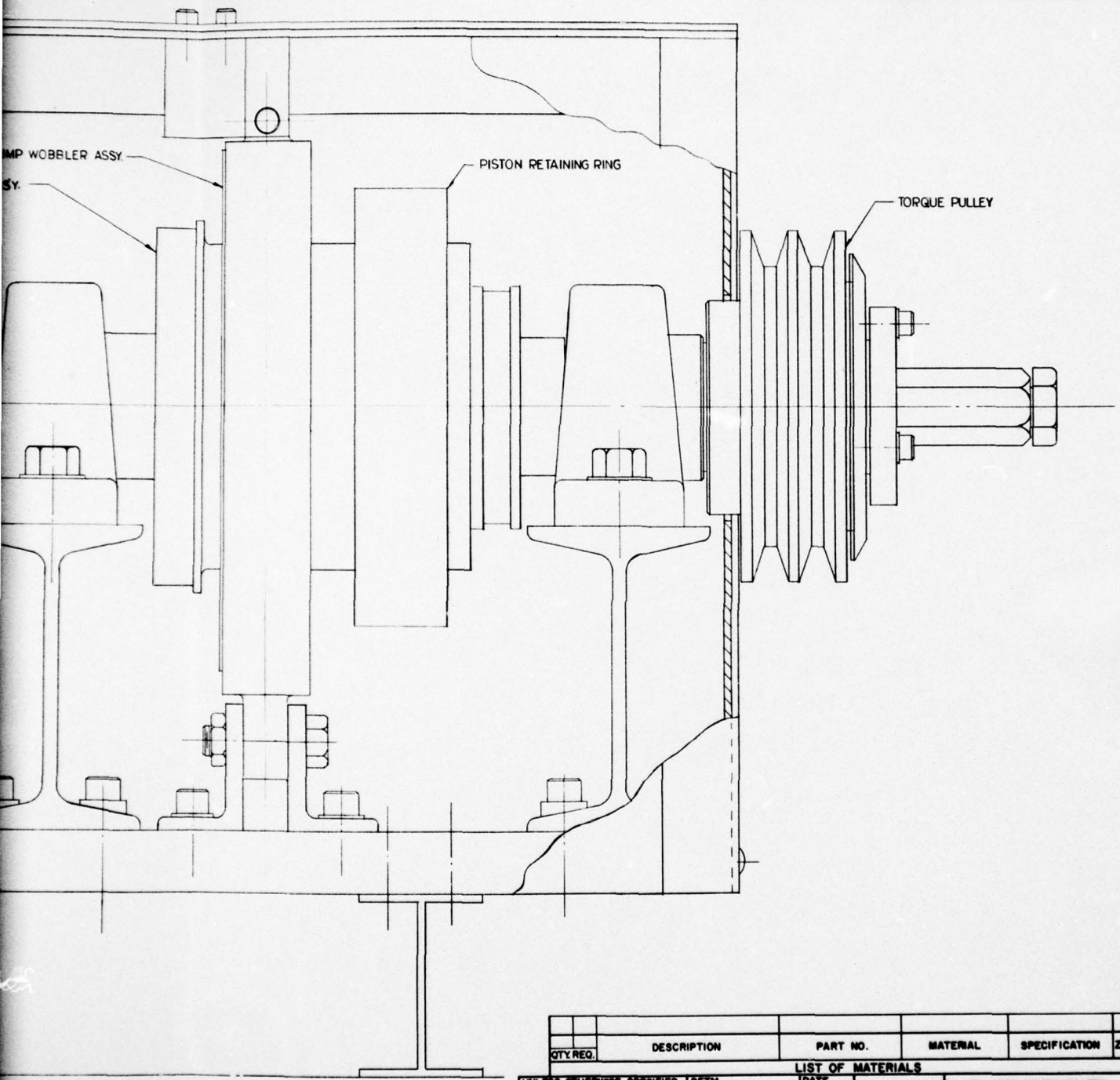

QTY. REQ.	DESCRIPTION	PART NO.	MATERIAL	SPECIFICATION	ZONE	ITEM

LIST OF MATERIALS

ITEM	QTY	NEXT ASSY	USED ON
APPLICATION			

UNLESS OTHERWISE SPECIFIED DIMENSIONS ARE IN INCHES

TOLERANCES ON:
FRACT. ± DECIMALS .XX ± .XXX ± ANGLES ±

MATERIAL

TREATMENT

FINISH

DFTM. R. Peter — DATE 7/16/69

DES. ENG.

CHKD.

APPD.

WORK ORDER NO. 595-01

CONTRACT NO.

ARINC RESEARCH CORPORATION

TITLE
TEST FIXTURE
B52H CSD MODEL 120 RD 02
HYDROSTATIC BEARING

SIZE D — DWG. NO. D 000263

SCALE 1/1 — SHEET 1 OF 1

2

Table 5—2. **LABORATORY-TEST INSTRUMENTATION**

Instrument	Manufacturer	Model	Used to Measure
Flowrator	Fischer & Porter Co.	10A3565A	Leakage flow
Pressure Gauge	Victor Equipment Co.		Supply-oil pressure
Temperature Gauge	Aschroft Corporation		Supply-oil temperature
Stroboscope	General Radio Co.	1531A	Cylinder-block speed
Potentiometer	Minneapolis-Honeywell	2745	Wobbler Temperature
Contamination Analysis Kit	Millipore Corp.	XX7104910	Supply-oil particulate contamination

5.4 RESULTS

5.4.1 Roller-Bearing Configuration

The roller-bearing configuration for the pump side of the constant-speed drive was installed on the test fixture, and data were obtained. Measurements of temperature rise, leakage-oil flow, and frictional drag torque were made at various combinations of input speed and supply pressure. The plotted data are presented in Figures 5—4 through 5—8. Some of the more significant aspects of these data are as follows:

- The maximum leakage-oil flow was 0.53 gpm and occurred at the maximum wobbler eccentricity of 0.35 inch, 1000-psig supply pressure, 4750-rpm cylinder-block speed, and 150°F supply oil temperature.
- The maximum frictional drag torque was 95 inch-pounds and occurred under the same operating condition as the maximum leakage flow.
- The maximum stabilized wobbler temperature was 308°F at 1000-psig supply pressure and 7000-rpm cylinder-block speed.

5.4.2 Hydrostatic-Bearing Configuration

Immediately after the hydrostatic-bearing-configuration test was initiated, it was apparent that excessive leakage was occurring at the pad/race interface. This leakage was so extensive, relative to ARINC Research's hydraulic-power-supply capability, that it was impossible to obtain precise data for comparison with the roller-bearing configuration. Therefore, although limited performance data were obtained, most testing of the hydrostatic-bearing configuration was devoted to the empirical solution of the leakage problem.

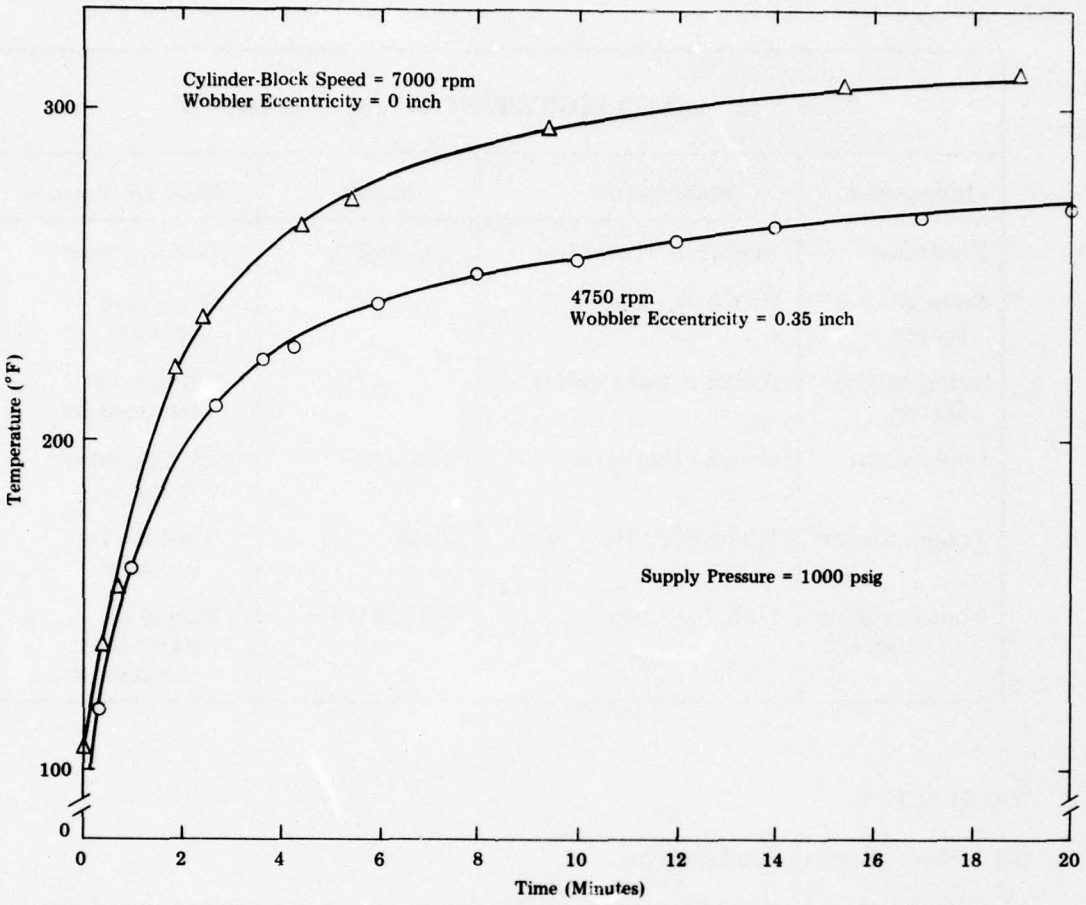

Figure 5—4. **WOBBLER TEMPERATURE VS. ELAPSED TIME, ROLLER-BEARING CONFIGURATION**

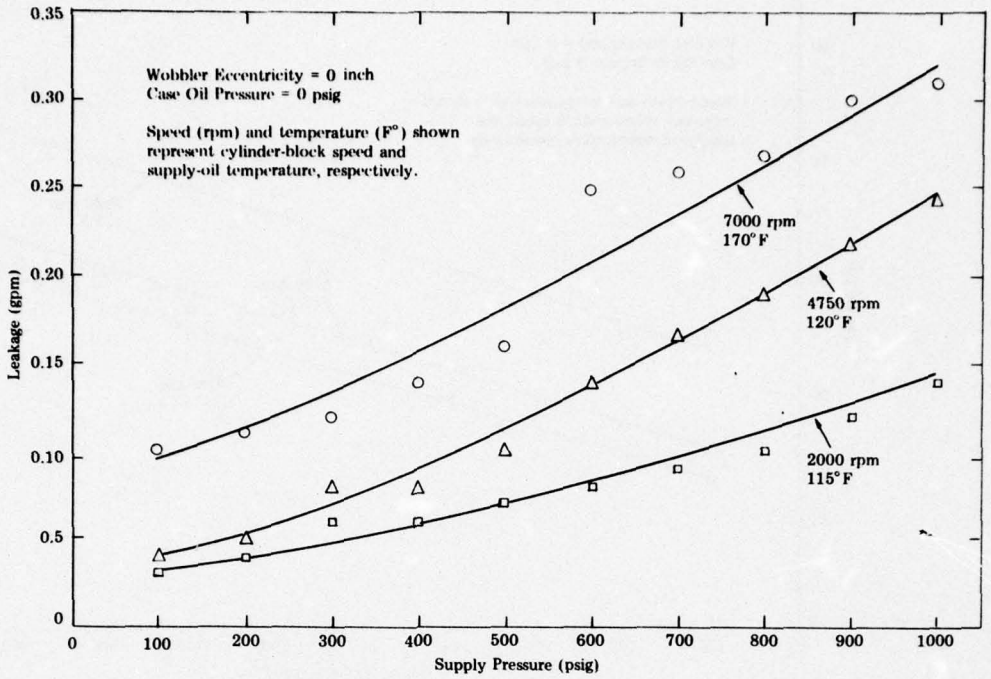

Figure 5—5. **OIL LEAKAGE VS. SUPPLY PRESSURE, ROLLER-BEARING CONFIGURATION (ECCENTRICITY 0 INCH)**

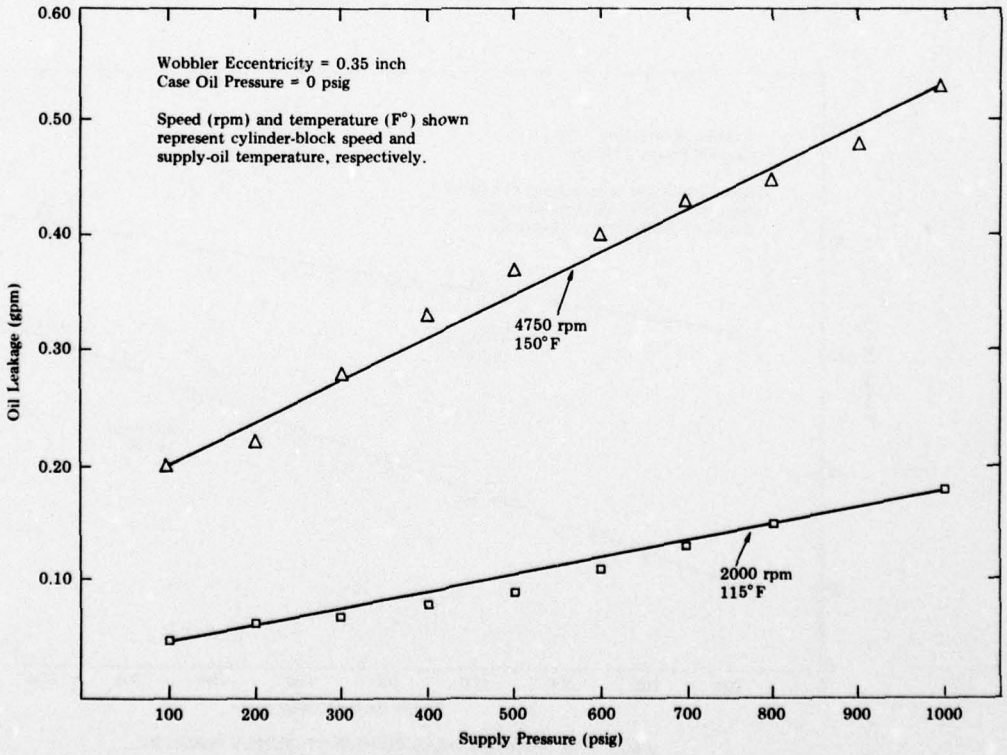

Figure 5—6. **OIL LEAKAGE VS. SUPPLY PRESSURE, ROLLER BEARING CONFIGURATION (ECCENTRICITY 0.35 INCH)**

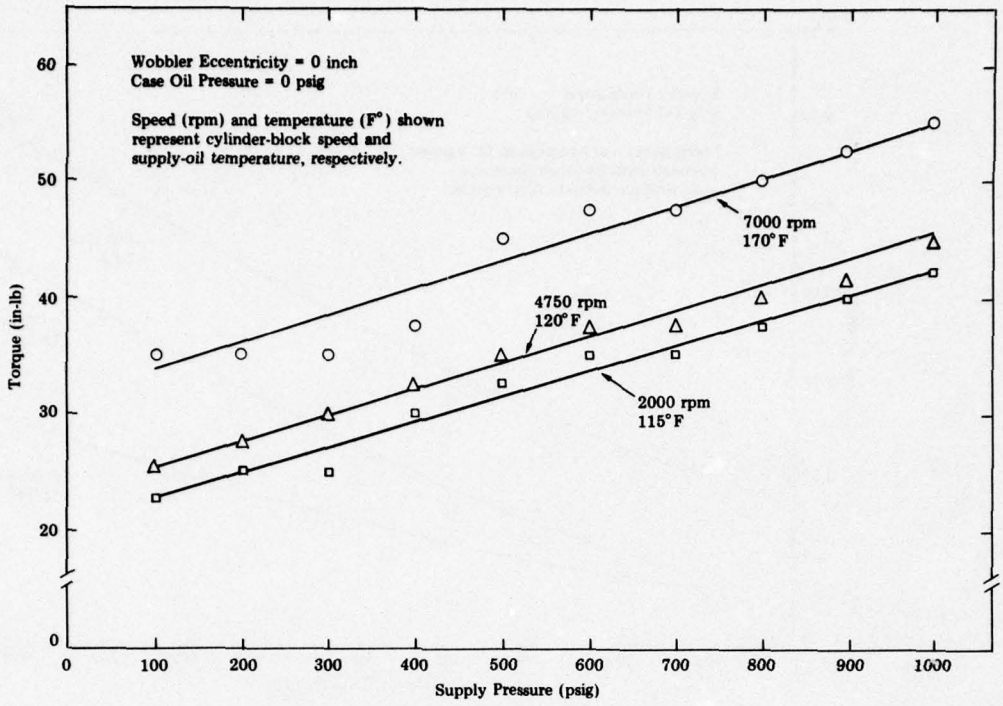

Figure 5—7. **WOBBLER DRAG TORQUE VS. SUPPLY PRESSURE, ROLLER-BEARING CONFIGURATION (ECCENTRICITY 0 INCH)**

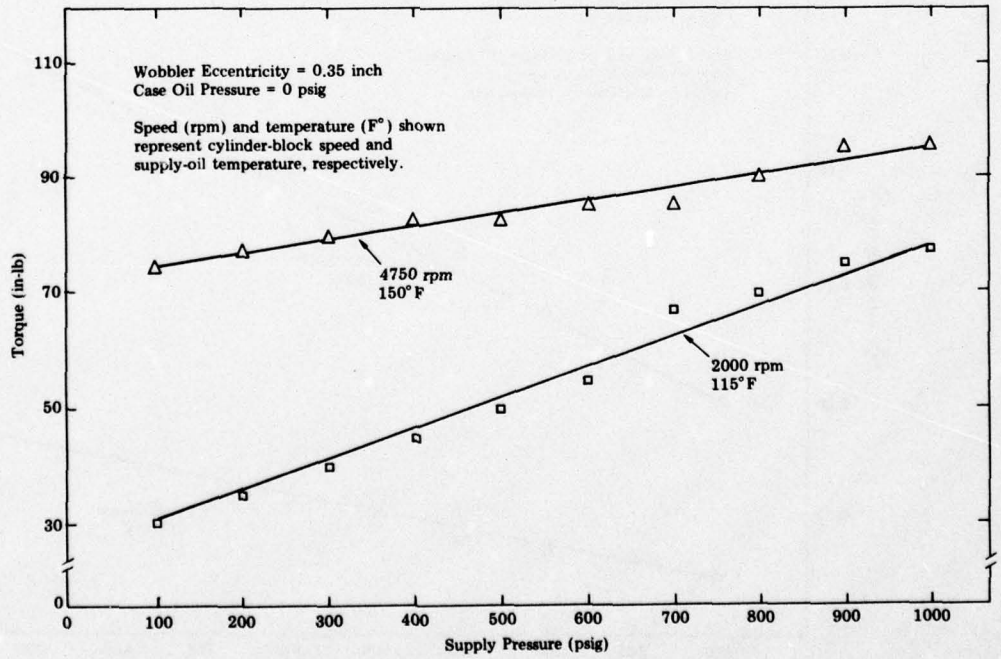

Figure 5—8. **WOBBLER DRAG TORQUE VS. SUPPLY PRESSURE, ROLLER-BEARING CONFIGURATION (ECCENTRICITY 0.35 INCH)**

5.4.2.1 Physical Data

When the prototype hydrostatic-bearing parts were received from the manufacturer, they were inspected for pertinent physical characteristics. Table 5—3 lists the weight of the hydrostatic-bearing parts for the pump.

Table 5—3. WEIGHT SUMMARY

Item	Part Number	Weight (pounds)	Quantity Required	Total Weight (pounds)
Piston	C-000415	0.078	18	1.40
Pad	C-000414	0.125	9	1.13
Race	C-000412	3.156	1	3.16
			Total	5.69

The knife-edge method was used to locate the center of gravity of a single piston/pad subassembly. This is shown in Figure 5—9. Figure 5—10 illustrates diametral measurements made on the race. These dimensions indicate that the race O.D. was 0.002″ out of round on the O.D., and that the O.D. was tapered 0.001″ total across its length. In addition, the race I.D. was found to be 0.001″ out of round on diameter; and the race-to-wobbler diametral clearance was 0.004″ to 0.006″ depending on race-to-wobbler relative angular position. Since the race-to-wobbler diametral clearance was at least double the race O.D. out of round, this condition presented no problem. The 0.001″ taper on the race O.D., however, could have been the recipient of a pressure gradient in the axial direction, causing the race to rub against the wobbler lip.

5.4.2.2 Performance Data

In the testing procedure for the roller-bearing configuration the pressure drop across the CSD was made the independent variable. It was against this pressure drop that dependent variables of leakage flow and drag torque were plotted, with speed as a parameter.

It was also planned to use this approach in the test procedure for the hydrostatic-bearing modification (see Appendix C). However, the leakage was so high that in most cases it was impossible to supply sufficient flow to the CSD to establish the required pressure drop across it. Therefore, in the testing of the hydrostatic bearing, supply flow was made either an independent variable or curve parameter and was physically adjusted by changing the supply-pump displacement.

When the hydrostatic-bearing modification was first assembled and operated with pads conforming exactly to ARINC Research Drawing C000414, a pressure drop of only 25 psi was obtained across the bearing at a supply flow of 0.68 gpm and input speed of 2000 rpm.

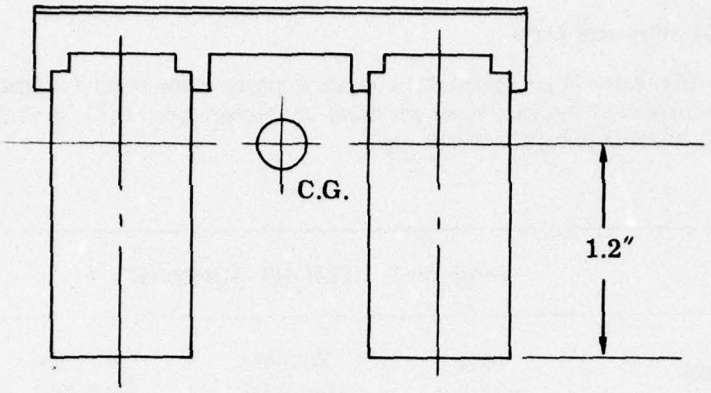

Figure 5—9. **CENTER-OF-GRAVITY LOCATION**

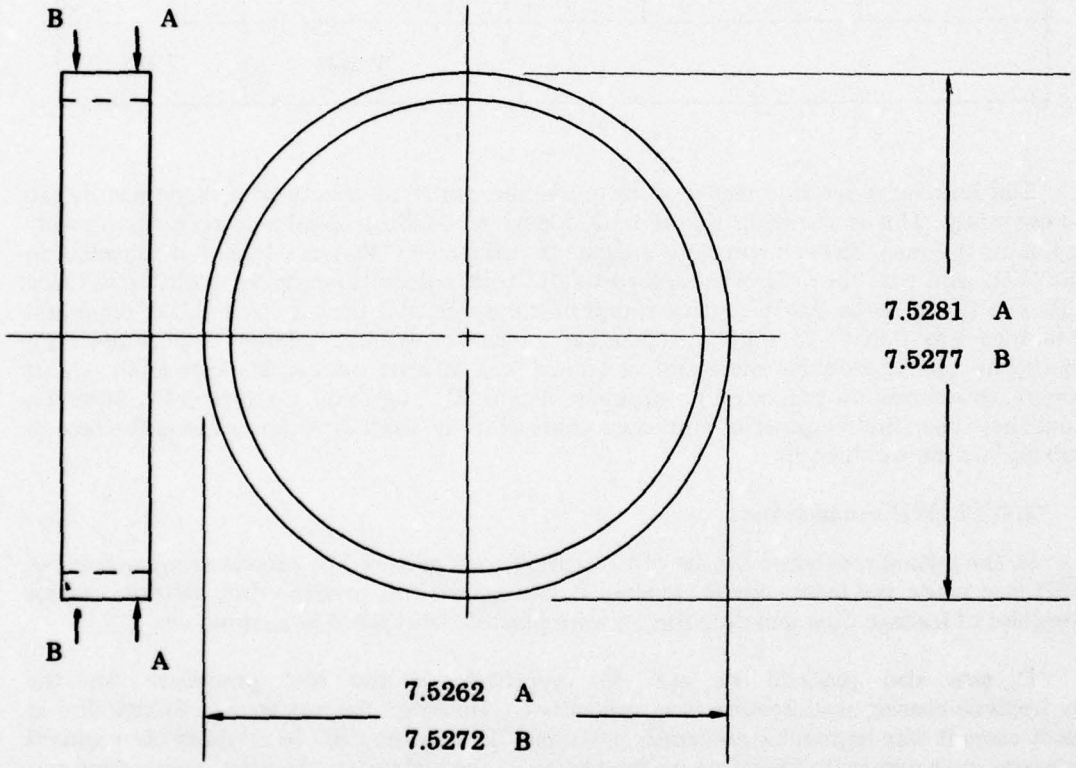

Figure 5—10. **ACTUAL RACE-DIAMETER MEASUREMENT**

REVISIONS				
SYM	ZONE	DESCRIPTION	DATE	APPROVED
A		REVISED AND REDRAWN, CENTER REMOVED	1/7/69	
		RECESS AND HOLE DIMENSIONS ADDED		

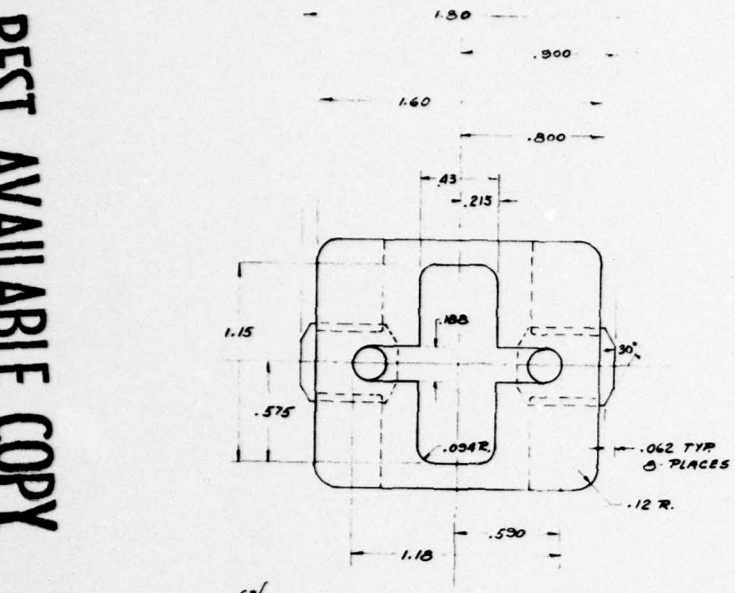

HARDNESS	MATERIAL	DASH NO.
BRINELL (3000/10) 170-185	AMPCO 15	-7
BRINELL (3000/10) 200-220	AMPCO METAL 18-22	-9
BRINELL (3000/10) 190-210	COPALLY. NO. 630	-11

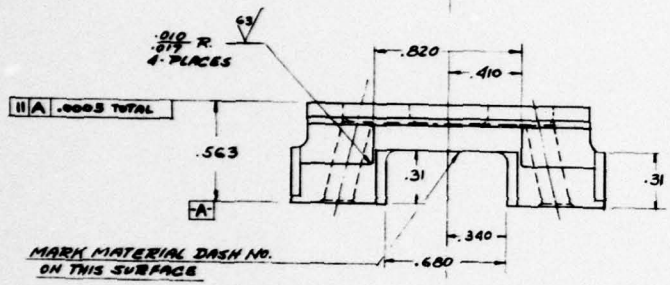

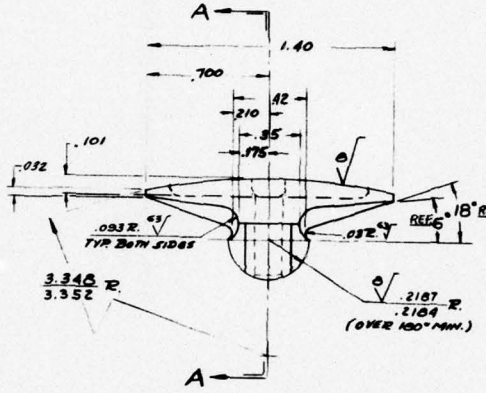

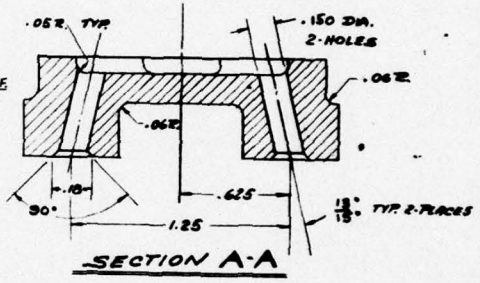

SECTION A-A

UNLESS OTHERWISE SPECIFIED
BREAK ALL EDGES .003 - .010

QTY. REQ.	DESCRIPTION	PART NO.	MATERIAL	SPECIFICATION	ZONE	ITEM

LIST OF MATERIALS

ITEM	QTY.	NEXT ASSY	USED ON
APPLICATION			

UNLESS OTHERWISE SPECIFIED DIMENSIONS ARE IN INCHES
TOLERANCES ON:
FRACT. ± DECIMALS .XX ±.01 .XXX ±.005 ANGLES ±3°

MATERIAL: SEE LIST
TREATMENT: SEE LIST
FINISH: 125 AND AS NOTED

DFTM. A.T.P. DATE 1/7/69
DES. ENG.
CHKD.
APPD.
WORK ORDER NO. 595-01
CONTRACT NO.

ARINC RESEARCH CORPORATION

TITLE
PAD
B-52H · CSD, MODEL 120RD02
HYDROSTATIC BEARING

SIZE C DWG. NO. C 000414
SCALE 2/1 SHEET 1 OF 1

4 3 2 1 D C A

Compared with the performance of the roller bearing, in which the pressure drop was 1000 psi, at 0.53 gpm, this performance was extremely poor. (Chapter 6 presents a theoretical discussion of the causes and solution to this excessive-flow-demand, or leakage, problem.) The pads were then lapped and additional data were taken. Figures 5—11 thorugh 5—13 illustrate leakage flow, pressure, and speed relationships for this condition.

The bearing pads were then modified according to ARINC Research Drawing A-000558. In addition, each of the piston bores was plugged and then drilled out to form a flow restriction. Figures 5—14 through 5—17 illustrate the supply-pressure/leakage-flow relationship for various cylinder-block input speeds. Although these restrictors did decrease the leakage by throttling the flow, they eventually caused scoring damage to the bearing, as discussed in Chapter 6.

Figure 5—18 shows the improvement of the modified pad over the original pad. Here, 16 pistons were plugged solid while the two feeding flow to the pad being tested were equipped with 0.050″-diameter restrictors. For this test, the race was removed from the wobbler and the pad recess was in communication with one race orifice.

During the hydrostatic-bearing test, at no time under any operating condition did the wobbler temperature exceed 150°F nor the oil temperature 130°F. Both of these temperatures occurred with the modified pads (A-000558) and with 0.040″-diameter restrictors in each piston at an input speed of 7800 rpm. Observation confirmed that for all operating conditions, the hydrostatic bearing was smoother and quieter in operation than the roller bearing.

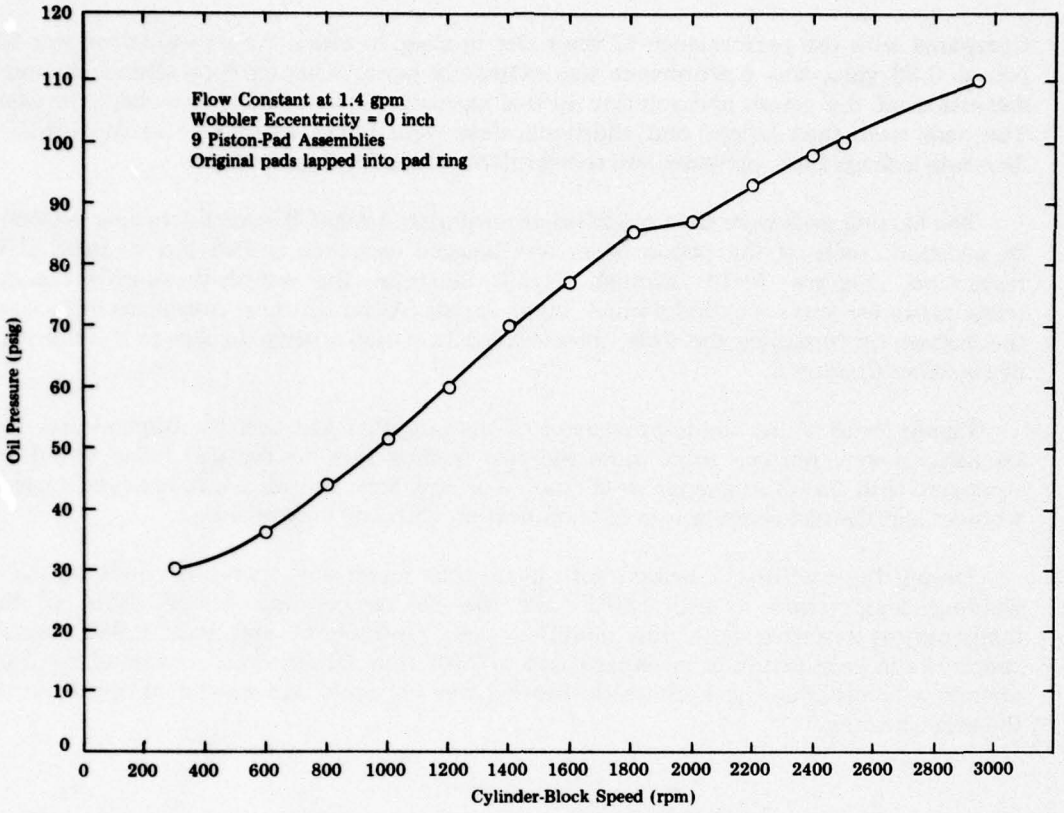

Figure 5—11. **OIL PRESSURE AS A FUNCTION OF CYLINDER-BLOCK SPEED**

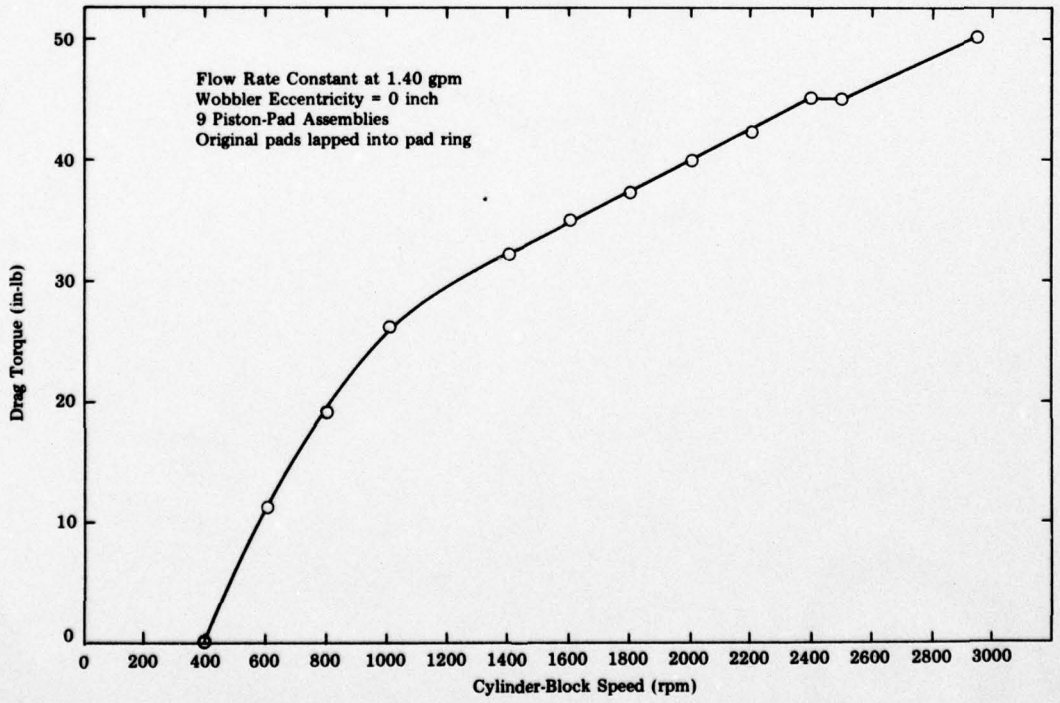

Figure 5—12. **DRAG TORQUE AS A FUNCTION OF CYLINDER-BLOCK SPEED**

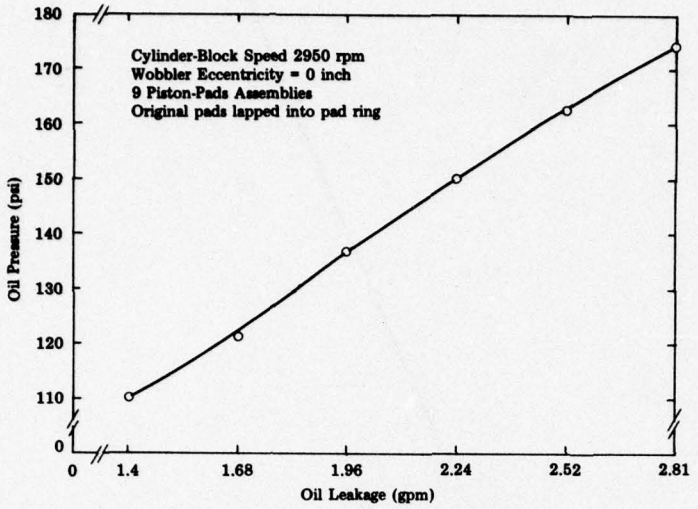

Figure 5—13. **OIL PRESSURE AS A FUNCTION OF OIL LEAKAGE**

Ⓐ CHANGED 5-3-69
Ⓑ CHANGED 5-21-69

Ⓑ MACHINE PAD-SUPPORT DOWN .010"

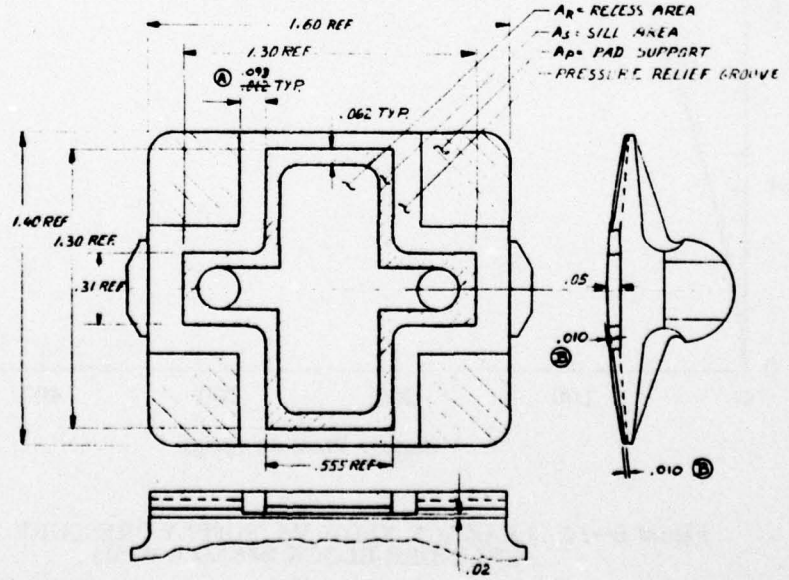

PAD-PRESSURE RELIEF GROOVE

A 000558

4/3/69 fg
4/7/69 R.F.

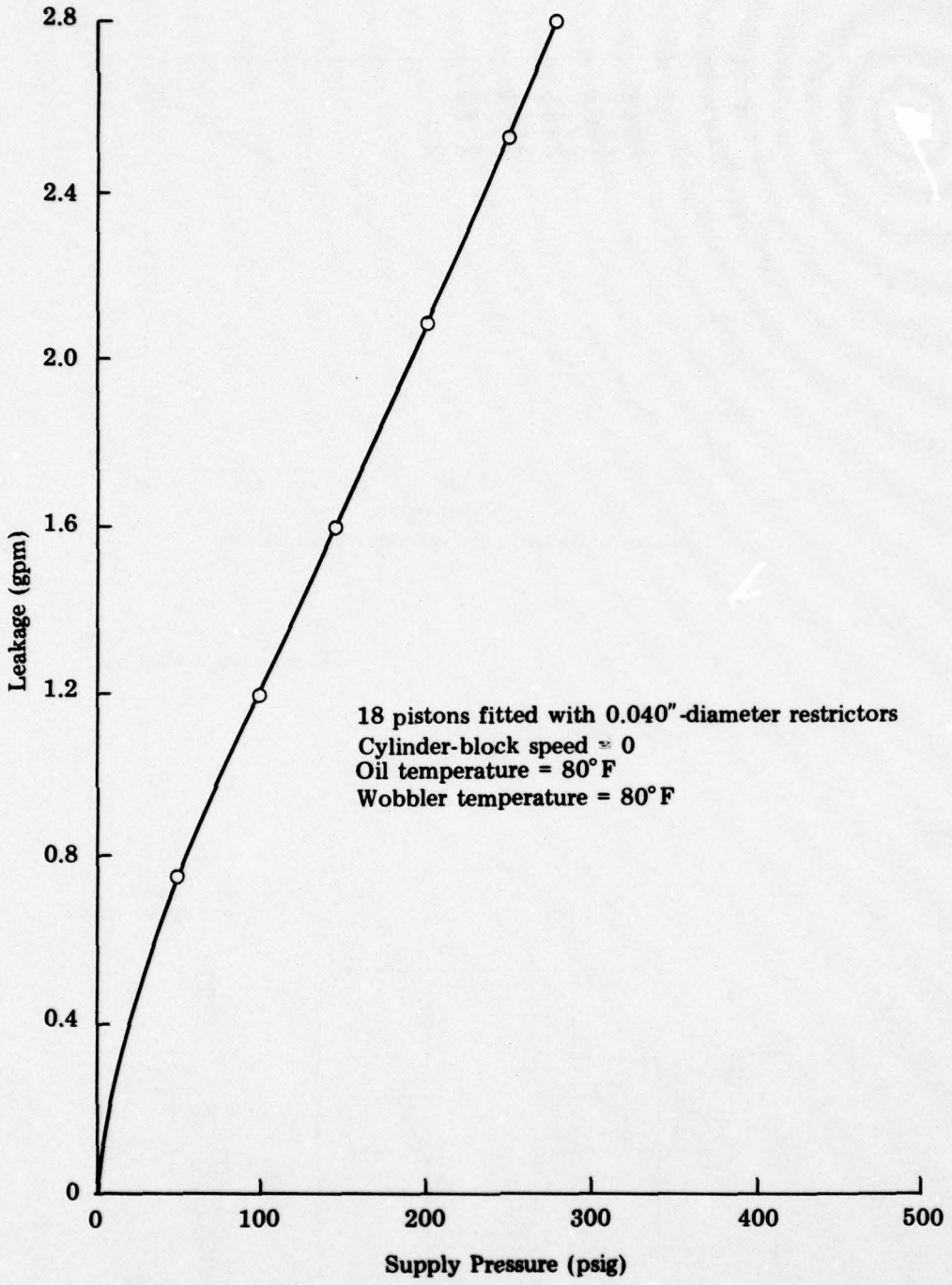

Figure 5—14. **LEAKAGE FLOW VS. SUPPLY PRESSURE (CYLINDER-BLOCK SPEED 0 RPM)**

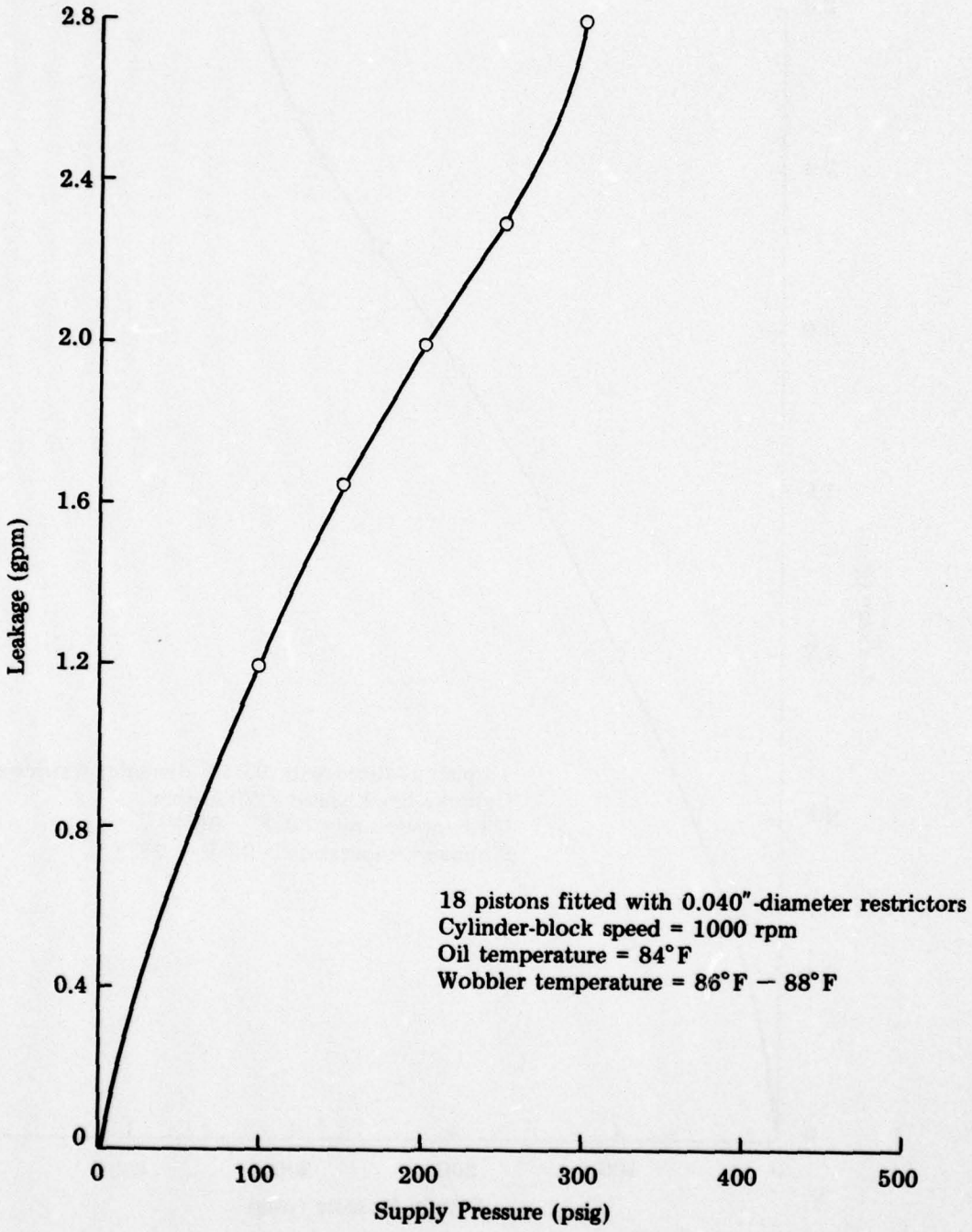

Figure 5—15. **LEAKAGE FLOW VS. SUPPLY PRESSURE (CYLINDER-BLOCK SPEED 1000 RPM)**

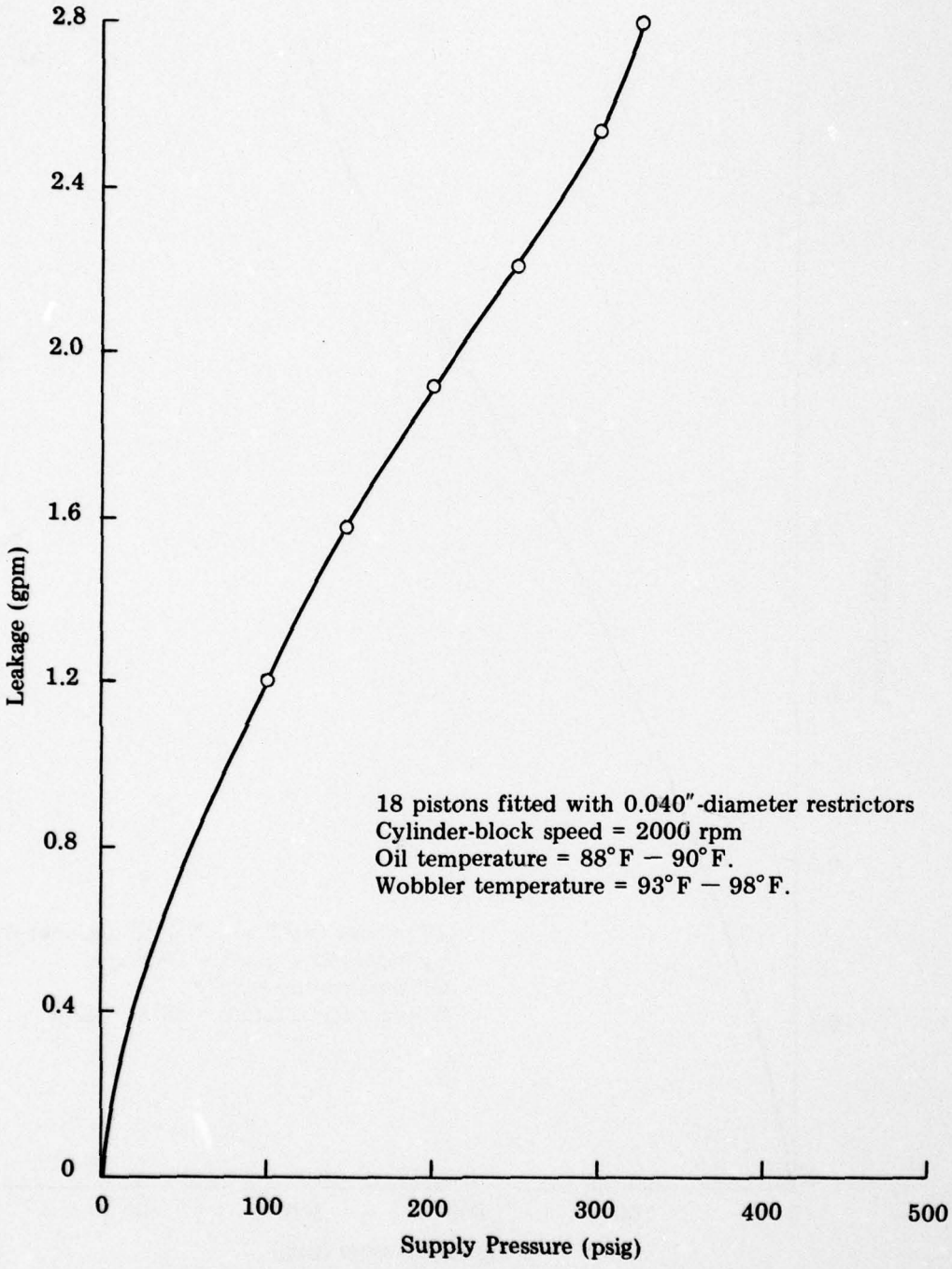

Figure 5—16. **LEAKAGE FLOW VS. SUPPLY PRESSURE (CYLINDER-BLOCK SPEED 2000 RPM)**

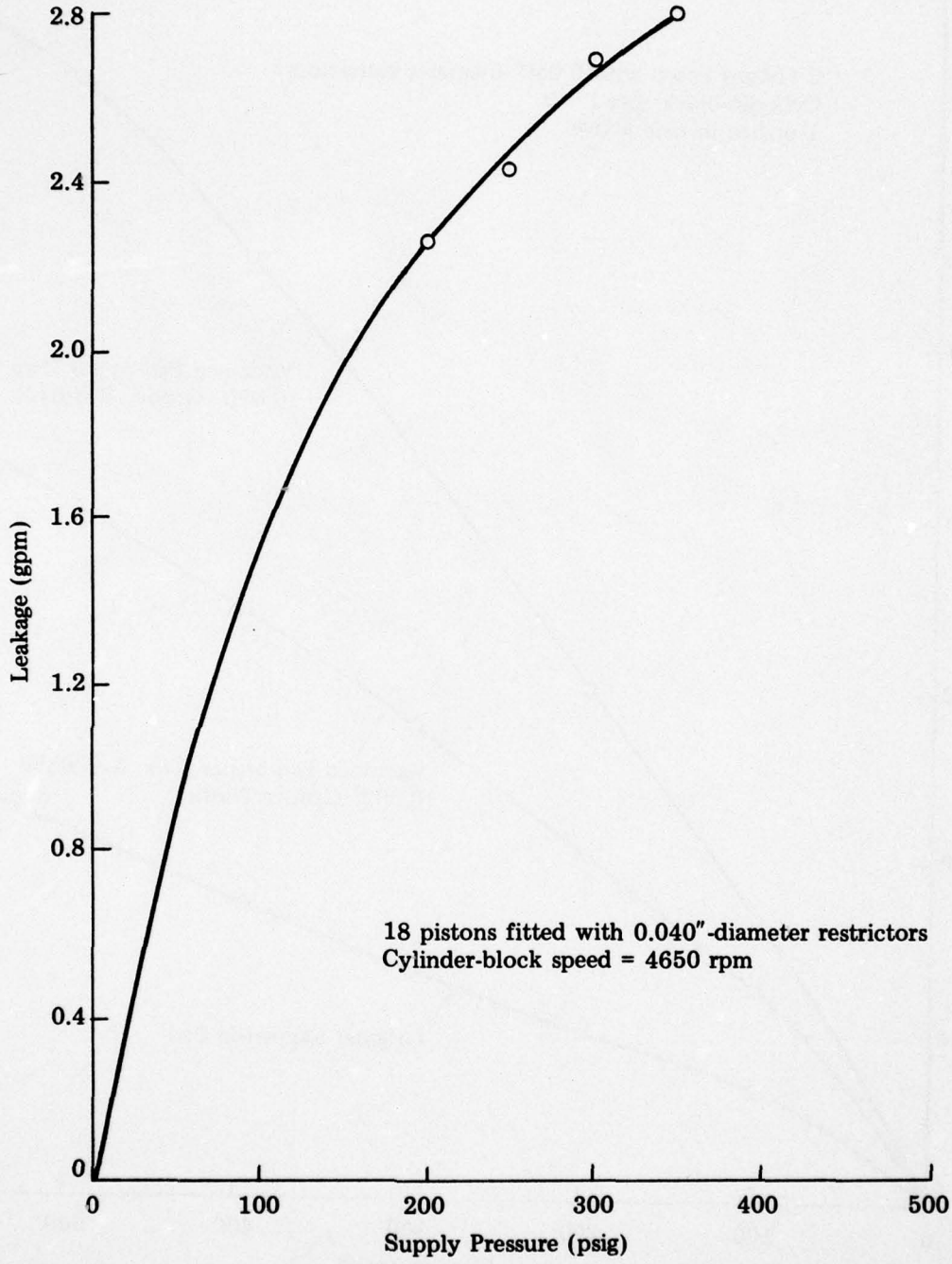

Figure 5—17. **LEAKAGE FLOW VS. SUPPLY PRESSURE (CYLINDER-BLOCK SPEED 4650 RPM)**

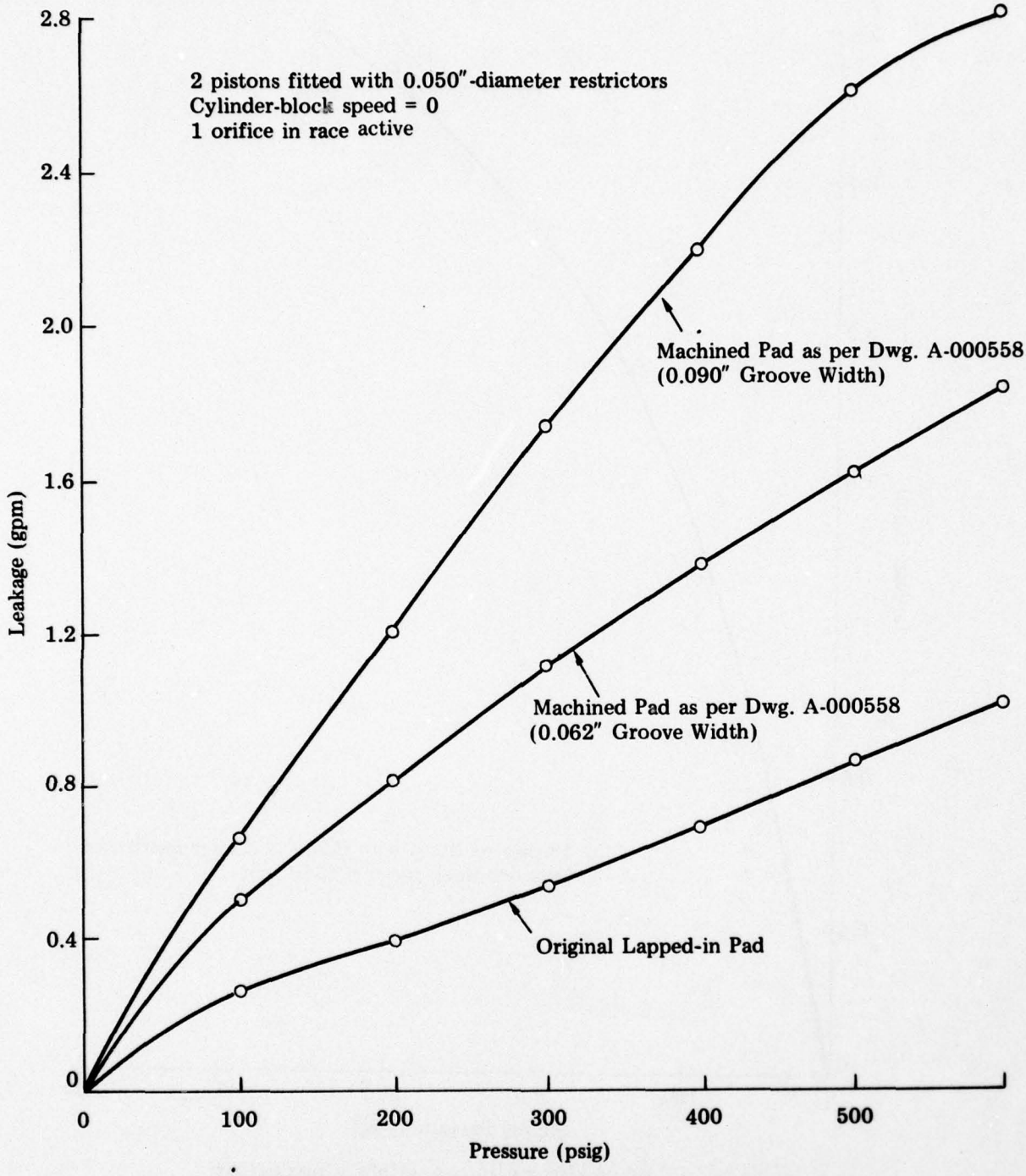

Figure 5—18. **LEAKAGE FLOW VS. SUPPLY PRESSURE (COMPARISON OF ORIGINAL AND MACHINED PADS)**

CHAPTER SIX

PROBLEM AREAS

6.1 PAD/RACE INTERFACE LEAKAGE

Excessive leakage at the pad/race interface made most of the test data obtained for the hydrostatic-bearing modification meaningless. This leakage is shown as Q_L in Figure 6—1.

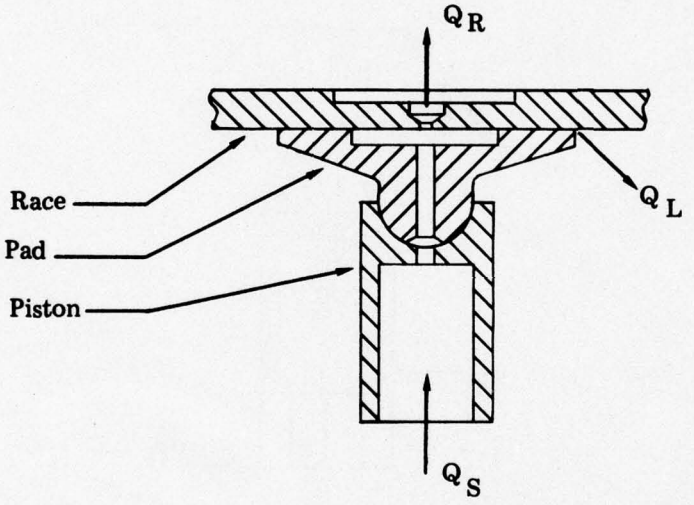

Figure 6—1. **FLOW DESIGNATION**

Its existence is detrimental to satisfactory system performance for the following reasons:

- It tends to cause a reduction in the oil pressure within the pad recess, thereby reducing the flow through the hydrostatic bearing, Q_R. This in turn decreases the load-carrying capacity of the bearing and increases the chance of race damage due to metal-to-metal contact.
- It increases the total system-flow demand to values in excess of what can be supplied feasibly.

6.1.1 Causes of Interface Leakage

ARINC Research Corporation determined that there are essentially three contributors to the leakage problem:

(1) Hydrostatic lift-off forces, which cause a separation between the pad and race

(2) Light metal-to-metal bearing stress over the pad sill area

(3) Misalignment of the cylindrically contoured mating surfaces of the pad and race.

6.1.1.1 Hydrostatic Lift-Off

Initially, it was assumed that if the pad recess area (A_r) were made smaller than the piston face area (A_p), the resulting net outward radial force would maintain a metal-to-metal contact seal between the pad sill area (A_s) and the race I.D. Inherent in this assumption was negligible hydrostatic-pressure distribution across the sill area. Testing has shown that this seal is incapable of isolating the pressurized oil within the recess, resulting in a pressure distribution across the pad surface similar to that illustrated in Figure 6—2.

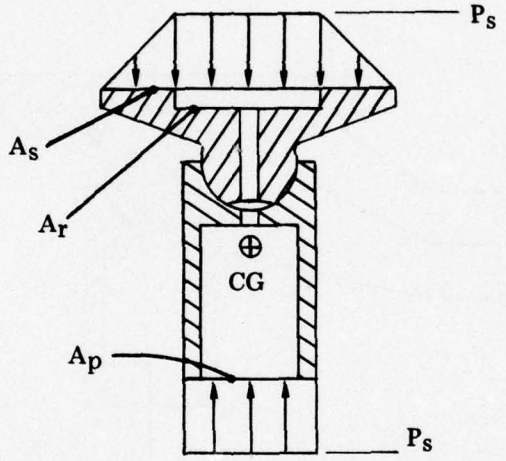

Figure 6—2. **PRESSURE LOADING**

The net hydrostatic separating force at the pad/race interface, assuming linear pressure gradient across the sill, is given by F_S:

$$F_S = F_1 - F_2 \tag{17}$$

where

$$F_1 = P_S A_r + \tfrac{1}{2} P_S A_S \tag{18}$$

$$F_2 = P_S A_p + \frac{W}{g}\left[r_{cg} \left(\frac{d\theta}{dt}\right)^2 + \frac{d^2 r}{dt^2}\right] \tag{19}$$

For various operating conditions, F_2 can be obtained directly from Figures 4—4 through 4—7. Analysis based on these equations indicated that, except for cases of high input speed and low supply pressure, $F_1 > F_2$ and a net separating force existed at the interface.

To remedy this situation, ARINC Research Corporation reduced the pad-sill effective area by machining pressure-relief grooves in the pad surface as shown in Figure 6—3. This, in effect, reduced the sill-area factor (A_s) in Equation 18 from the total sill area to the significantly smaller inner sill area.

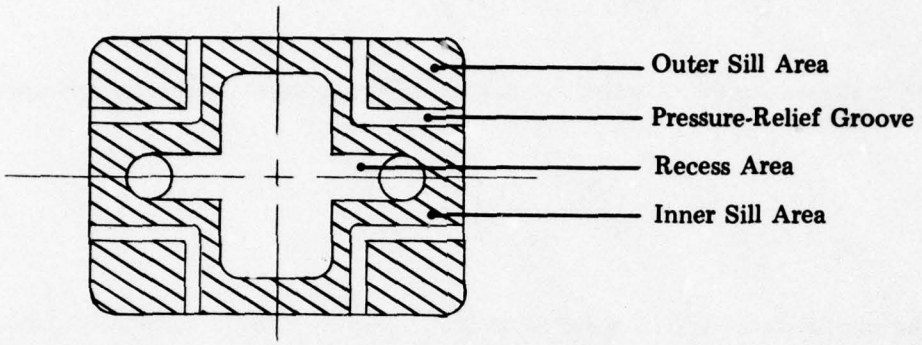

Figure 6—3. PAD MODIFICATION

The original total sill area was 1.60 sq in. After the grooves were machined, the sill area capable of supporting a hydrostatic pressure gradient (inner sill area) was 0.34 sq in. Testing showed that this modification resulted in a significant reduction in interface leakage. However, the leakage persisting in spite of this improvement was still considered excessive.

6.1.1.2 Sill Metal-to-Metal Bearing Stress

Although the machining of the pressure-relief grooves in the pad surface essentially eliminated the hydrostatic lift-off or separating tendency, excessive leakage still persisted at the interface. One explanation for this condition is that the sill bearing stress was too light to seal the high-pressure oil within the recess. Although the inner sill area is the only area capable of supporting a hydrostatic pressure distribution, the sum of both the inner sill area and outer sill area must be used in computing metal-to-metal bearing stress.

Equation 18 can be manipulated for the condition of zero hydrostatic lift-off force and resulting metal-to-metal bearing stress by substituting the sill bearing stress (S_b) for the pressure-gradient factor. Thus

$$F'1 = P_s A_r + S_b A_s \quad \text{where } A_s \text{ is the total sill area.} \tag{20}$$

Since there is now no net separating force,

$$F'_1 = F_2 = P_s A_p + F_i \tag{21}$$

where

$$F_i = \frac{W}{g}\left[r_{cg}\left(\frac{d\theta}{dt}\right)^2 + \frac{d^2 r}{dt^2}\right] \tag{22}$$

The bearing stress can now be solved for in terms of the appropriate areas, supply pressure, and inertial force:

$$S_b = \left(\frac{1}{A_s}\right) F_i + \left(\frac{A_p - A_r}{A_s}\right) P_s \tag{23}$$

Since the inertial force (F_i) is speed-dependent, speed becomes a convenient parameter against which the bearing stress can be plotted. This was done as shown in Figure 6—4 for a 167-HP alternator load condition. In this figure the pad-recess oil pressure is also plotted against input speed to illustrate the magnitude difference between the oil pressure and the sill bearing stress. Only the discharge side of the pump element is considered. The discontinuity at 4475 rpm is due to the alternator load's cutting in at this point.

It appeared that a further reduction in interface leakage would require an increase in sill bearing stress. One method of achieving this increase is to install restrictors in the piston bores to throttle the flow through the piston, thereby creating a pressure differential across the piston-pad assembly. This is illustrated in figure 6—5.

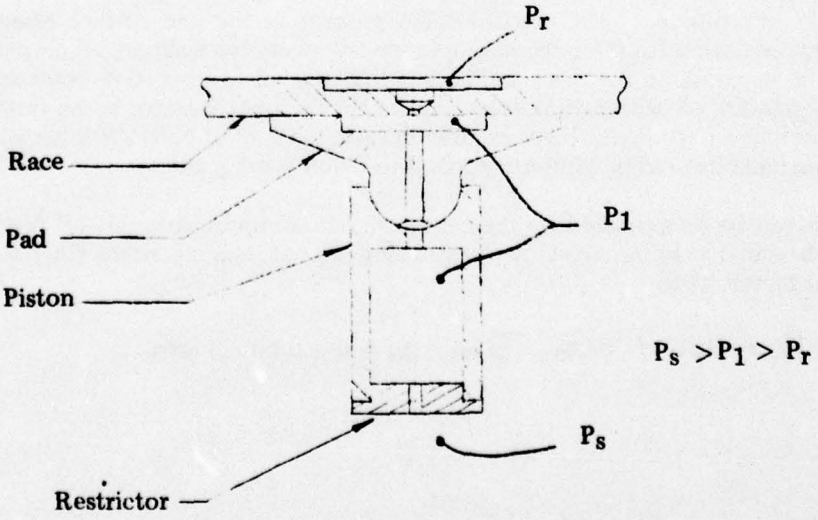

Figure 6—5. **RESTRICTOR INSTALLATION**

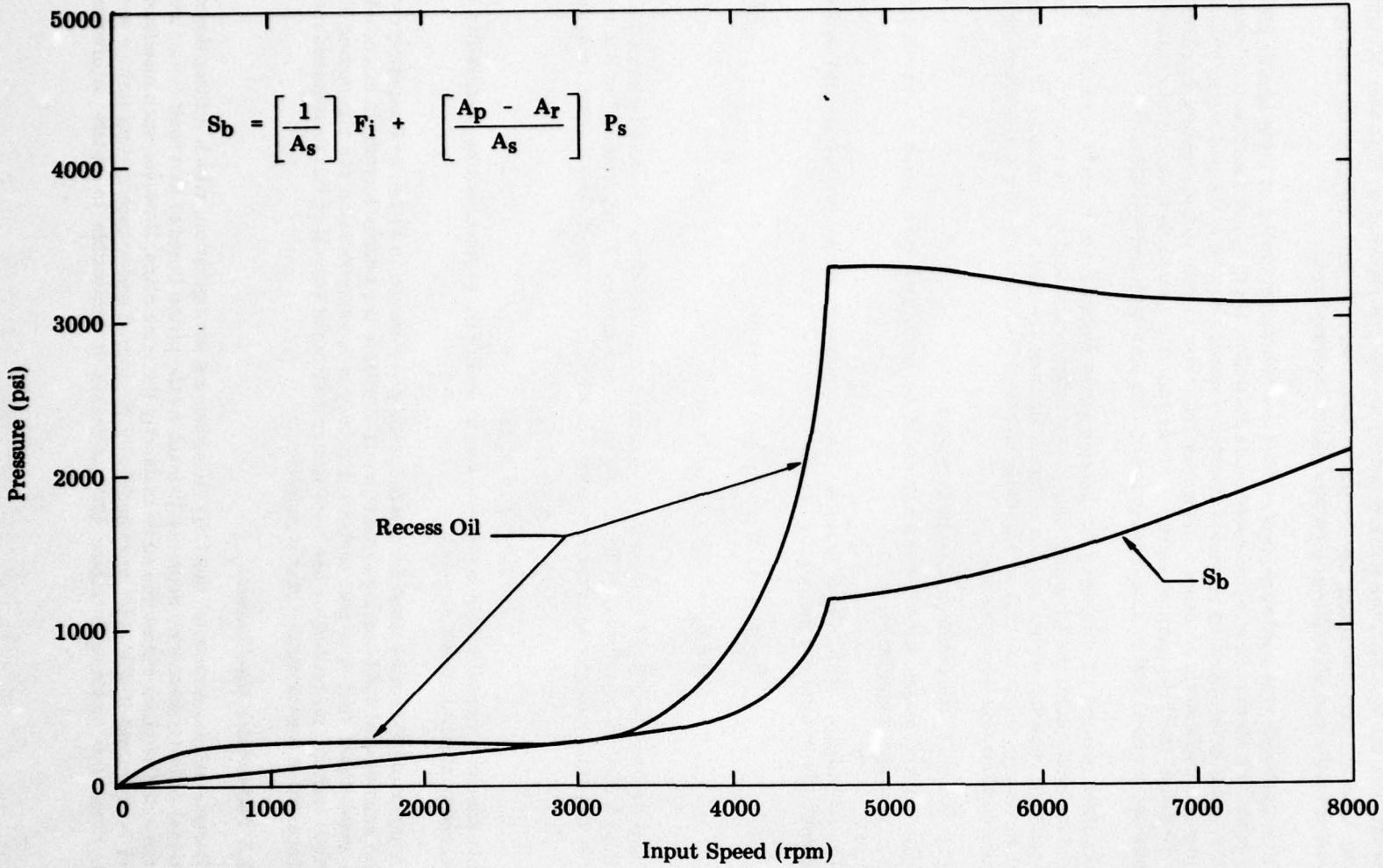

Figure 6–4. **OIL AND SILL BEARING PRESSURE AS A FUNCTION OF INPUT SPEED**

The pad recess area was originally manufactured smaller than the piston face area. When the restrictors are installed, the pressure acting on the pad recess area (P_1) also becomes smaller than the pressure acting on the piston face area (P_s). This increases the load to be supported by the pad sill and thus increases pad-sill bearing stress.

This approach was hardware-implemented and laboratory-tested at input speeds up to 7800 rpm. The combination of recess-pressure reduction ($P_1 < P_s$) and increased sill-bearing loading was not sufficient to eliminate interface leakage. However, the pad recess pressure was lowered sufficiently to cause a dangerous reduction in race recess pressure P_r. This in turn decreased the load-carrying capacity of the race and caused metal-to-metal contact of the race and wobbler and scoring damage to the race periphery and wobbler I.D.

Another method of increasing sill bearing stress would be to modify the pad surface areas. This method has the advantage that piston restrictors would not be required. The race load-carrying capacity would not be reduced, because the pad recess pressure (P_1) would equal the supply pressure (P_s) as originally intended. To calculate new pad surface areas, two principal criteria were observed:

(1) Pad sill bearing stress had to be increased.

(2) No hydrostatic lift-off tendency could be permitted, even under a hypothetical zero-speed condition.

In accordance with these criteria, two equations were developed and solved simultaneously to establish the required areas:

$$S_b A_s + P_s A_r - A_p P_s - F_i = 0 \tag{24}$$

$$0.5 A_s + A_r - k A_p = 0 \tag{25}$$

For zero hydrostatic lift-off tendency under a zero-speed condition, k must be equal to or less than 1.0. Various values of k from 0.80 to 1.0 and ratios of S_b/P_s from 0.7 to 0.9 were used in the equations and the required areas (A_s and A_r) calculated. The selected areas are:

$$A_s = 0.59 \text{ sq in.}$$
$$A_r = 0.44 \text{ sq in.}$$

In this selection, consideration was also given to feasibility of manufacture, availability of space, and configuration requirements.

A curve of sill bearing stress for this proposed pad is shown in Figure 6—6 superimposed on the existing pad's sill-bearing-stress curve to illustrate the relative increase in magnitude. It is emphasized that this pad represents merely a recommendation for eliminating the interface leakage; no prototype has been made. Additional aspects of this recommendation are discussed in the remainder of this chapter.

6.1.1.3 Pad-to-Race Misalignment

Because of the nature of the CSD roller-bearing configuration, which utilizes domed individual pistons, there is no necessity to machine the piston bores so that their center lines and the cylinder-block center line all lie in exactly the same plane. However, such machinery would be required if the existing cylindrically contoured pad-to-race mating surface were used. Since the pad/race interface leakage makes it impossible to obtain satisfactory

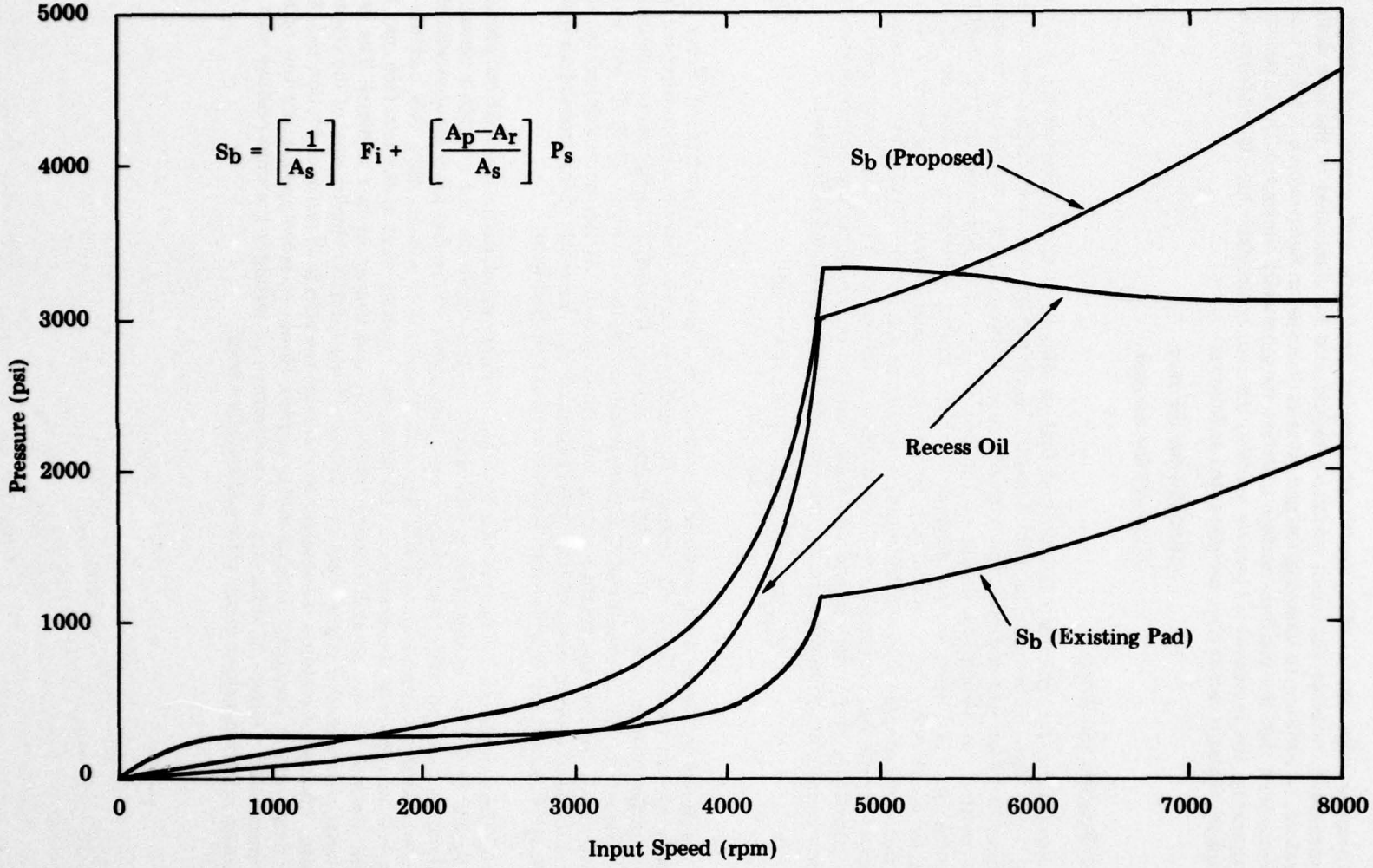

Figure 6—6. **OIL AND SILL BEARING PRESSURE AS A FUNCTION OF INPUT SPEED**

performance with the existing hydrostatic-bearing prototype and a new pad design is recommended, possible alignment problems should also be eliminated in the new design. Therefore, in addition to changing the pad areas as discussed in Subsection 6.1.1.2, it is also recommended that the pad/race surface interface be spherically contoured. Detail drawings incorporating the increased sill-bearing loading, the zero hydrostatic lift-off tendency, and the spherical pad/race interface are presented as follows:

C-000428 for the race

C-000429 for the pad

6.1.2 Friction and Wear

Essentially, this chapter has indicated that to stop the leakage between the pad and race, these two parts must be held together more tightly. However, regardless of the tightness between pad and race, the relative motion between the two will remain the same. This motion, or oscillatory sliding of the pad on the race, is caused by the wobbler eccentricity. The instantaneous magnitude of the sliding velocity is a function of the wobbler eccentricity, input speed, and cylinder-block angular position. Figure 6—7 shows the locus of instantaneous relative sliding velocities as a function of cylinder-block angular position for the full eccentric (e = 0.35) wobbler position and 4475-rpm input speed. For the calculation of PV factors and frictional horsepower, no single instantaneous-velocity value was used, but rather the average velocity, which can be defined as follows:

$$V_{average} = \frac{1}{2\pi} \int_0^{2\pi} |V| \, d\theta \qquad (26)$$

As shown in Figure 4—1, wobbler eccentricity is a function of input speed. From this relationship, an entire family of instantaneous sliding-velocity curves can be constructed for many different input speeds. Then the average velocity for each of these can be calculated from Equation 26. The results of this calculation are plotted in Figure 6—8. At any given input speed, the average relative sliding velocity (Figure 6—8) can be multiplied by the metal-to-metal bearing stress at that speed (Figure 6—6). The result of this calculation is the bearing PV factor, and it serves as an indication of anticipated wear.

Pad/race interface PV factors as a function of input speed were calculated and plotted in Figure 6—9. The quantitative values shown in this figure do not constitute absolute criteria; they do indicate, on a relative basis, that higher PV factors are associated with the recommended modification. ARINC Research Corporation believes that this increase is required to eliminate the leakage. In addition, the resulting wear at the interface may be slight because of the good boundary lubrication and change in race material. The race material recommended is gray cast iron instead of the E-52100 bearing steel of the original design. The use of cast iron is necessary to minimize the effects of pad/race friction and also to ensure against periphery scuffing during startup. However, prototype manufacture of the recommended pad/race modification and resumption of testing is the only positive way to evaluate interface-leakage elimination and interface wear.

REVISIONS			
SYM	ZONE	DESCRIPTION	DATE	APPROVED

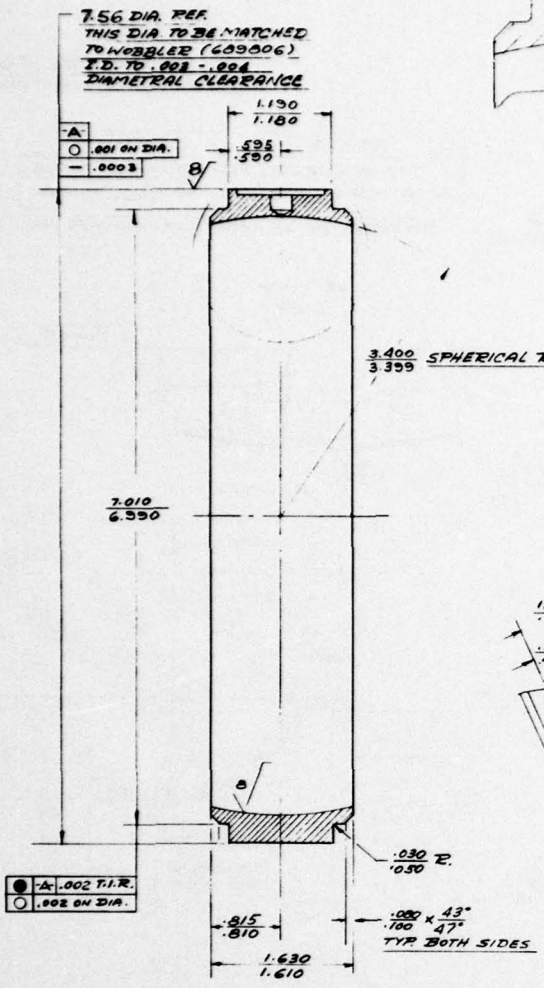

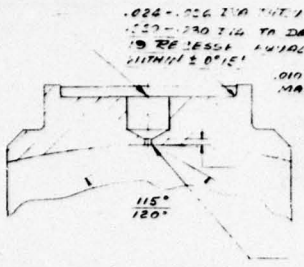

SCALE DOUBLE SIZE

HOLE EDGE MUST BE SHARP & FREE FROM BURRS

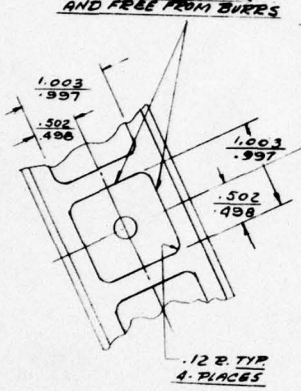

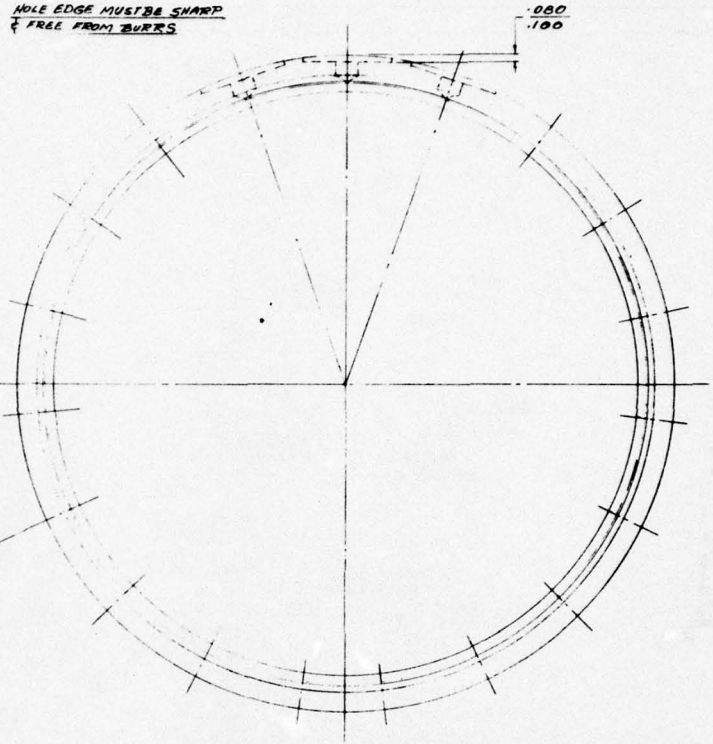

UNLESS OTHERWISE SPECIFIED BREAK ALL EDGES .003 - .010

BEST AVAILABLE COPY

MATERIAL :
SAE - J431 AG 3500
AIRCRAFT QUALITY PEARLITIC GRAY CAST IRON
220 - 240 BRINELL HARDNESS

QTY. REQ.	DESCRIPTION	PART NO.	MATERIAL	SPECIFICATION	ZONE	ITEM

LIST OF MATERIALS

ITEM	QTY.	NEXT ASSY	USED ON
APPLICATION			

UNLESS OTHERWISE SPECIFIED DIMENSIONS ARE IN INCHES
TOLERANCES ON:
FRACT. ± DECIMALS .XX ± .XXX ± ANGLES ±

MATERIAL: SEE NOTE
TREATMENT: SEE NOTE
FINISH: AS NOTED

DFTM. K. R. — DATE 7-1-69
DES. ENG. R.T.W. — DATE 7-8-69
CHKD.
APPD.
WORK ORDER NO. 595-01
CONTRACT NO.

ARINC RESEARCH CORPORATION

TITLE
RACE, PUMP
B52H CSD MODEL 120 RD02
HYDROSTATIC BEARING

SIZE C — DWG. NO. C 000428
SCALE 1/1 & 2/1 — SHEET 1 OF 1

REVISIONS				
SYM	ZONE	DESCRIPTION	DATE	APPROVED

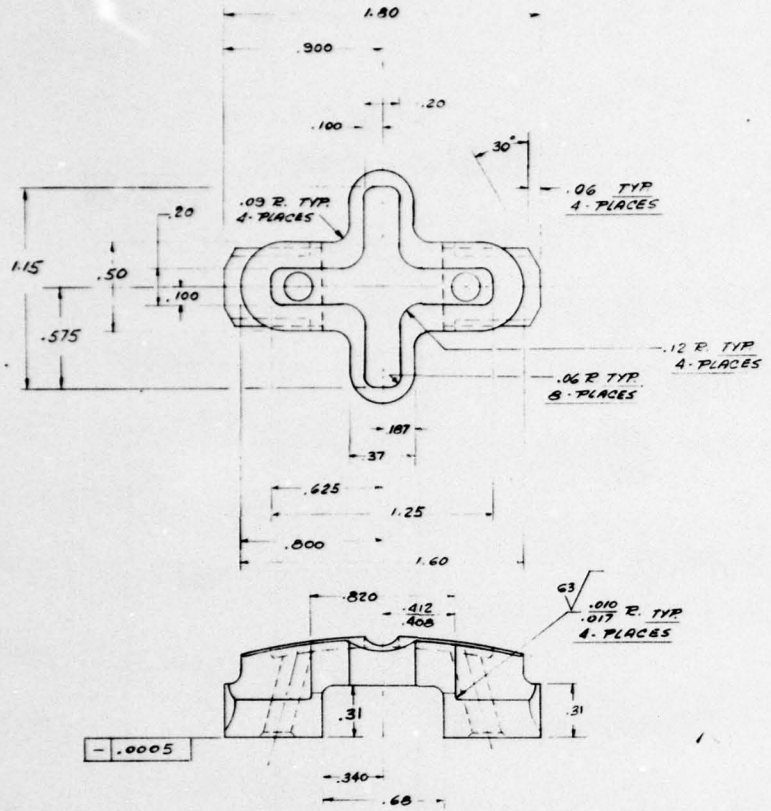

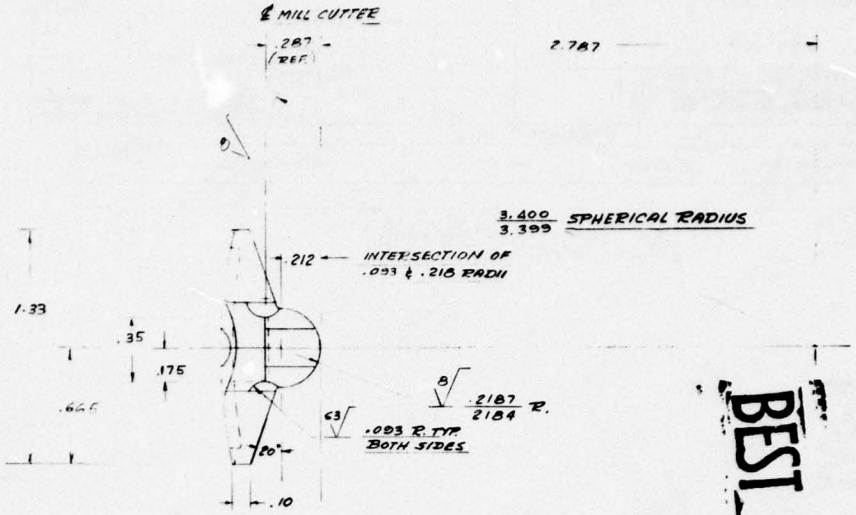

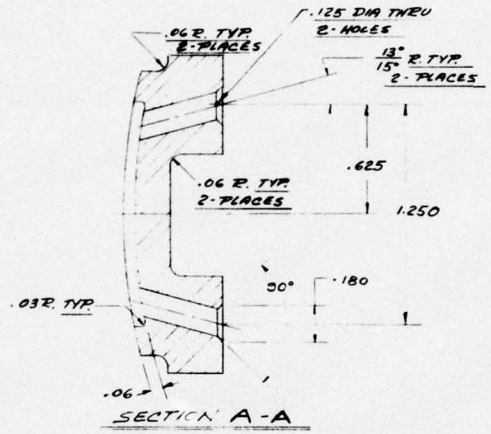

SPHERICAL RAD. REF.

MAY BE MADE FROM EITHER OF THE FOLLOWING

HARDNESS	MATERIAL
BRINELL 3000/10 200 - 220	AMPCO METAL 18 - 22
BRINELL 3000/10 190 - 210	COP. ALLY. NO. 630

UNLESS OTHERWISE SPECIFIED
BREAK ALL EDGES .003 - .010

QTY. REQ.	DESCRIPTION	PART NO.	MATERIAL	SPECIFICATION	ZONE	ITEM

LIST OF MATERIALS

UNLESS OTHERWISE SPECIFIED DIMENSIONS ARE IN INCHES TOLERANCES ON: FRACT. ± DECIMALS .XX ± .01 .XXX ± .005 ANGLES ± 1°	DFTM. K. M.S.	DATE 7/2/69	ARINC RESEARCH CORPORATION
	DES. ENG. R. F. W.	7-8-69	TITLE PAD B52 H CSD MODEL 120 RD 02 HYDROSTATIC BEARING
MATERIAL SEE LIST	CHKD.		
TREATMENT SEE [illegible]	APPD.		
FINISH [illegible]	WORK ORDER NO. 595-01		SIZE C DWG. NO. [illegible] 429
	ACT N	SCALE	SHEET OF 1

ITEM [illegible] NEXT ASSY APPLI[illegible] USED ON [illegible]

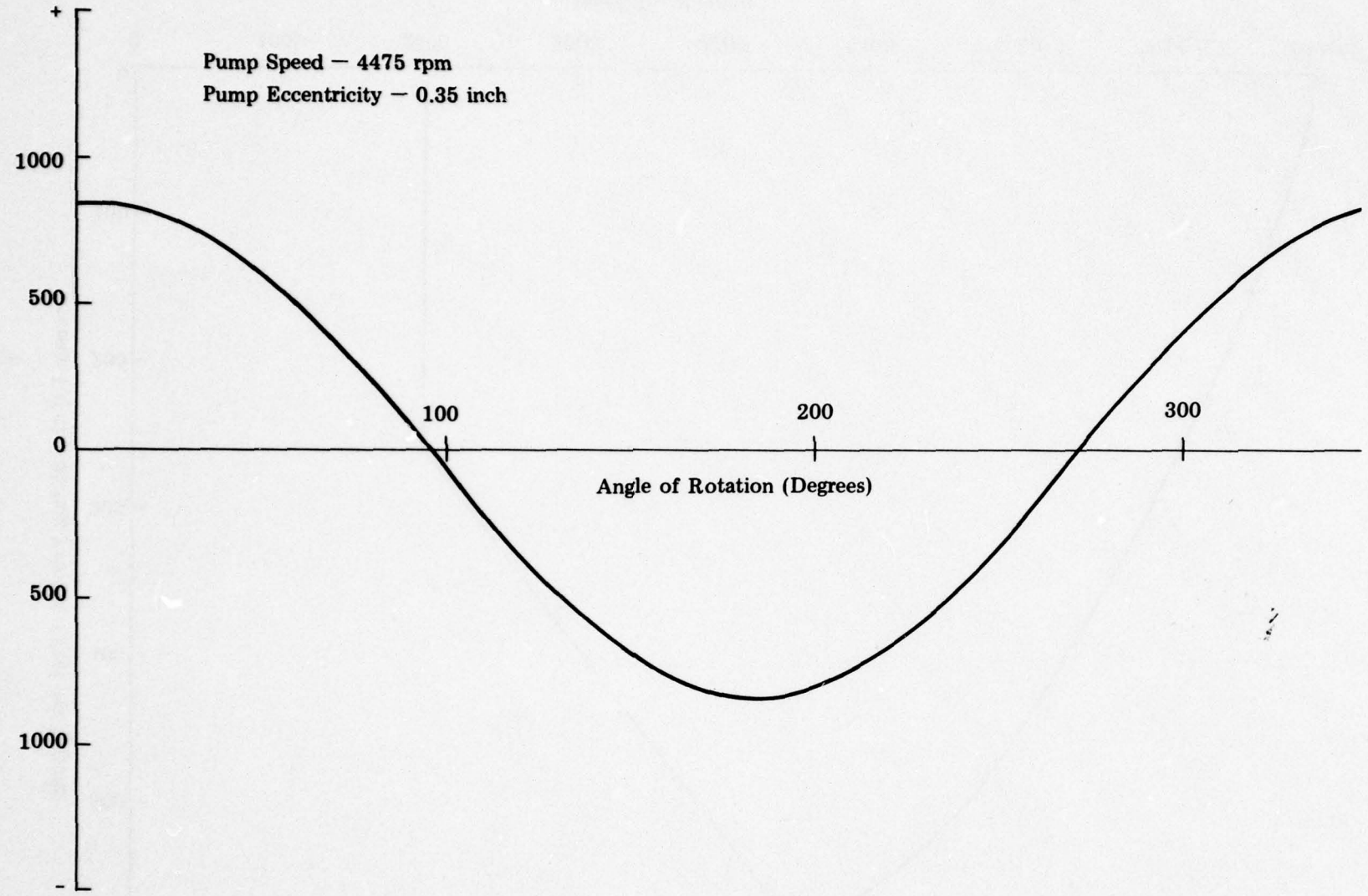

Figure 6—7. **SLIDING VELOCITY OF PAD ON RING VS. ANGLE OF ROTATION**

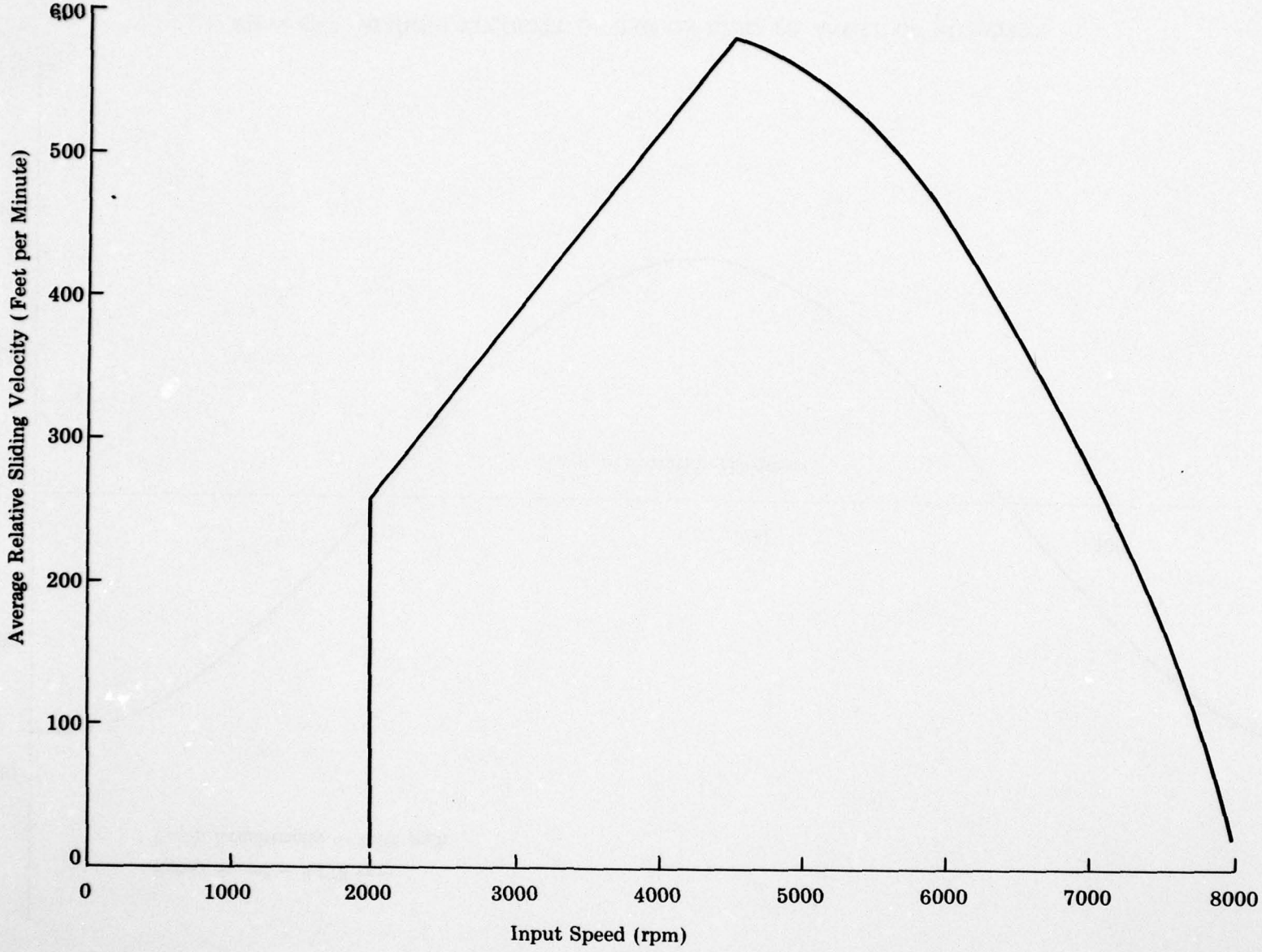

Figure 6—8. **AVERAGE RELATIVE SLIDING VELOCITY OF PAD ON RACE AS A FUNCTION OF INPUT SPEED**

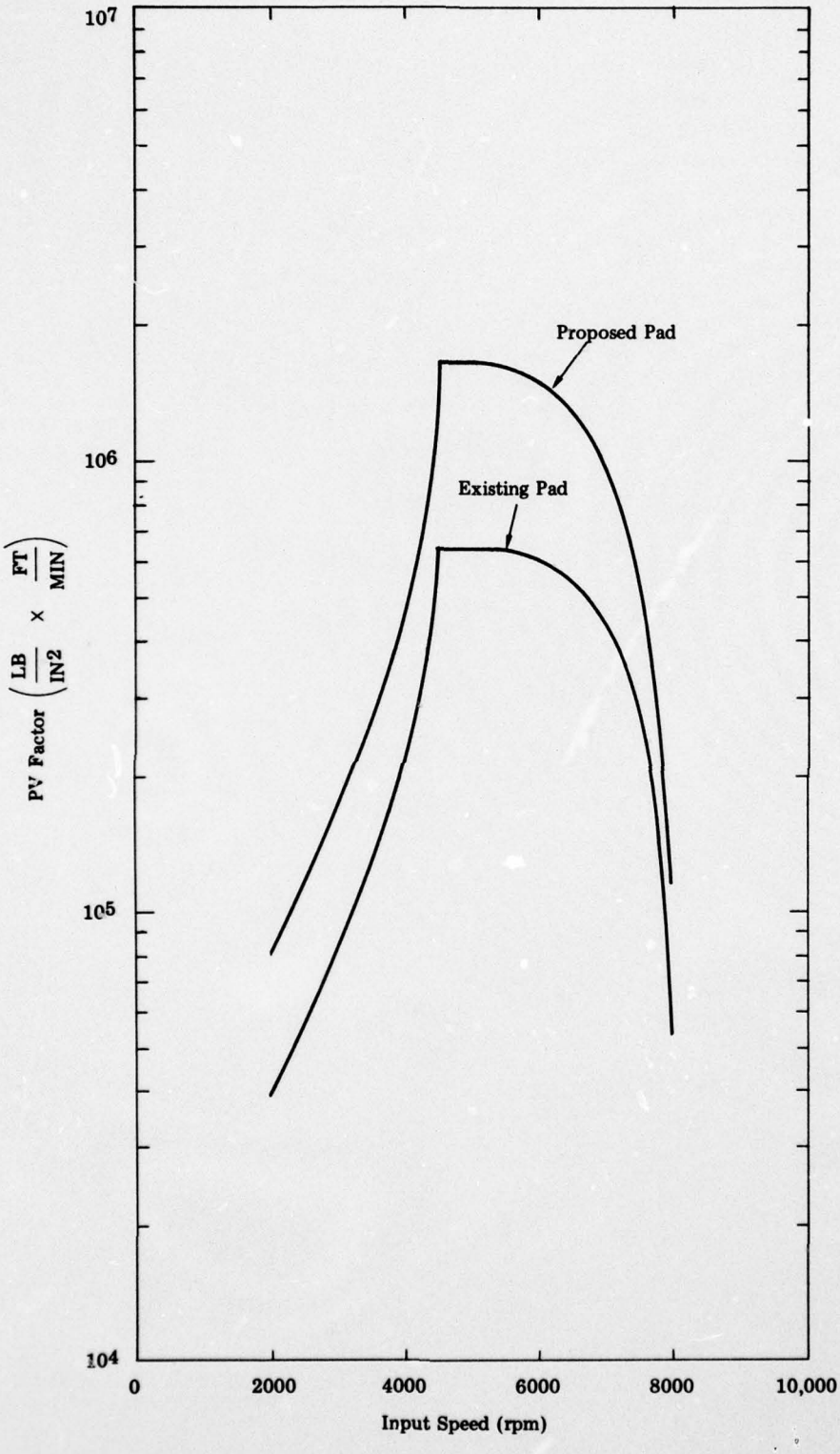

Figure 6—9. **PV FACTOR AS A FUNCTION OF INPUT SPEED (PUMP DISCHARGE SIDE, 167-HP LOAD)**

CHAPTER SEVEN

CONCLUSIONS

The objective of Phase I of this program was to design, fabricate, and test an experimental-model hydrostatic-bearing system for the pump side of the CSD and to validate its technical feasibility. The initiation of Phase II will depend on the judgment of OCNE engineers concerning the results of Phase I.

7.1 FEASIBILITY

The final determination of the feasibility of a hydrostatic-bearing system lies with OCNE engineering. Their decision will be predicated on system parameters such as oil flow, temperature build-up, wear characteristics, friction, material, and tolerance requirements, and the interaction of these parameters with CSD supporting devices.

In view of the excess leakage at the pad/race interface, ARINC Research Corporation believes that the prototype hydrostatic bearing will be judged unfeasible by the evaluating engineers at OCNE. However, the cause of the leakage has been determined, and a pad/race modification to eliminate the leakage has been designed and presented. ARINC Research Corporation, therefore, believes that the following course of action should be taken:

(1) Establish an interim project to fabricate and test the proposed modification to eliminate interface leakage

(2) Re-evaluate feasibility

(3) Perform Phase II effort if the results of the feasibility re-evaluation are positive.

7.2 PHASE II

Phase II of the program will consist of detailed engineering analysis of the entire CSD system, including the CSD, oil reservoir, oil cooler, oil lines, and filters.

A preliminary ECP will be prepared and parts will be fabricated to modify one complete 120RD02 CSD. It is proposed that the modified CSD be tested in a laboratory environment at the OCAMA facility. Initial testing procedures should include a minimum of 10 starts and stops with running time increasing from 1 hour to 20 hours. After an accumulation of 100 hours of successful operation, it is recommended that two additional drives be modified, installed on aircraft, and flight-tested.

Additional Phase II efforts will include finalizing the hydrostatic-system design and preparing a complete engineering data package (ECP). This package will consist of a complete set of reproducible engineering drawings necessary for the manufacture of all parts associated with the CSD modification and revision of applicable overhaul instructions.

REFERENCES

1. Maleev, V. L. and Hartman, J. B., *Machine Design*, 3rd Ed., International Textbook Company, Scranton, Pennsylvania, 1954.

2. Phelan, R. M. *Fundamentals of Mechanical Design*, McGraw-Hill Book Company, Inc. New York, 1962.

3. Rothbart, H. A., *Mechanical Design and Systems Handbook*, McGraw-Hill Book Company, Inc., New York, 1964.

4. Merritt, H. E., *Hydraulic Control Systems*, John Wiley and Sons, Inc., New York, 1967.

5. Beer, F. P. and Johnston, E. R., *Mechanics for Engineers*, McGraw-Hill Book Company, Inc., New York, 1957.

6. Rippel, H. C., *Cast Bronze Hydrostatic Bearing Design Manual*, Cast Bronze Bearing Institute, Inc., Cleveland, Ohio, 1963.

APPENDIX A

ACCELERATION ANALYSIS

The following sketch and equations show the determination of radial acceleration required for calculating tne radial inertial load in Chapter 4.

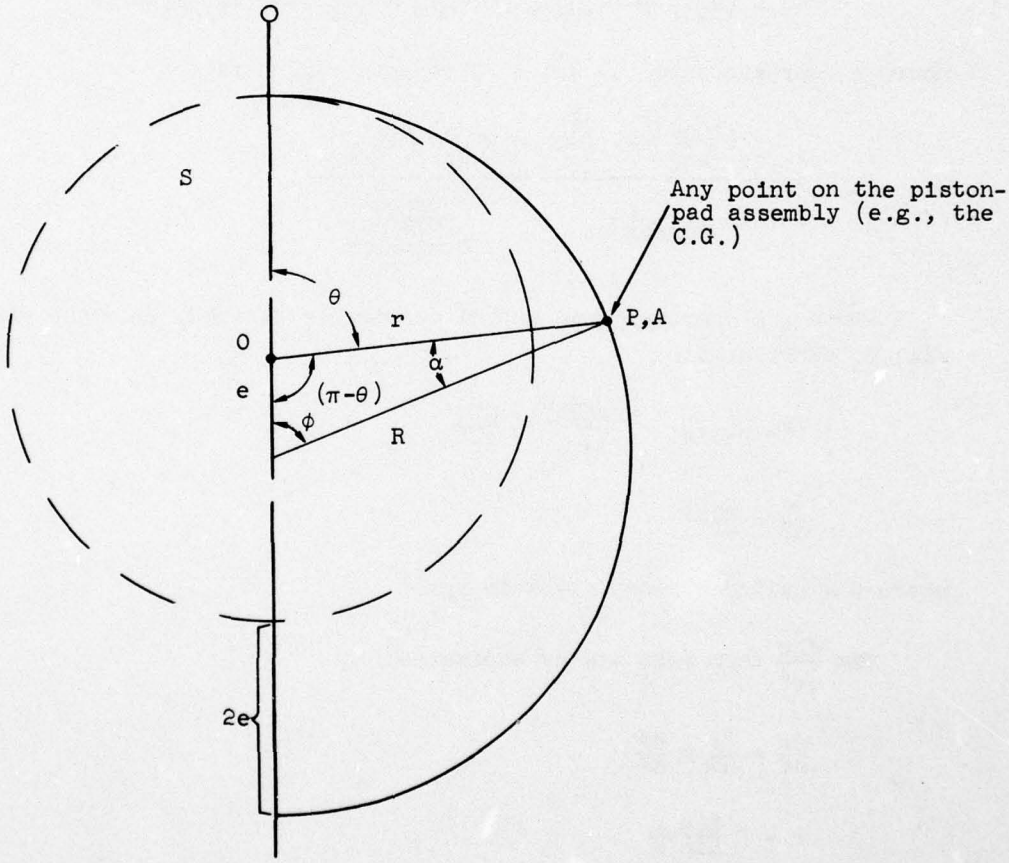

$$\frac{e}{\sin \alpha} = \frac{R}{\sin (\pi-\theta)}$$

$$\sin (\pi-\theta) = \sin \theta$$

$$\alpha = \text{Sin}^{-1}\left[\frac{e}{R}\,\text{Sin}\,\theta\right]_{\theta=0}^{180^\circ}$$

$$\left.\begin{aligned}\phi &= \pi - (\pi-\theta) - \alpha = \theta-\alpha \\ r &= R\,\frac{\text{Sin}\,\phi}{\text{Sin}\,\theta}\end{aligned}\right\}\ 0<\theta<\pi$$

$$a_P = a_A \twoheadrightarrow a_{P/S} \twoheadrightarrow a_C$$

where

a_P = Absolute acceleration of point P

a_C = Coriolis component

$$a_P = (a_A)_r \twoheadrightarrow (a_{P/S})_r \twoheadrightarrow (a_C)_r \twoheadrightarrow (a_A)_t \twoheadrightarrow (a_{P/S})_t \twoheadrightarrow (a_C)_t$$

where r represents radial and t represents tangential.

$$a_P = \underbrace{r\left(\frac{d\theta}{dt}\right)^2 \twoheadrightarrow \frac{d^2r}{dt^2}}_{\substack{\text{Radial}\\ \text{Component}}} \twoheadrightarrow \underbrace{2\left(\frac{d\theta}{dt}\right)\left(v_{P/S}\right)_r}_{\substack{\text{Tangential}\\ \text{Coriolis}\\ \text{Component}}}$$

Since the inertial load on the bearing is desired, only the radial components will be considered:

$$(a_P)_{\text{Radial}} = r\left(\frac{d\theta}{dt}\right)^2 + \frac{d^2r}{dt^2}$$

$$\frac{d\theta}{dt} = \frac{2\pi N}{60}$$

where N = cylinder-block speed in rpm.

The $\frac{d^2r}{dt^2}$ term must now be evaluated:

$$\frac{dr}{dt} = \frac{dr}{d\theta} \times \frac{d\theta}{dt}$$

$$r = R\,\frac{\text{Sin}\,\phi}{\text{Sin}\,\theta}$$

$$\frac{dr}{d\theta} = R\left[\frac{\text{Cos}\,\phi}{\text{Sin}\,\theta} \times \frac{d\phi}{d\theta} - \frac{\text{Sin}\,\phi\,\text{Cos}\,\theta}{\text{Sin}^2\theta}\right]$$

$$\frac{d^2r}{d\theta^2} = R\left[\frac{\text{Cos}\,\phi}{\text{Sin}\,\theta} \times \frac{d^2\phi}{d\theta^2} - \frac{2\,\text{Cos}\,\phi\,\text{Cos}\,\theta}{\text{Sin}^2\theta} \times \frac{d\phi}{d\theta} - \frac{\text{Sin}\,\phi}{\text{Sin}\,\theta} \times \left(\frac{d\phi}{d\theta}\right)^2 + \frac{\text{Sin}\,\phi}{\text{Sin}\,\theta} + \frac{2\cdot\text{Sin}\,\phi\,\text{Sin}\,\theta\,\text{Cos}^2\theta}{\text{Sin}^4\theta}\right]$$

$$\frac{d\phi}{d\theta} = 1 - \frac{d\alpha}{d\theta}$$

$$\frac{d^2\phi}{d\theta^2} = - \frac{d^2\alpha}{d\theta^2}$$

$$\frac{d\alpha}{d\theta} = \frac{\left(\frac{e}{R}\right) \text{Cos } \theta}{\sqrt{1-\left(\frac{e}{R} \text{ Sin } \theta\right)^2}}$$

$$\frac{d^2\alpha}{d\theta^2} = \frac{\left(\frac{e}{R}\right)^3 \text{Sin } \theta \text{ Cos}^2 \theta}{\left[1 - \left(\frac{e}{R}\right)^2 \text{Sin}^2\theta\right]^{3/2}} - \frac{\frac{e}{R} \text{ Sin } \theta}{\left[1 - \left(\frac{e}{R} \text{ Sin } \theta\right)^2\right]^{1/2}}$$

$$\frac{d^2r}{dt^2} = \frac{dr}{d\theta} \times \frac{d^2\theta}{dt^2} + \left(\frac{d\theta}{dt}\right)^2 \times \frac{d^2r}{d\theta^2}$$

At a constant input speed,

$$\frac{d\theta}{dt} = \text{Constant}$$

$$\frac{d^2\theta}{dt^2} = 0$$

$$\frac{d^2r}{dt^2} = \left(\frac{d\theta}{dt}\right)^2 \frac{d^2r}{d\theta^2}$$

APPENDIX B

COMPUTER FLOW DIAGRAM

The hydrostatic-bearing computer analysis described in Chapter 4 is represented by the following sketch of bearing geometry and by the flow diagram that appears on the following page.

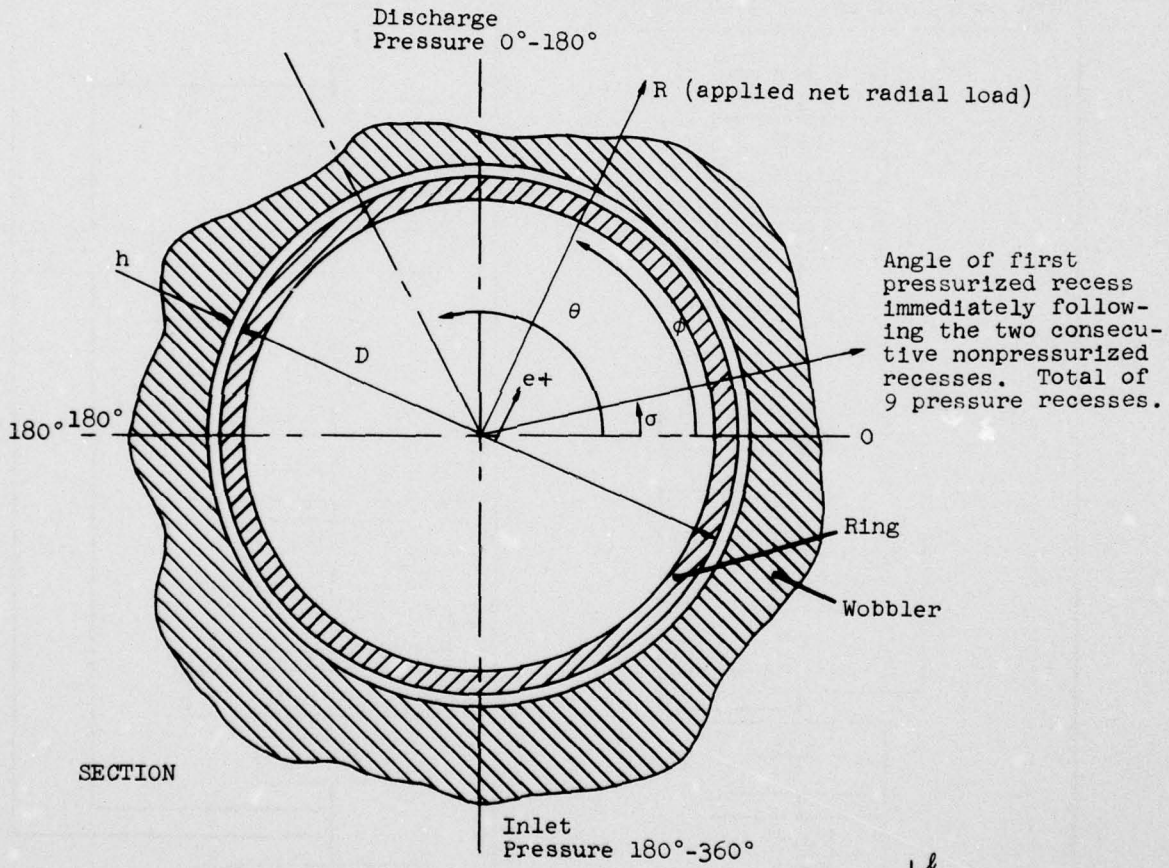

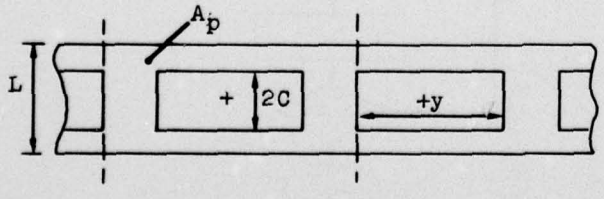

VIEW OF RING OUTER SURFACE

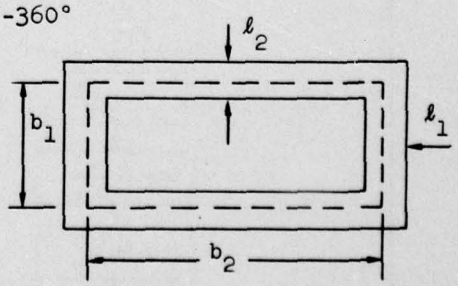

IDEALIZED RECESS/SILL GEOMETRY

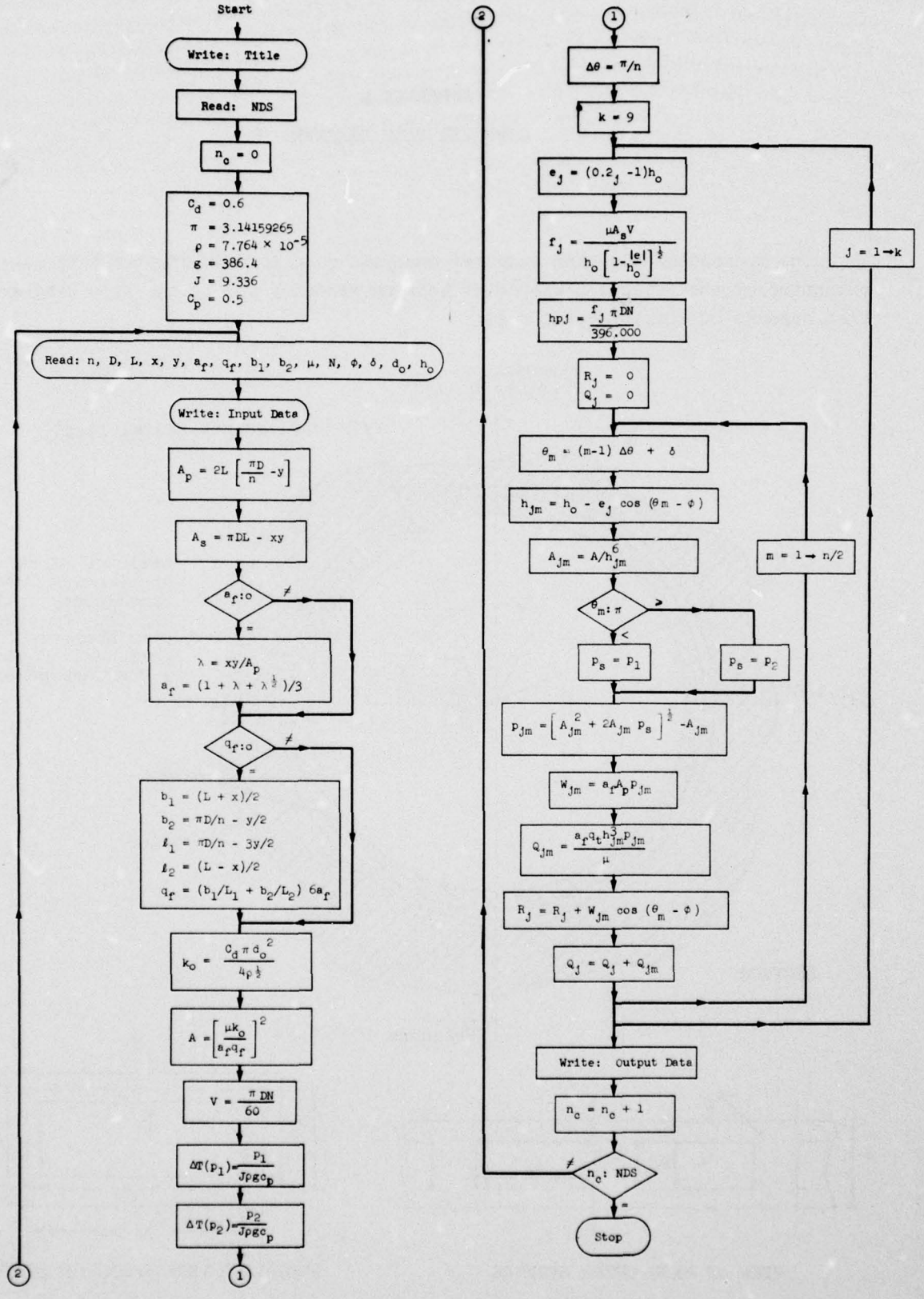
Start
Write: Title
Read: NDS
$n_c = 0$
$C_d = 0.6$
$\pi = 3.14159265$
$\rho = 7.764 \times 10^{-5}$
$g = 386.4$
$J = 9.336$
$C_p = 0.5$
Read: n, D, L, x, y, a_f, q_f, b_1, b_2, μ, N, ϕ, δ, d_o, h_o
Write: Input Data
$A_p = 2L\left[\frac{\pi D}{n} - y\right]$
$A_s = \pi DL - xy$
a_f:o
$\lambda = xy/A_p$
$a_f = (1 + \lambda + \lambda^{\frac{1}{2}})/3$
q_f:o
$b_1 = (L + x)/2$
$b_2 = \pi D/n - y/2$
$\ell_1 = \pi D/n - 3y/2$
$\ell_2 = (L - x)/2$
$q_f = (b_1/L_1 + b_2/L_2)\, 6a_f$
$k_o = \frac{C_d \pi d_o^2}{4\rho^{\frac{1}{2}}}$
$A = \left[\frac{\mu k_o}{a_f q_f}\right]^2$
$V = \frac{\pi DN}{60}$
$\Delta T(p_1) = \frac{p_1}{Jpgc_p}$
$\Delta T(p_2) = \frac{p_2}{Jpgc_p}$
1
2
$\Delta\theta = \pi/n$
$k = 9$
$e_j = (0.2_j - 1)h_o$
$f_j = \frac{\mu A_s V}{h_o\left[1 - \frac{|e|}{h_o}\right]^{\frac{1}{2}}}$
$hp_j = \frac{f_j \pi DN}{396.000}$
$R_j = 0$
$Q_j = 0$
$\theta_m = (m-1)\,\Delta\theta + \delta$
$h_{jm} = h_o - e_j \cos(\theta_m - \phi)$
$A_{jm} = A/h_{jm}^6$
θ_m: π
$p_s = p_1$
$p_s = p_2$
$p_{jm} = \left[A_{jm}^2 + 2A_{jm} p_s\right]^{\frac{1}{2}} - A_{jm}$
$W_{jm} = a_f A_p p_{jm}$
$Q_{jm} = \frac{a_f q_f h_{jm}^3 p_{jm}}{\mu}$
$R_j = R_j + W_{jm} \cos(\theta_m - \phi)$
$Q_j = Q_j + Q_{jm}$
m = 1 → n/2
j = 1 → k
Write: Output Data
$n_c = n_c + 1$
n_c: NDS
Stop

APPENDIX C

HYDROSTATIC-BEARING EXPERIMENTAL TEST

The following procedure was prepared for testing the prototype hydrostatic-bearing configuration:

SECTION I - GENERAL PROCEDURE

A. Inspect New Parts

1. Dimensional Checks

   a. Wobbler I.D.
   b. Ring O.D.
   c. Ring I.D.
   d. Piston O.D.
   e. Pad Knuckle Diameter
   f. Pad Run-out

2. Visual Observations

   a. Surface Finishes
   b. Fits

B. Weigh New Parts

1. Piston
2. Pad
3. Ring

C. Determine approximate C.G. of piston and pad.

D. Photograph wobbler, pistons, pads, and ring, with emphasis on wear areas.

E. Flush oil-supply system, making periodic contamination analysis until an SAE-class-5 supply is achieved.

F. Install new in-line filter, flush briefly, and check contamination. Photograph contamination-analysis filter under magnification.

G. Thoroughly clean new parts, cylinder block, and all related hardware; then assemble in accordance with the following:

1. Cleanliness

   All test specimens and fixture parts must be free of foreign matter, both internally and externally. To accomplish this, submerge and wash parts in Government Specification P-D-680 solvent and air-blow dry.

2. Lubrication

   a. All test-specimen parts must be lightly coated with clean MIL-L-7808 oil after cleaning and prior to assembly. Do not lubricate screws or threads that retain the pump plate.

   b. O-ring seals should be lubricated with either MIL-L-7808 oil or a very light coat of acryloid HF 825 prior to assembly.

3. Demagnetization

   All specimen parts must be demagnetized prior to lubrication and assembly.

4. Assembly (see ARINC Research Drawing C-000419)

   a. Install cylinder block on test-fixture center shaft. Make absolutely sure that both cross-feed holes of the small shaft open unrestricted into the cylinder block's center cavity. If the assembly is incorrect, one of the feed holes may be covered by the larger shaft.

   b. Place pump wobbler flat on a bench, with the threaded screw holes used to fasten the pump-plate ratining ring facing upward. Fit the pump race (C-000412) into the wobbler. Extreme caution must be observed to ensure that the recess feed holes are facing the direction of rotation as shown on Drawing C-000419, Zone 2-C. Install the pump-plate retaining ring and secure with the appropriate washers and screws. Torque the screws to 75-85 in-lb.

   c. Install 18 domed motor pistons on motor side of cylinder block and retain with aluminum ring. Make sure ring is concentric and balanced.

   d. To each pad (C-000414) attach two pistons (C-000415) and then install each piston-pad assembly into the cylinder block. These may be temporarily retained with a rubber band around the pads for assembly into the wobbler. Pads of identical material must be grouped together.

   e. Install the wobbler and cylinder block on the test fixture in exactly the same way as for testing the roller-bearing configuration. Check line-up of wobbler to cylinder block, using Teflon plug and dial indicator.

REVISIONS				
SYM	ZONE	DESCRIPTION	DATE	APPROVED
A		REVISED AND REDRAWN TO SHOW RECESS DIMENSIONS	1-7-69	[illegible]

7.56 REF.
THIS DIA. TO BE MATCHED TO WOBBLER (689806) I.D. TO .003 - .004 DIAMETRAL CLEARANCE

-A-
○ .001 ON DIA.
— .0003

.815 / .805

.595 / .590

.010 R. MAX.

7.010 / 6.990

6.705 / 6.695

.030 R. / .050

◎ A .002 TIR
○ .002 ON DIA.
— .0005

1.190 / 1.180

.080 / .100 X 43° / 47°
TYP. BOTH SIDES

1.630 / 1.610

.030 / .050

.060 REF.

94°30' REF.

.024 - .026 DIA. THRU
.220 - .230 DIA. TO DEPTH SHOWN
19 RECESSES EQUALLY SPACED WITHIN ± 0°15'

.030 / .025

115° / 120°

HOLE EDGE MUST BE SHARP AND FREE FROM BURRS

RECESS, TYP. - 2X

.115 / .125

1.110 / 1.125

R.

.502 / .498

1.003 / .997

RECESS EDGE SHARP AND FREE FROM BURRS

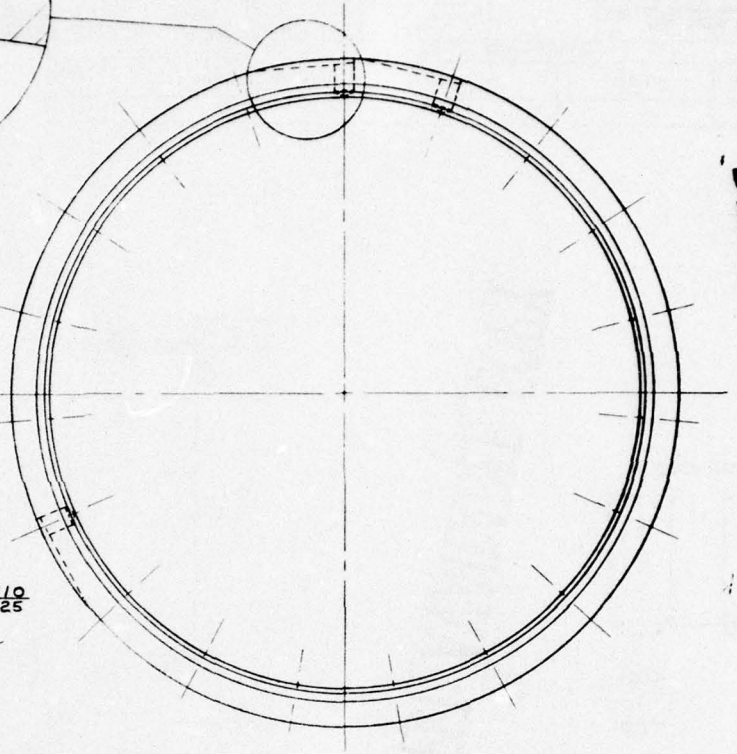

BEST AVAILABLE COPY

UNLESS OTHERWISE SPECIFIED
BREAK ALL EDGES .003 - .010

QTY. REQ.	DESCRIPTION	PART NO.	MATERIAL	SPECIFICATION	ZONE	ITEM

LIST OF MATERIALS

ITEM	QTY.	NEXT ASSY	USED ON
APPLICATION			

UNLESS OTHERWISE SPECIFIED DIMENSIONS ARE IN INCHES
TOLERANCES ON:
FRACT. ± DECIMALS .XX ± .XXX ± ANGLES ±

MATERIAL: AISI-E-52100

TREATMENT: HARDEN 58-62 R_c

FINISH 125 V

DFTM.	R. F. Wambaugh	1-7-69
DES. ENG.	R. F. Wambaugh	1-7-69
CHKD.	[illegible]	[illegible]
APPD.		

WORK ORDER NO. 595-01

CONTRACT NO.

ARINC RESEARCH CORPORATION

TITLE
RACE - PUMP
B 52H CSD MODEL 120RD02
HYDROSTATIC BEARING

SIZE C | DWG. NO. C-000412

SCALE | SHEET 1 OF 1

REVISIONS				
SYM	ZONE	DESCRIPTION	DATE	APPROVED
A		DELETE TABLE 1	9/17/68	RLS
B	3 D	HOLE DIA. ADDED. NOTE 4, 5 DELEATED	1/7/69	RSB

NOTES:

1 BREAK SHARP CORNERS
\.020

~~MACHINE PISTON O.D. TO MATCH INDIVIDUAL BORE CYLINDERS WITH A .0003" TO .0005" CLEARANCE BETWEEN PISTON O.D. AND CYLINDER I.D.~~
~~MARK MATCHED PISTON-CYLINDER SETS~~

	PART NO.	GROUP	BORE 'd'	DIAMETER 'D'
MOTOR	C000415-1	WW	.525 / .545	.66640-.66655
	-2	XX		.66655-.66670
	-3	YY		.66670-.66685
	-4	ZZ		.66685-.66700
	-5	CC		.67130-.67145
	-6	DD		.67145-.67160
	-7	EE		.67160-.67175
	-8	AA		.66700-.66715 (A)
	-9	FF		.67175-.67190
PUMP	-10	WW	.565 / .585	.71340-.71355
	-11	XX		.71355-.71370
	-12	YY		.71370-.71385
	-13	ZZ		.71385-.71400
	-14	CC		.72240-.72255
	-15	DD		.72255-.72270
	-16	EE		.72270-.72285
	-17	AA		.71400-.71415
	-18	FF		.72285-.72300

TABLE 1

3. HEAT TREAT PER AISI 52100

~~4 HOLE SIZE WILL BE SPECIFIED AT A LATER DATE~~

5 DO NOT USE 8 SURFACES FOR HARDNESS TESTS

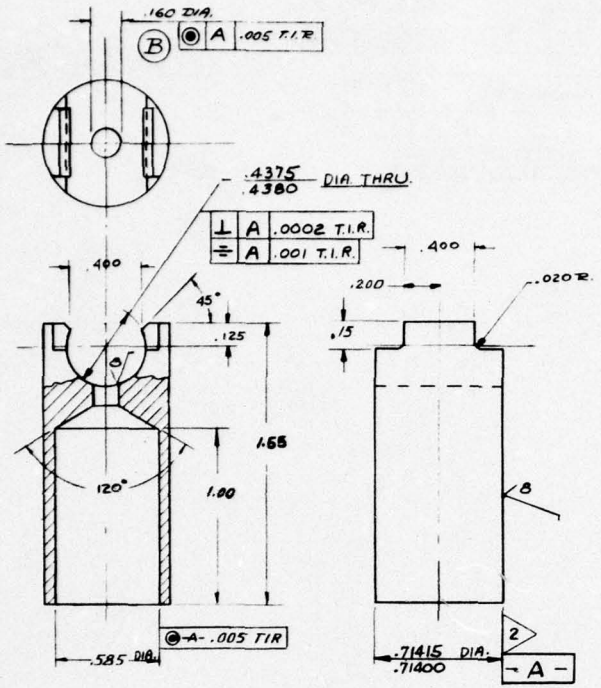

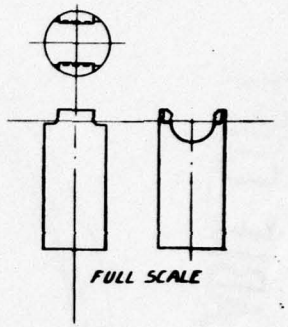

QTY. REQ.	DESCRIPTION	PART NO.	MATERIAL	SPECIFICATION	ZONE	ITEM

LIST OF MATERIALS

ITEM	QTY.	NEXT ASSY	USED ON
APPLICATION			

UNLESS OTHERWISE SPECIFIED DIMENSIONS ARE IN INCHES
TOLERANCES ON:
FRACT. ± | DECIMALS .XX ±.01, .XXX ±.005 | ANGLES ± 3°
MATERIAL: AISI-E-52100
TREATMENT: HARDNESS 58-62 Rc
FINISH: 125 AND AS NOTED

		DATE
DFTM.		10/28/68
DES. ENG.		
CHKD.		11-21-68
APPD.		11/21/68

WORK ORDER NO. 595 01
CONTRACT NO.

ARINC RESEARCH CORPORATION

TITLE
PISTON
B 52 H CSD 120 RD 02
HYDROSTATIC BEARING

SIZE C | DWG. NO. C 000415

SCALE 2/1 | SHEET 1 OF 1

f. Before testing, bleed any air trapped within the specimen out the plug end of the center shaft.

H. Flush (low pressure, zero speed) through specimen; check contamination; photograph analysis filter.

I. Begin test

1. Conditions for the first two hours (break-in), using the vari-drive, are as follows:

a. Eccentricity = 0
b. Supply pressure = 250 psig
c. Speed = 500 to 2000 rpm in 500-rpm increments every 30 minutes

2. During break-in, wobbler temperature, drag torque, supply-oil temperature, and leakage flow are to be monitored continuously. If any of these factors begins to deviate abnormally (e.g., wobbler temperature exceeds 325°F), the test must be terminated.

J. First Tear-Down and Inspection

1. The following visual observations should be made:

a. Wear Patterns, Fits, Surface Finishes

· Side of pump race where it runs against bronze pump plate
· Bronze-pump-plate surface against which race runs
· Wobbler lip against which race runs
· O.D. and I.D. of race
· Pad swivel and ring contact surface
· Piston swivel and O.D.
· Cylinder bores

b. Cleanliness of Oil-Flow Restrictors in Race

2. Prior to reassembly, all parts must be throughly cleaned and the system flushed as described in paragraphs G and H.

K. Data Collection

1. After the first tear-down obtain required data for Section III.

2. Obtain lower-speed data first, progressing to the high-speed (7000 rpm) data last.

L. Preliminary Endurance Test

1. After data collection, run continuously under the following operating conditions until the total accumulated running time (including break-in and data collection) is 50 hours:

a. Supply pressure = 500 psig
b. Eccentricity = 0
c. Speed = 7000 rpm

2. From 50 hours to 150 hours accumulated time, operating conditions are:

   a. Supply pressure = 1000 psig
   b. Eccentricity = 0
   c. Speed = 7000 rpm

M. Perform second tear-down and inspection in a manner identical to the first (Paragraph J).

N. Intermediate Test

1. From 100 to 150 hours accumulated time; same operating conditions as L.2.

O. Endurance Test

1. From 150 to 175 hours accumulated time, operating conditions are:

   a. Supply pressure = 500 psig
   b. Eccentricity = 0.35 inch
   c. Speed = 4750 rpm

2. From 175 to 230 hours accumulated time, operating conditions are:

   a. Supply pressure = 1000 psig
   b. Eccentricity = 0.35 inch
   c. Speed = 4750 rpm

P. Data collection after 230 hours

1. Obtain data per Section III and Paragraph K.

2. Test described in Section III Paragraph D not required here.

Q. Final Tear-Down and Inspection

1. Visual observation per Paragraph J.1.

2. Dimensional checks per Paragraph A.1.

3. Photographs per Paragraph D.

NOTE: Observations not specifically called for are to be recorded together with date, time, and phase of this test at which the observation is made.

SECTION II

A. Throughout the test, check and record the following at the intervals stated:

1. Every 30 minutes

AD-A054 699 ARINC RESEARCH CORP ANNAPOLIS MD F/G 20/5
HYDROSTATIC-BEARING MODIFICATION FOR MODEL 120RD02 CONSTANT-SPE--ETC(U)
AUG 69 R F WAMELING, G K GANTSCHNIGG F34601-69-C-1400
UNCLASSIFIED 595-01-1-990 NL

2 OF 2
ADA
054699

END
DATE
FILMED
6-78
DDC

a. Wobbler temperature
b. Drag torque
c. Flow (if readable on flowrator)

2. Every 25 hours

a. Contamination analysis

B. An elapsed-time record must be kept to indicate the total accumulated running time as well as the total accumulated time at each operating condition and when during the test the running time was accumulated.

SECTION III - DATA REQUIRED

A. Oil leakage (gpm) vs. supply pressure (psig) over a pressure range of 250 to 1000 psig for each of following at stabilized supply-oil temperature:

1. Eccentricity = 0

a. Cylinder-block speed = 0 rpm
b. Cylinder-block speed = 2000 rpm
c. Cylinder-block speed = 4750 rpm
d. Cylinder-block speed = 7000 rpm

2. Eccentricity = 0.35 inch

a. Cylinder-block speed = 2000 rpm
b. Cylinder-block speed = 4750 rpm

B. Wobbler drag torque (in-lb) vs. supply pressure (psig) over pressure range of 250 to 1000 psig for each of the following at stabilized supply-oil temperature:

1. Eccentricity = 0

a. Cylinder-block speed = 2000 rpm
b. Cylinder-block speed = 7000 rpm

2. Eccentricity = 0.35 inch

a. Cylinder-block speed = 2000 rpm
b. Cylinder-block speed = 4750 rpm

C. Stabilized supply-oil and wobbler temperatures.

D. Wobbler temperature (°F) vs. time (minutes) at supply pressure of 1000 psig for the following:

1. Cylinder-block speed = 4750 rpm, eccentricity = 0.35 inch

2. Cylinder-block speed = 7000 rpm, eccentricity = 0